

CLOSURE ESTIMATIONS FROM UNDERGROUND OBSERVATIONS AND THEIR COMPARISON TO CLOSURE FROM ELASTIC NUMERICAL MODELLING

Obakeng Rakumakoe

A research report submitted to the Faculty of Engineering and the Built Environment,
University of the Witwatersrand, Johannesburg, in partial fulfilment of the requirements for
the degree of Master of Science in Engineering.

Johannesburg, October 2017

Declaration

I Obakeng Rakumakoe (Student number: 0307475G) am a student registered for MSc(Eng) Mining in the year 2017. I hereby declare that this research report is my own unaided work. I have read the University Policy on Plagiarism and hereby confirm that no Plagiarism exists in this report. I also confirm that there is no copying nor there is any copyright infringement. It is being submitted for the Degree of Master of Science to the University of the Witwatersrand, Johannesburg. It has not been submitted before for any degree or examination in any other University.

Date:

Signature:.....

ABSTRACT

The gold reserves in South Africa have been mined for decades, depleting all the easily accessible reserves. In pursuing the deeper reserves South African mining industry has for many years led the development of mining and particularly rock engineering. Various design criteria and tools have been developed and used by South African rock engineers in different mining environments.

It must also be understood that these criteria were developed decades ago in different mining environments compared to where mining is currently taking place. In using these design criteria one needs to look at the relevance of such criteria and question if they are still applicable or if new criteria are required. Scheepers et.al, (2012) reviewed the design criteria used in designing ultra-deep narrow reef stopes in the West Wits and identified that there was no clear correlation between the design criteria used and the seismicity which is the highest FOG risk in ultra-deep mines. They then decided to use modelled elastic closure as design parameter which can be correlated to seismicity.

This report details an investigation into the correlation of the modelled elastic closure to the estimated closure from underground and how modelled closure can be adjusted to better reflect the anticipated closure underground. The investigation was conducted using underground observations and stoping width estimations using installed timber support and numerical modelling results (MAP3D).

Before correlating the modelled closure and the estimated closure, it was critical to understand the basis of the work done by (Scheepers et.al, 2012) in correlating the modelled closure to seismic hazard. McGarr, (1976) introduced the concept of correlating seismic energy to volume changes in stope. However this correlation was on the basis that the closure in the stope is only as a result of seismic failure. This was the basis of work done by (Scheepers et.al, 2012) in correlating volume change due to seismicity (seismic potency) to modelled closure.

It must be understood that (Scheepers et.al, 2012) aim was not for the modelled closure to reflect underground closure, however was to give an indication of the anticipated seismic activity relative to closure. This report further looks at what would the underground closure be relative to the modelled closure which has been used as a design parameter against seismicity.

This report showed no correlation between the 0.27m modelled closure determined by Scheepers et.al, (2012) for Mponeng mine to the estimated closure. Through (Scheepers et.al, 2012) work, it was also shown that the correlation of potency to modelled closure was only in the first 10000m² of mining a new raise line. Seismic potency is highly dependent on the seismic moment of a seismic event and the larger the event, the larger the seismic potency without any consideration to the mining layout.

The elastic modelled closure was found to be on average only 55.3% of the estimated closure. The MAP3D model only considered the elastic properties of the rock and did not take into account any discontinuities or non-homogeneity in the rock mass, hence the large difference to the measured closure. It is important to note that seismic potency and elastic closure modelled do not take into account critical factors that contribute to both rock mass deformation and seismicity in deep mines. More work is required to gain a better understanding on the correlation of rock mass deformation in ultra-deep mines to seismicity.

Of importance from the research is to acknowledge that the use of modelled elastic closure should always be supported with a good understanding of the actual rock mass behaviour. The elastic properties used in numerical modelling programs could be varied in such a way that the elastic modelling results can closely depict the actual rock mass behaviour in terms of closure. Accurate estimation of closure would be useful in the design of support systems and mining layouts in ensuring the stability of excavations for the required periods.

Closure can be estimated by conducting underground measurements and calculated by running numerical modelling programs. Better correlations between the two results would be possible once the elastic properties used in a model are varied until the results obtained from the model are similar to the underground measurements.

The inclusion of the backfill material into the elastic model has significant influence on the resultant closure. This was shown by varying the stoping width used in the model. In a pure elastic model without backfill the stoping width has no influence on the resultant modelled closure as it is evident in the elastic closure formula by (Malan, 2003) which does not take into account stoping width. Varying the poisson's ration has very little influence of the modelled closure while the adjustments to the young's modulus has a significant influence to the modelled closure.

ACKNOWLEDGEMENTS

First, I would like to pass my deepest appreciation to Thabo Semfeng (Rock Engineering Management Trainee at Mponeng mine) who assisted in gathering data and taking photos during underground visits and A.A. Steyn (Rock Engineering Manager, Mponeng Mine 2012-2014) who allowed me the time to conduct the investigation. I would also like to thank my supervisor Prof Halil Yilmaz who always availed himself for consultation and guidance and also pass my appreciation to the Mponeng Mine's rock engineering department for always willing to assist.

Lastly to my wife Keitsile Edith Rakumakoe, thank you for the support, believing in me and the endless inspiration, you made this research possible.

TABLE OF CONTENTS

CHAPTER 1. INTRODUCTION.....	1
1.1. Purpose of Study	1
1.2. Research Background/Context.....	1
1.3. Research Motivation	6
1.4. Problem Statement	6
1.5. Assumptions	6
1.6. Research Objective.....	6
1.7. Context of the Research Report	6
CHAPTER 2. LITERATURE REVIEW.....	8
2.1. Ultra-deep mining	8
2.2. Seismicity and mining	9
2.3. Energy Release Rate (ERR) as a design criterion	11
2.5. Sequential grid mining method	13
2.6. Stope closure (elastic convergence)	14
2.7. Aspects of closure in deep level hard rock mines,	17
2.7.1. Effects of rock mass properties and stress on closure	18
2.7.2. Effects of time on closure	21
2.7.3. Effects of support on closure	22
2.8. Correlation of seismic Potency and elastic closure	23
2.9. Closure monitoring and measurements	25
2.9.1. Estimation of the closure using the deformation of installed support.	26
2.10. Numerical modelling as a design tool	28
2.10.1. Numerical Modelling Methods	29
2.11. Conclusions	29
CHAPTER 3. EXPERIMENT AND DATA COLLECTION.....	30
3.1. Continuous closure monitoring instruments	30
3.2. Experiment site selection	31
3.3. Continuous closure monitoring at 104-65 Raise line (Site A) using closure loggers	34
3.4. Underground stope closure measurements using timber pack support.	37
3.4.1. 104-65 Raise Line Underground Measurements	37
3.4.2. 113-52 Raise underground measurements.....	39
3.4.3. 116-52 Raise Underground measurements.....	42

3.4.4.	120-36 Raise underground measurements.....	43
3.5.	Model building to simulate closure (Using MAP3D).....	44
3.5.1.	Experiment Model.....	47
3.5.2.	Modelled closure results per raise line assessed.....	49
3.6.	Analytical calculation of closure.....	53
CHAPTER 4. DATA ANALYSIS		55
4.1.	Underground measured closure.....	55
4.1.1.	116-52 Raise closure analysis.....	55
4.1.2.	104-65 Raise closure analysis.....	57
4.1.3.	113-52 Raise closure analysis.....	59
4.1.4.	120-62 Raise closure analysis.....	61
4.2.	Correlation between modelled closure and estimated closure	64
4.3.	Conclusions	65
CHAPTER 5. DISCUSSION OF RESULTS		66
5.1.	Elastic modelled closure vs estimated closure	66
5.2.	Correlation between estimated closure and modelled closure	68
5.3.	Influence of rock mass properties on closure.....	71
5.4.	Conclusions	72
CHAPTER 6. SUMMARY AND CONCLUSIONS.....		73
6.1.	Summary	73
6.2.	Conclusions	74
CHAPTER 7. RECOMMENDATIONS FOR FUTURE WORK.....		78
CHAPTER 8. References		79

LIST OF FIGURES

Figure 1. Cumulative seismic potency against area mined in square meters for the six raise lines used in the study (Scheepers et.al, 2012).	3
Figure 2. Cumulative seismic potency (calculated) vs cumulative production graph for the raise lines in the study. The thick black line is the average and the thin red line is the positive standard deviation (Scheepers et.al, 2012).	3
Figure 3. Combined modelled volumetric closure against area mined for the six raise lines (Scheepers et.al, 2012).....	4
Figure 4. Modelled closure for Mponeng VCR mining using MAP 3D. (Scheepers et.al, 2012)	4
Figure 5. Seismic events of magnitude 2.0 and larger for Mponeng Mine VCR mining since 1986. (Scheepers et.al, 2012).....	5
Figure 6. Plan view showing three raise lines a, b and c with raise a having the new design with strike pillars and b and c mined with the old design.....	5
Figure 7. Surface and subsurface distribution of the Witwatersrand Super Group, Dominion Group and Mesoarchean granite-greenstone basement domes. (Jooste, 2013)	9
Figure 8. The number of damaging bursts vs. ERR on the VCR and CLR for the period Jan. 1975 to Dec. 1976 (Spottiswoode et.al, 2000).....	11
Figure 9. A typical longwall mining layout. (Russo-Bello and Murphy, 2000).....	13
Figure 10. Sequential grid mining layout. (Ryder and Jager, 2002)	14
Figure 11. Stress around a deep level stope face. The deformation outside the fractured zone is elastic and in the fractured zone is inelastic. (Ryder and Jager, 2002).....	15
Figure 12. Incremental enlargement of a parallel sided stope panel. It is assumed that both sides of the stope are mined simultaneously (Ryder & Jager, 2002).....	17
Figure 13. Creep rate versus axial stress for quartzite and lava (Drescher and Handley, 2003)	18
Figure 14. Fracturing in bedded rock mass around a tabular stope with backfill (Kirsten and Stacey, 1988).....	20

Figure 15.	Typical continuous stope closure after blasting and the definition of closure terms (Malan, 2003).....	21
Figure 16.	Stress – strain graphs of different backfill tests at different porosities (Ryder and Jager, 2002).....	22
Figure 17.	Detailed view of the raise lines used in the back analysis (Scheepers et.al, 2012).	24
Figure 18.	Schematic of the four-peg closure/ride station (Ryder and Jager, 2002).....	25
Figure 19.	Idealized closure monitoring system with a closure logger in every panel (Malan, Kononov, Coetzer, Janse van Rensburg, & Spottiswoode, 2000).....	26
Figure 20.	Timber packs deformation due to stope closure in the back area.	28
Figure 21.	Rockwatch Logger and accessories used in monitoring closure, (Groundwork, 2013). (A) Rockwatch logger, (B) Grabber and (C) PC with Rockwatch software.	31
Figure 22.	Plan view of Mponeng mine indicating experiment sites: A) 104-65 Raise. B) 113-52 Raise. C) 116-52 Raise. D) 120-36 Raise.....	32
Figure 23.	Plan view of 104-65 (A), 113-52 Raise (B), 116-52 Raise (C) and 120-36 Raise (D) with the gullies to be measured.	33
Figure 24.	Position of the closure loggers in the 104-65 W9 panel. (1) Logger 260, (2) Logger 671, (3) Logger 877.....	34
Figure 25.	Logger 260 installed on the North shoulder of the W9 cleaning gully.....	35
Figure 26.	Closure readings from three closure loggers installed at 104-65 raise between 12 November 2012 to 08 January 2013.	36
Figure 27.	104-65 experiment site and MRM mapping results in the W10 panel.	37
Figure 28.	Closure observed on timber pack in the 104-65 W9 cleaning gully.....	38
Figure 29.	Closure observed on timber pack and elongates in the W11 cleaning gully.	39
Figure 30.	Closed gully shoulders and highly deformed timber packs in the W10 gully. ...	39
Figure 31.	113-52 experiment site.....	40
Figure 32.	Photos of the E8 gully cleaning gully showing deformed support	41
Figure 33.	View into E7 stope from the E7 cleaning gully and view of the E7 gully.	41

Figure 34.	Highly deformed timber pack in the E6 gully and almost complete closure into the E6 stope.	41
Figure 35.	116-52 experiment site indicating the points where measurements were taken.	42
Figure 36.	120-36 experiment site indicating the points where measurements were taken	43
Figure 37.	Minimal deformation observed on the packs in the W6 cleaning gully.	44
Figure 38.	Little signs of deformation on the timber packs in the W7 cleaning gully.....	44
Figure 39.	Closure in the stopes using element size of 20m.	46
Figure 40.	Closure in the stopes using element size of 10m.	46
Figure 41.	Stress state used in the model and the elastic rock properties for quartzite rock.	48
Figure 42.	The elastic rock properties for shale and the material properties of the backfill material.	48
Figure 43.	Points where modelled closure was measured similar to underground in 120-36 raise line.	49
Figure 44.	Modelled closure with points where measurement were taken in 116-52 raise line.	50
Figure 45.	Modelled closure with points where measurements were taken in the 113-52 raise line.	51
Figure 46.	Modelled closure 104-65 raise line with poits where measurements were taken.	52
Figure 47.	Closures determined at each point in 116-52 raise.	56
Figure 48.	116-52 raise layout indicating the position of the W6 and E4 gullies, with the E4 gully closer to the abutment.	57
Figure 49.	Closures determined at each point in 104-65 raise.	58
Figure 50.	Layout of the 104-65 raise indicating the measured points in the W11, W10 and W9 gullies relative to the centre.	59
Figure 51.	Closures determined at each point in 113-52 raise.	60

Figure 52. Layout of the 113-52 raise indicating the measured points in the E8, E7 and E6 gullies relative to the centre.	61
Figure 53. Closures determined at each point in 120-36 raise.	62
Figure 54. Layout of the 120-36 raise indicating the measured points in the W6 and W7 gullies relative to the centre.	63
Figure 55. Frequency distribution graph of the difference between modelled closure and estimated closure.	65
Figure 56. Modelled closure at the same points in 113-52 raise line as closure estimations .	66
Figure 57. Cross section A-A of an elastic closure model.	67
Figure 58. Typical fracturing and discontinuities formed around a tabular stope in deep mines (Napier et.al, 1998).	67
Figure 59. Mining sequence in a sequential grid raise line.	68
Figure 60. Photo of the 104-66 Raise. The pack on the raise shoulders were installed with a full cut ledge at 2.4m high and currently measure only 0.5m in height.	70
Figure 61. Closure in one of the strike gullies on the Eastern side of the 104-66 raise line.	71
Figure 62. Calibration results for 116-52 raise line.	76
Figure 63. Calibration results for 113-52 raise line.	77

LIST OF TABLES

Table 1.	Different parameters used in mine design and the values according to mining depth (Jager and Ryder, 1999).	16
Table 2.	Uniaxial compression creep test results (Drescher and Handley, 2003)	19
Table 3.	Experiment sites and their different environment.	32
Table 4.	Closure monitoring result from 104-65 raise line.	36
Table 5.	104-65 stope closure measurement results.	38
Table 6.	113-52 stope closure measurement results.	40
Table 7.	116-52 stope closure measurement results.	42
Table 8.	120-36 stope closure measurement results.	43
Table 9.	Modelled results of 120-36 raise at indicated points in Figure 42	49
Table 10.	Modelled closure results for 116-52 raise	50
Table 11.	Modelled results for 113-52 raise at indicated points in Figure 44	51
Table 12.	Modelled closure results of 104-65 raise at indicated points in Figure 45.	52
Table 13.	Mechanical properties of the quartzite and shale rock used in the calculations.	53
Table 14.	Calculated convergence at each experiment point per raise line.	53
Table 15.	Input parameters used in the calibration exercise.	76

LIST OF ACRONYMS

AGA	AngloGold Ashanti
BEM	Boundary element method
CLR	Carbon leader reef
ERR	Energy release rate
FOG	Fall of ground
MRM	Mineral resource management
RMR	Rock mass rating
SW	Stoping width
VCR	Ventersdorp contact reef

CHAPTER 1.INTRODUCTION

1.1. Purpose of Study

With the gold reserves remaining in the Wits basin laying deeper into the earth's crust, new methods must be developed to address challenges arising with the increasing depth. The depths being planned for mining in the future, if South Africa is still to be a major role player in the gold production, are the depths that could not be imagined five decades ago. This study will probably be one of the many studies to come as South African gold mines surge deeper to access reserves and continuously aim for safer operations. The purpose of the study is to compare the elastic modelled closure to the closure estimated from underground observations and measurements.

1.2. Research Background/Context

Mponeng mine currently holds the record of being the World's deepest mine operating at depths of between 2,400m and 3,900m (AngloGold Ashanti, 2013). The mine is located near Carletonville approximately 80km from the City of Johannesburg. Two main economical reefs can be found in the mine's lease area, being the Ventersdorp Contact Reef (VCR) and the Carbon Leader Reef (CLR). Mponeng Mine was commissioned in 1986 and has up to date only mined the VCR as this is intersected earlier and the CLR is only intersected at 3600m depth within the lease area.

The upper most VCR was mined using a long wall mining method without backfill up to 89 level at 2700m depth. The mining method was changed to sequential grid with backfill from 89 level to the lowest 120 level at 3400m depth. The change of mining methods will be discussed section 2.4 of this report. With the mining getting deeper, the seismic activity on the mine also increased. The introduction of pre-conditioning methods saw a significant decrease in seismic related accidents and incidents particularly face bursting. (Mahne, 2004)

Scheepers et.al, 2012, conducted back analysis to see the influence of the current design and mining method to the seismic activity being experienced. From the numerical modelling back analysis conducted in six different raise lines (Figure 1) it was determined that the current mine design experienced hazardous levels of seismic potency when cumulative seismic potency is $>1100\text{m}^3$ and the area mined $>30\,000\text{m}^2$ (Figure 2). They concluded that the modelling of the

six raise lines and the resulting cumulative average volumetric closure corresponds with the area mined (Figure 3). The slope of the volumetric closure vs area mined graph matched that of cumulative seismic potency vs area mined. The slope in Figure 3 at 30 000m² is 0.27m which is the average modelled closure (Scheepers et.al, 2012). This indicated that when the modelled closure exceeds 0.27m, hazardous levels of seismicity would be experienced, hence the 0.27m modelled closure became the design parameter to maintain acceptable levels of seismicity. Following this assessment, they also recommended that the modelled closure can be kept below 0.27m by introducing 30m wide strike pillars after every 100m on dip in a raise line.

The correlation between the closure and the seismicity can be demonstrated by Figure 4 which is the modelled closure and Figure 5 which is the seismic events of magnitude 2 and above at Mponeng Mine since 1986. In Figure 4 the warmer colours indicate higher closure values and the grey represent closure in excess of 0.5m in the absence of backfill. The events in Figure 5 are represented by spheres with size and colour scaled to magnitude (warmer colours indicate larger events) (Scheepers et.al, 2012). The area on the mine with the highest modelled closure also has a high number of seismic events.

The current design calls for 180m between dip stabilizing pillars of 30m width. One side of the raise is mined first up to the pillar position and during this stage the seismic response is very low. When the opposite side is mined up to the pillar position with the span being extended to its maximum length of 180m the seismic response increases and larger magnitude events are experienced. (Scheepers et.al, 2012). In most cases the final ground close to the pillar (+/-10m) is lost due to increased seismic activity and bad ground conditions. Figure 6 shows lost ground close to the final pillar position.

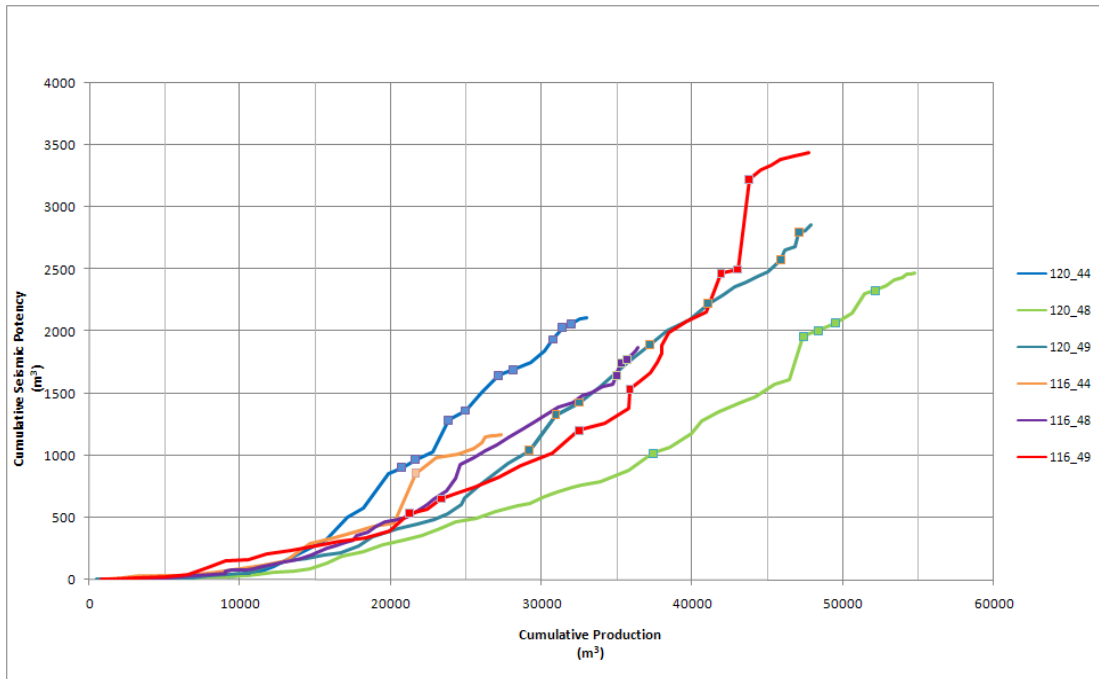


Figure 1. Cumulative seismic potency against area mined in square meters for the six raise lines used in the study (Scheepers et.al, 2012).

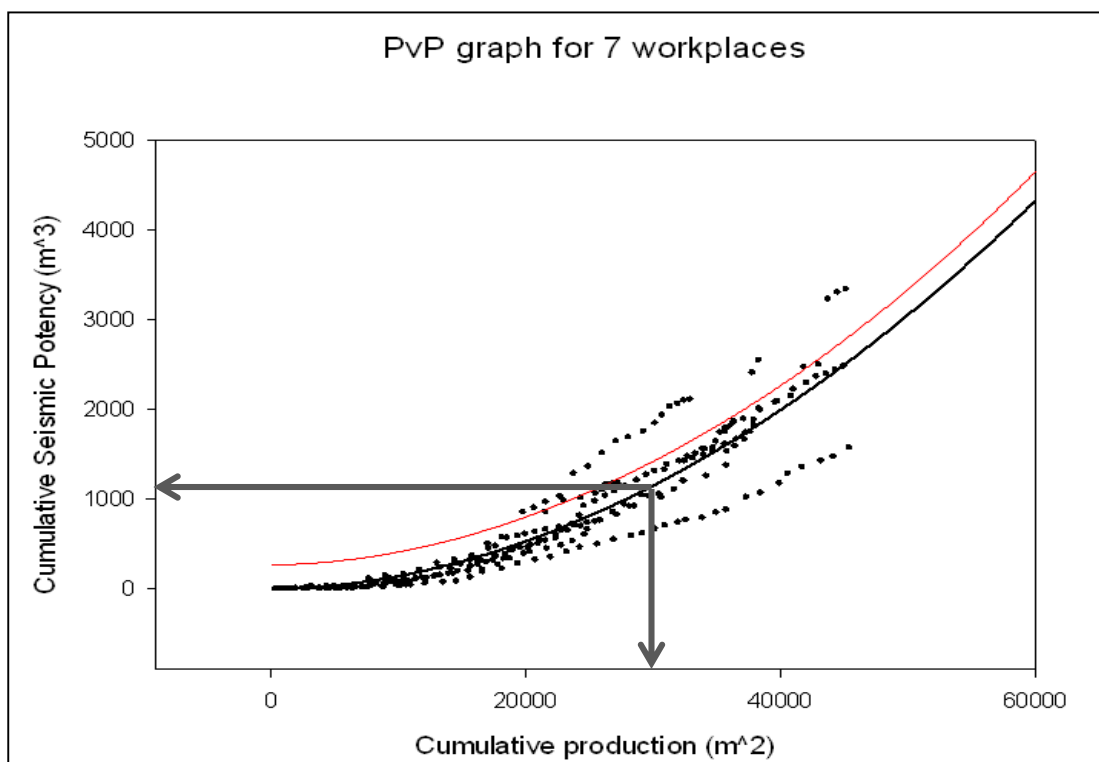


Figure 2. Cumulative seismic potency (calculated) vs cumulative production graph for the raise lines in the study. The thick black line is the average and the thin red line is the positive standard deviation (Scheepers et.al, 2012).

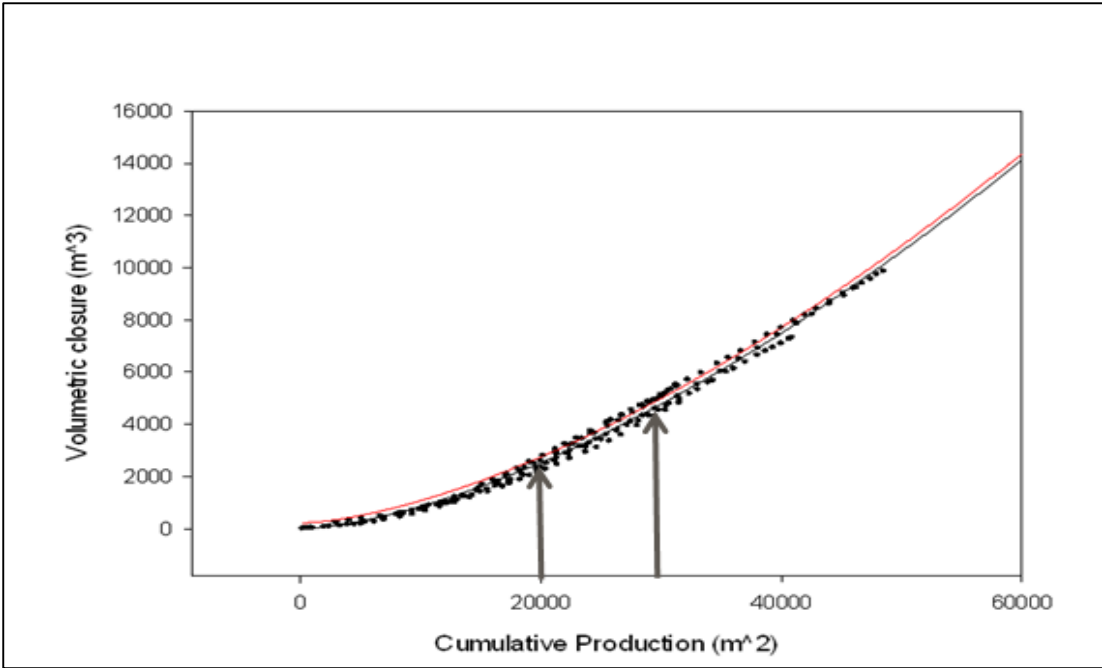


Figure 3. Combined modelled volumetric closure against area mined for the six raise lines (Scheepers et.al, 2012).

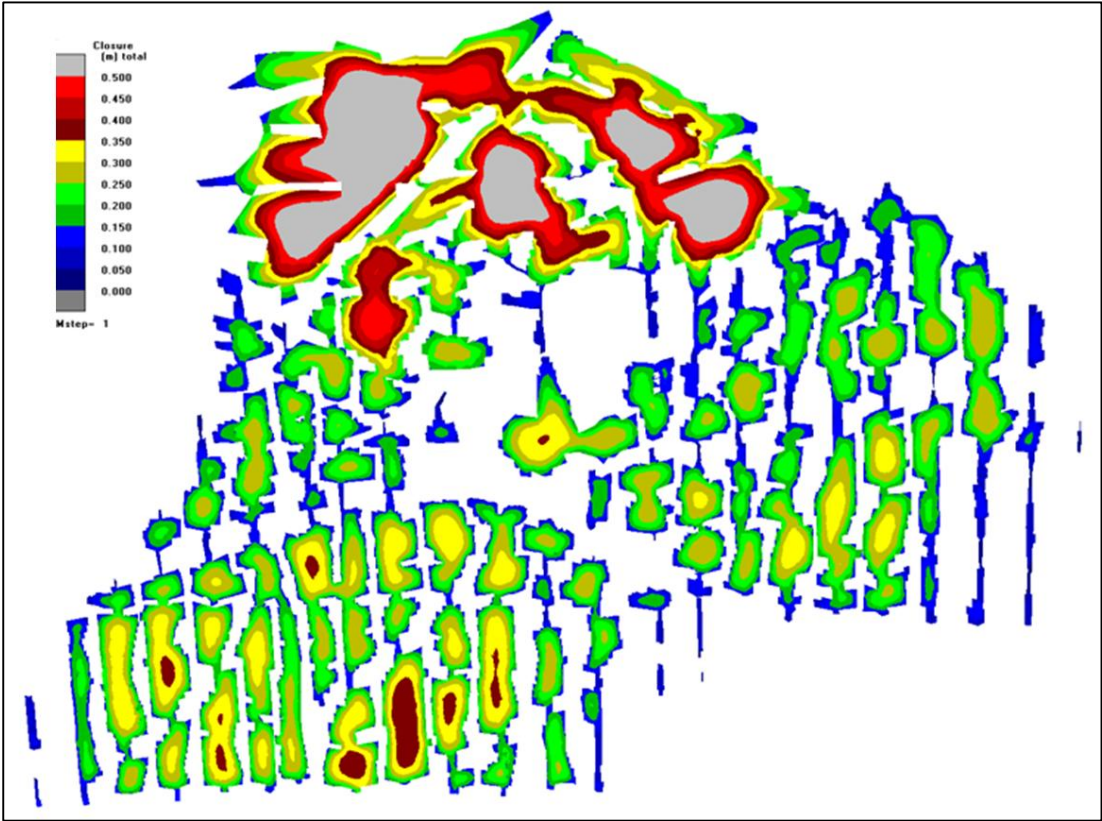


Figure 4. Modelled closure for Mponeng VCR mining using MAP 3D. (Scheepers et.al, 2012)

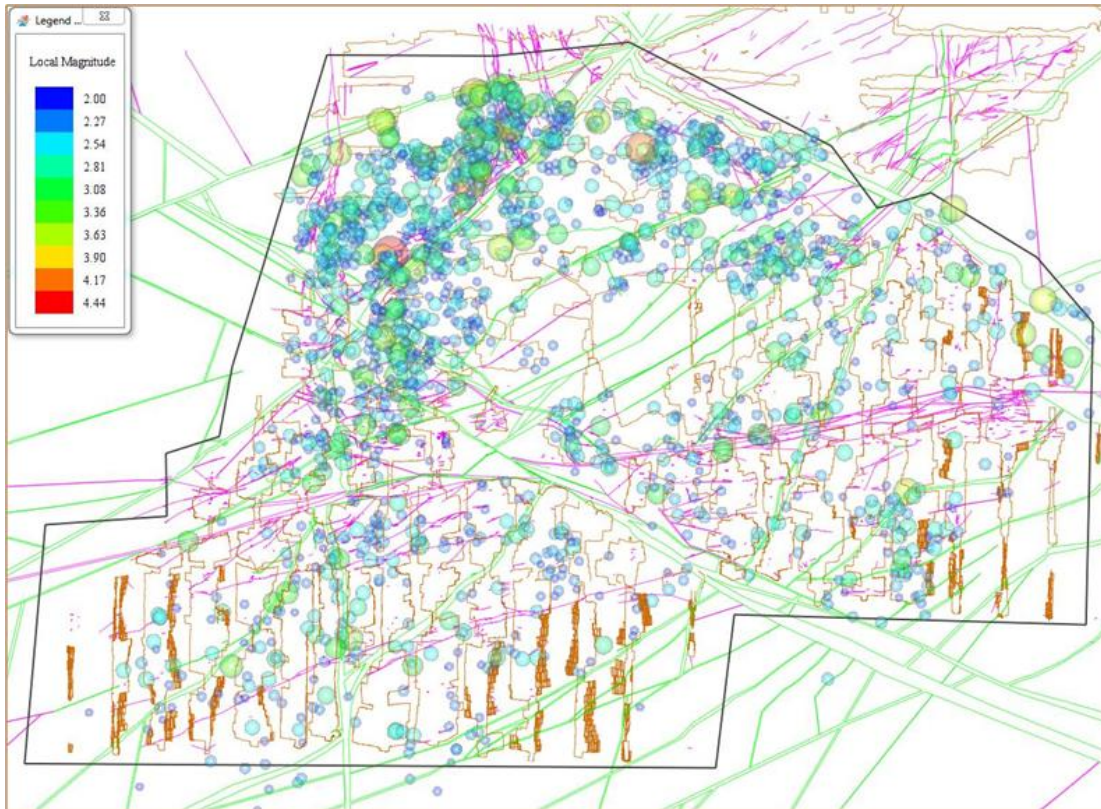


Figure 5. Seismic events of magnitude 2.0 and larger for Mponeng Mine VCR mining since 1986. (Scheepers et.al, 2012)

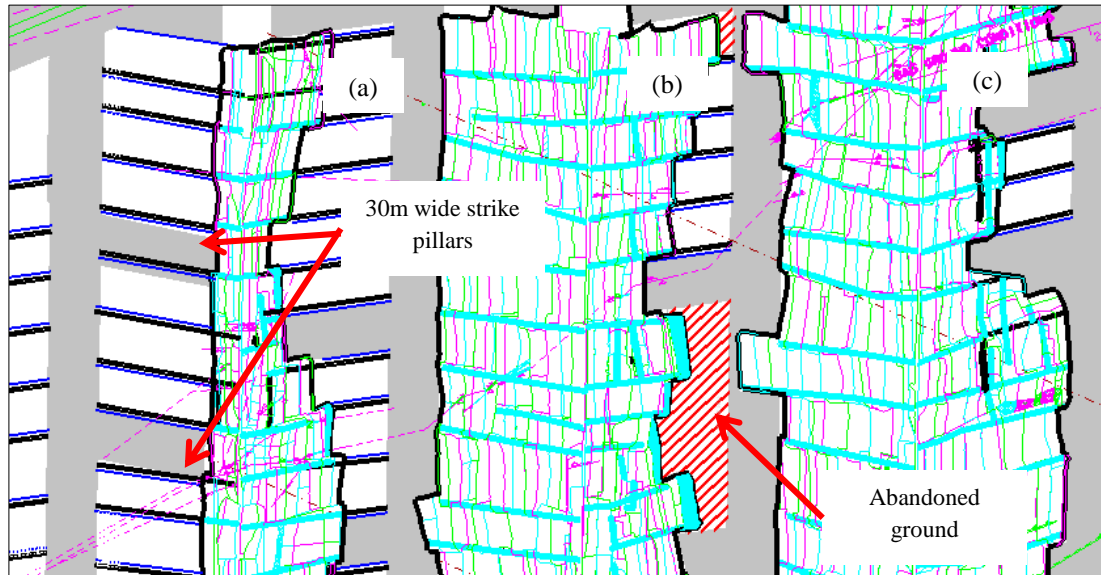


Figure 6. Plan view showing three raise lines a, b and c with raise a having the new design with strike pillars and b and c mined with the old design.

1.3. Research Motivation

The inclusion of the strike stabilizing pillars is intended for reducing closure. However this only speaks to the modelled closure and not the underground closure. This brought an opportunity to further refine the use of the modelled closure to also represent the anticipated underground closure. This research attempts to compare the estimated closure underground to the elastic modelled closure. Adjustments in the modelling parameters would enable better correspondence with the estimated closure. The use of modelled closure would then give a good indication of the anticipated rock mass deformation underground.

1.4. Problem Statement

The 0.27m modelled closure recommended by Scheepers et.al, (2012) was not based on underground measurements but purely on the elastic properties of the rock mass. Scheepers et.al, (2012), used the elastic modelling program MAP3D to determine the closure in the mined out area and compared it to the seismic response. The underground environment does not behave elastically and this will present a challenge as the elastically modelled closure will differ from the actual closure. This then brings a question that: How does the elastically modelled deformation (closure) compare to the actual underground closure?

1.5. Assumptions

In order to obtain meaningful results and analysis from this research the following basic rock mechanics assumptions must be applied in numerical modelling.

- The rock mass is isotropic and continuous
- The stress is distributed evenly throughout the mine.
- The backfill has the same properties at its placement.

1.6. Research Objective

The main objective of this research project is:

- To compare the elastic modelled closure to the estimated underground closure

1.7. Context of the Research Report

The research report is presented in seven chapters including the introduction chapter. The chapters are sequenced to enable follow of the thought process and understanding to the reader.

The first chapter with the research work (Chapter 2) is the literature review. The literature review chapter sets the context of the research, looking at similar work that has been done in the past in order to gain better understanding of the subject. The chapter focuses on understanding rock mass deformation “closure” and what are the main contributing factors and how they contribute to the closure. The chapter also covers the correlation of closure to seismicity and the assumptions applied in the determination of the elastic closure modelled to represent seismic hazard. Furthermore the chapter discusses the different methods used in measuring closure and how numerical modelling is used to estimate closure.

Chapter 3 is research field work and data collection for the project. This chapter covers the process and methods used to measure observed closure underground and how the numerical models were configured and run. The results are presented in this chapter.

In Chapter 4 the results and observation in Chapter 3 are analysed to assess the correlation between observed and estimated underground closure with the numerical modelling closure. Chapter 5 discusses the findings in Chapter 4 and elaborates on the factors that could have contributed to the findings and how these findings influence the understanding on rock mass deformation in ultra-deep mines.

Chapter 6 is the summary and conclusions which briefly describes the steps followed in the research and the outcomes in each step. Then final conclusions are provided with regards to the set objectives of the research. Chapter 7 gives recommendations for further work that can be carried out regarding the subject to gain a better understanding on the use of elastic numerical modelling to represent inelastic rock mass deformation.

CHAPTER 2. LITERATURE REVIEW

The aim of the literature review was to gain an understanding on the challenges faced with designing layouts for ultra-deep mines and to understand the main objectives of these layouts. This understanding would enable to assess which parameters are suitable for design of layouts. It would also enable the assessment of the practicability of using elastically modelled closure to represent underground closure. The first part of the literature review looks at the history of gold mining in South Africa leading to the current ultra-deep mines faced with the challenge of mining induced seismicity. Then the review looks at the mining methods that have been developed and employed in the past to manage seismicity such as sequential grid mining method and the parameters that were used in the design of these mining layouts, specifically the Energy Release Rate (ERR). A review on the correlation of seismicity and the rock mass deformation, forms a base for assessing the correlation of elastically modelled closure to modelled closure due to seismic failure.

The review covers the different deformation monitoring methods and their limitations. Finally it looks at the use of elastic numerical modelling codes, specifically MAP3D, for use in inelastic rock mass environment.

2.1. Ultra-deep mining

The gold bearing reefs of the Witwatersrand (Figure 7) were not always at great depths as they are currently found. The discovery of gold in 1886 saw the development of what came to be known today as the city of gold, Johannesburg. Mining started near the present-day Johannesburg in the gold bearing reef outcrops. As the mining stopes extended deeper and reached depth of several hundred meters, the first mining-induced seismicity and its hazardous manifestation, rock bursting, were encountered in the early 1900s. (Durrheim, 2010)

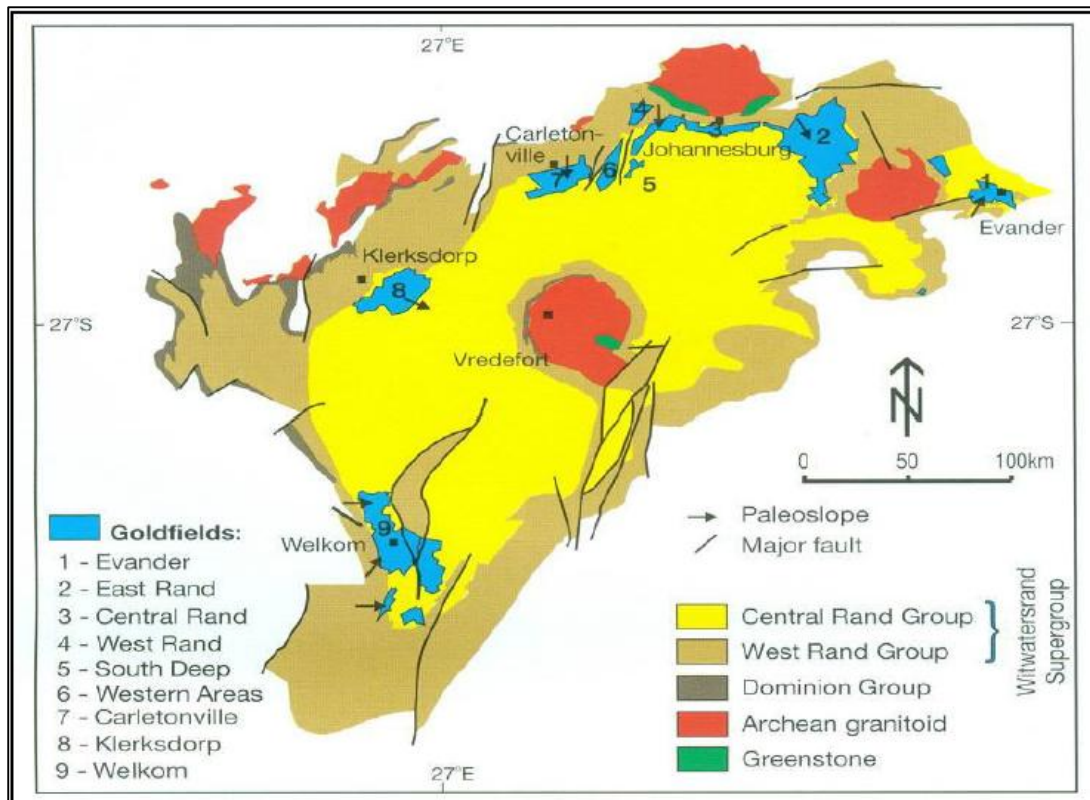


Figure 7. Surface and subsurface distribution of the Witwatersrand Super Group, Dominion Group and Mesoarchean granite-greenstone basement domes. (Jooste, 2013)

2.2. Seismicity and mining

Since the first encounter of mining induced seismicity there have been several committees created to determine the source and the cause of the earth tremors and develop ways to mitigate the hazards associated with seismicity. Research work over the years has focused on three main areas:

- (i) development of macro-layouts (e.g. sequential grid) and regional support (e.g. backfilling) to control the release of seismic energy through the geometry and sequence of mining. The released seismic energy is proportional to the released seismic moments;
- (ii) development of support units and systems to limit rock burst damage; and
- (iii) mine seismology, which seeks to develop techniques to continually assess the seismic hazard and control seismic activity (e.g. through the rate of mining). (Durrheim, 2010)

The history of the South African deep level hard rock mining and its challenges with seismicity is well summarized by Durrheim, (2010). This report came about in an attempt to manage and reduce seismicity occurring in the stope. In this section the aim is to show the relationship between closure and the seismic activity.

The mining taking place in the Wits basin is referred to as tabular narrow reef mining due to the narrow gold bearing conglomerate reefs. Mining generally advanced in the strike direction creating large spans and as mining followed the reef deeper the seismicity problem began to manifest itself both on surface as damage to civil engineering structures, buildings or houses and underground as collapse or damage of mine workings (Riemer and Durrheim, 2012). Seismic event occurring on mines have been grouped into two source mechanism, the crush type events and the shear type events.

For both of these mechanisms to occur the following conditions must exist; a substantial zone of overstressed rock must exist in a state of unstable equilibrium, a sufficient change in stress must take place and lastly the failure structure must undergo a significant and sufficiently rapid stress drop (Jager & Ryder, 1999). These conditions generally exist underground in the areas such as ahead of the advancing stopes face, pillars created in the stope, abutments and geological structures. These areas are the main sources of seismic events. Continuous closure monitoring conducted in deep stopes has shown that large seismic events are accompanied by significant stope closure (Jager & Ryder, 1999).

In the introduction it was shown how seismic potency was correlated to closure. Scheepers et.al, (2012) attempted to show this correlation by comparing the area mined with modelled closure volume then comparing area mined with seismic potency. From this comparison of both modelled closure and seismic potency to mined volume, they drew a correlation between seismic potency and closure.

Seismic potency represents the volume of rock, of whatever shape, associated with co-seismic inelastic deformation at the source. Potency refers to the strain change at the source and the source volume (Mendecky et.al, 2010). Potency is a volume measure hence it could be compared to production volume. The seismic potency is calculated as: (McGarr, 1976)

$$P = M/G \tag{1}$$

Where: M is the Seismic moment (MJ) and G is the Modulus of Rigidity (GPa)

2.3. Energy Release Rate (ERR) as a design criterion

ERR has been one of the most commonly used tool for designing mining layout for deep and ultra-deep mines (>3500m deep). The concept was introduced in the early 1960s as a measure to calculate the stress and energy changes around the tabular mining stope (Jager and Ryder, 1999). ERR is simply defined as the one half of the potential energy that is created during removal of rock per unit face area mined. The one half is stored in the rock mass as strain energy and the other half is released in the form of shearing/crushing/heating of the fracture zone in front of the face and the rate at which the latter is released is referred to as the energy release rate (ERR) and determined from equation 2 below. (Jager & Ryder, 1999)

$$ERR = \frac{1}{2} \sigma^p S^p \text{ (MJ/m}^2\text{)} \quad (2)$$

Where: S^p is the closure measured at the centre of the stope

σ^p is the resultant stress due to mining.

It is important to note that ERR is not a direct expression of seismicity. Most of the energy realised is released a-seismically in the mechanisms described above. However Spottiswoode et.al, (2000) carried out studies in deep level longwall mining and observed a positive correlation between ERR and occurrence of seismic damages in stopes. Figure 8 shows the correlation obtained by Spottiswoode et.al, (2000) with a clear distinction between the two different environments and that a higher ERR translates to increased seismic damage.

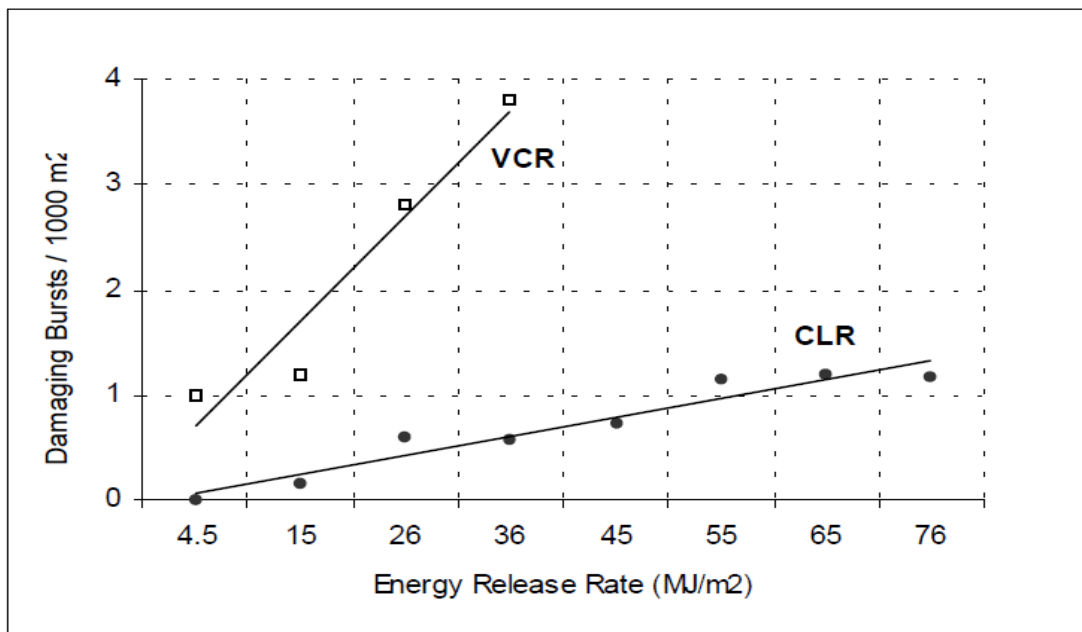


Figure 8. The number of damaging bursts vs. ERR on the VCR and CLR for the period Jan. 1975 to Dec. 1976 (Spottiswoode et.al, 2000)

Most of the data was gathered when the support system and mining layouts were different from today. The use of pillars was not as extensive as it is today and backfill was not used. Today almost 80% of the geological structures are left with bracket pillars around them reducing seismic events occurring along these structures and pillars (Spottiswoode et.al, 2000). With the current mining methods, the correlation between ERR and seismicity does not hold and in his report Lachenicht, (2001) looks at what other parameters that are best suited for the current mining and support systems. Spottiswoode et.al, (2000) also agrees with Lachenicht, (2001) that for the current mining systems, a more detailed mechanistic relationship between rock mass deformation and seismicity is required than that provided by ERR.

2.4. Ultra deep mining Methods

The mining methods used in ultra-deep mining are centred on the same principles, which are to minimize the mining span, reduce total closure and maintain average ERR on the mining face. Western Deep level mines have always employed the longwall mining method. Tau Tona mine stopped the use of longwall (Figure 9) with strike stabilizing pillars spaced 240m apart in 2010. (Russo-Bello and Murphy, 2000). These stabilizing pillars form one of the main components of the strategy to reduce ERR and the number of seismic events.

Seismic events are mainly associated with the mining faces and the presence of geological structures ahead of the advancing longwall (Russo-Bello & Murphy, 2000). It is thought that the two main attributes of strike stabilizing pillars are to reduce the longwall span, effectively reducing closure, and their role in ‘clamping’ the surface of a potential slip at intervals along its length. (Russo-Bello and Murphy, 2000).

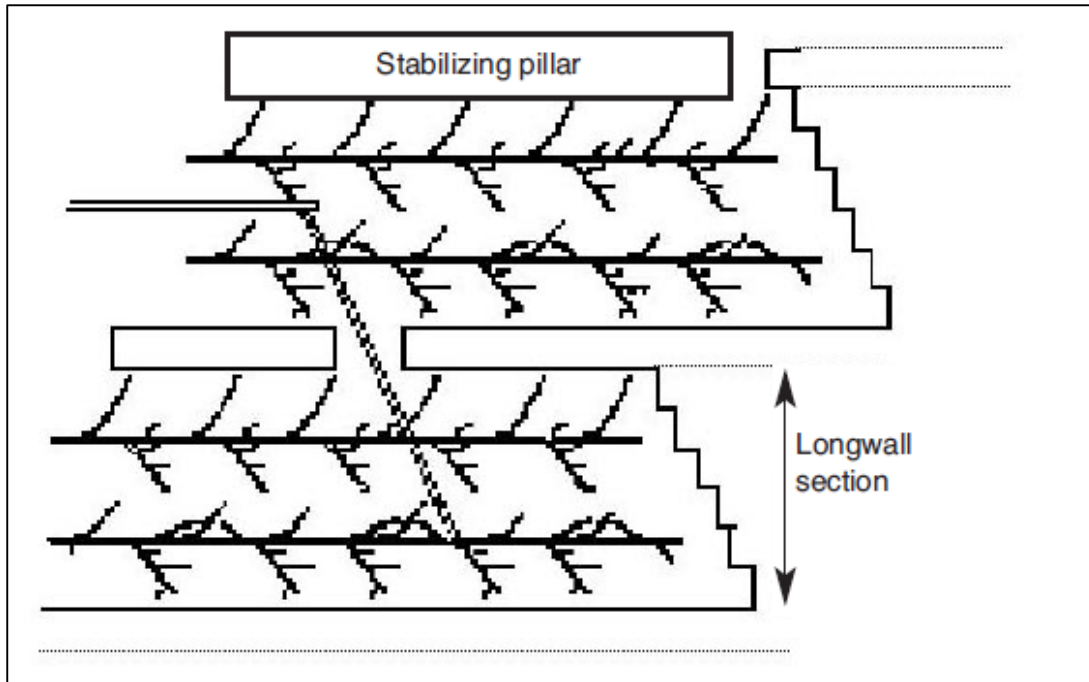


Figure 9. A typical longwall mining layout. (Russo-Bello and Murphy, 2000)

The favoured orientation of stabilizing pillars has changed from strike to dip, with the predevelopment of tunnels allowing hazardous structures to be detected and bracket pillars to be planned prior to stoping (Durreheim et.al, 2005). This method is referred to as the sequential grid.

2.5. Sequential grid mining method

During the development of sequential grid mining (Applegate, 2001) as mentioned by Handley et.al, (2000) showed that the ERR peak could be kept at acceptable levels by implementing a proper sequence of mining where stope spans were kept to a minimum. ERR has been used as the measure of ground conditions and seismic response in the development of sequential grid in Figure 10.

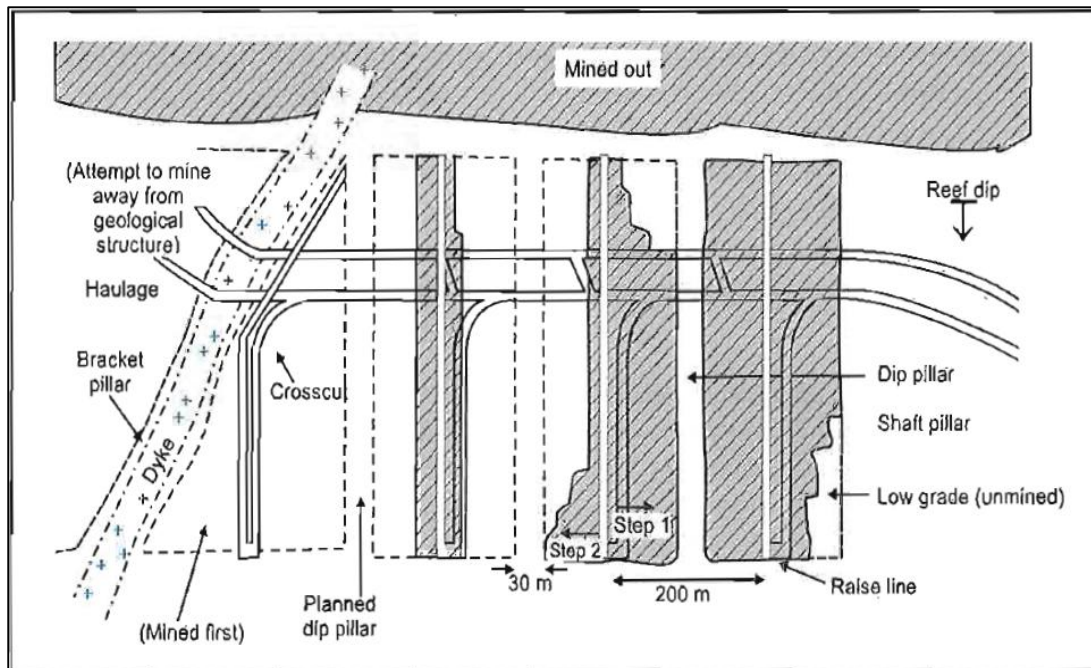


Figure 10. Sequential grid mining layout. (Ryder and Jager, 2002)

In their work on Mponeng Mine (Scheepers et.al, 2012) showed that there is correlation between seismic potency and modelled closure. Scheepers et.al, (2012) then concluded that seismic hazard is directly related to the closure volume or mining volume. Therefore closure needs to be reduced to reduce the seismic hazard (Scheepers et.al, 2012). By doing so they moved away from using ERR and other design parameters and focused on closure in the design of mining layouts. It is important to note that closure is an integral part of ERR, but unlike ERR, closure can be monitored and measured to correlate to the seismic response.

2.6. Stope closure (elastic convergence)

In deep level mines the rock mass is under compression and is said to behave elastically (Ryder and Jager, 2002). When mining takes place and there are small spans created in the stope, the rock mass is allowed to relax and the deformation taking place is referred to as elastic convergence. As mining spans increase the fractured zone around the stope increases and the back area of the stope is in the de-stressed zone. According to Ryder and Jager, (2002) the deformation taking place in this zone is of inelastic nature and this results in closure occurring behind the face. Malan, (2003) described closure as the sum of the convergence and inelastic movements caused by fracturing and the slip and opening of discontinuities such as bedding planes. Figure 11 below shows closure occurring behind a stope face in the fractured zone.

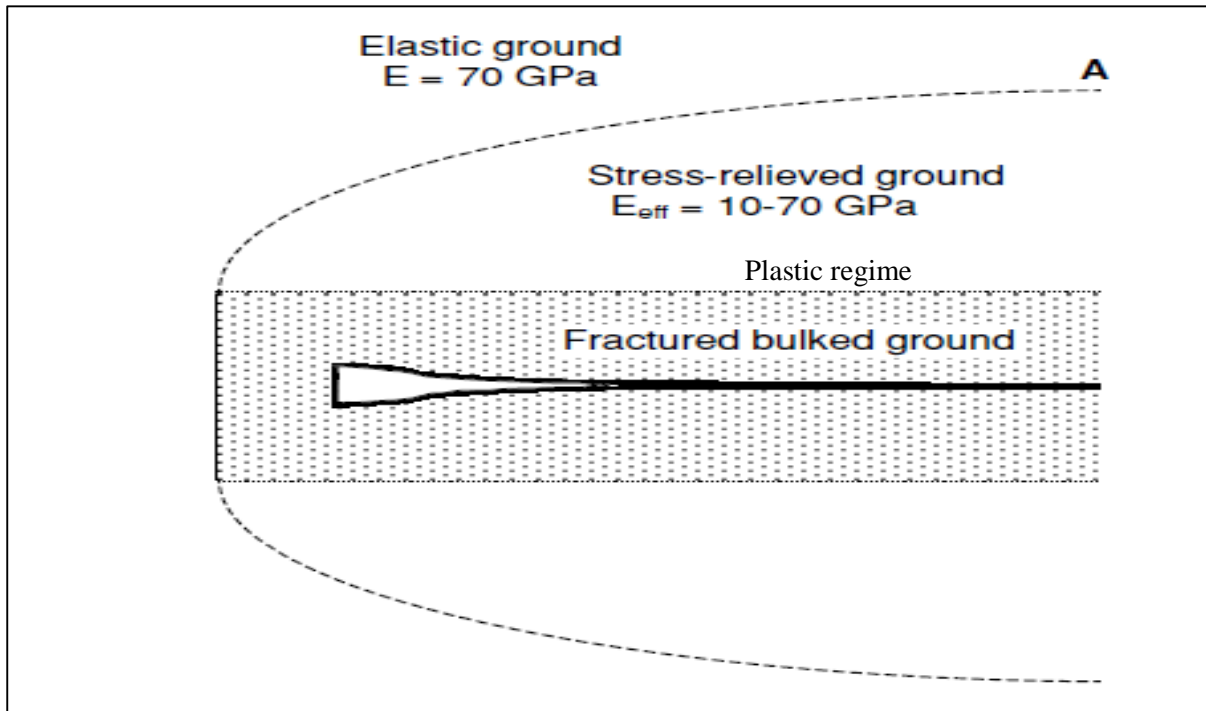


Figure 11. Stress around a deep level stope face. The deformation outside the fractured zone is elastic and in the fractured zone is inelastic. (Ryder and Jager, 2002)

Closure can be broken into different components to describe the type of closure that is occurring. Some types of closures are time dependent closure, steady state closure and primary closure. The main differences between these closures are their time and rate of occurrence (Malan, 2003). This research report focuses mainly on the combination of these closures in the stope as this is said to be the main factor to mining induced seismicity and stope closure.

According to Milev and Spottiswoode, (1997) seismicity in deep level stope is influenced by the amount of the rock mass deformation. This was after Cook et.al, (1966) statement that the seismic energy is influenced by the volumetric closure of the excavation, taking into account the following factors:

- i. the mining method;
- ii. the amount of mining;
- iii. the geological setting; host rock types and structures and;
- iv. the virgin stress field prior to mining; including the depth.

The volumetric closure takes into account the three dimensional displacement of the rock mass which is not possible to measure underground. The closure is one dimension of the volumetric closure and this can be measured and quantified in the stopes. Table 1 shows the stope closure rates at different depths.

The mine designs and mining strategies with increasing depth have over the years been changed and altered with the aim of reducing the closure and in turn reducing seismic activity. Some of the changes include the development of the sequential grid mining method and the installation of backfill. This report also came about as a result of such an attempt to reduce closure with adjustments to existing mining layouts.

Table 1. Different parameters used in mine design and the values according to mining depth (Jager and Ryder, 1999).

Parameter	Shallow	Medium	Deep	Ultra-deep
Typical depth (m)	<1000	1000 - 2250	2250 - 3500	>3500
Typical ERR (MJ/m ²)	<8	8 – 40	40 – 80	>80
Vertical virgin stress (MPa)	<25	25 – 60	60 – 95	>95
Stress fracturing	Little/None	Moderate	Deep	V.Deep
Stope closure (mm/m advance)	Low (<10)	Mod.(10-30)	High(30-60)	V.High(>60)
Infl. of geology on h/w stability	Strong	Moderate	Moderate	Moderate?
Possible extent of FOG's	Can be large	Often small	Usually small	Small?
Rockburst hazard	Minimal	Mod.-Severe*	Severe*	V.Severe*?

Mathematical solutions to determine closure have also been developed over the years. Budavari, (1983) gave a simplified form of the well-known two dimensional elastic convergence solution which was first introduced by Salamon, (1968). The solution gives the convergence for a stope of half-span L for cases where there is no total closure in the back area assuming that the entire span was mined in a single step. Malan, (2003) modified the solution to allow the determination of the total closure measured at a specific point within the stope with incremental increases in span. The solution below (equation 3) represents the closure at a point.

$$\Delta S^T = \frac{4(1-\nu^2)W_z}{E} \left[\sqrt{(L+n\Delta\ell)^2 - x^2} - \sqrt{L^2 - x^2} \right] \quad (3)$$

for $x \leq L$ and

$$W_z = \rho g H$$

Where L is the length of a half span per specific raise line, X is the point where measurements are taken, $2L$ is the span of the stope, ρ is the density of the rock, g is gravitational acceleration, H is depth below surface, ν is Poisson's ratio, and E is the Young's modulus.

As X is the distance from the centre of the stope, the distance from the measuring position to the face is given by

$$d = L + n\Delta\ell - x \quad (4)$$

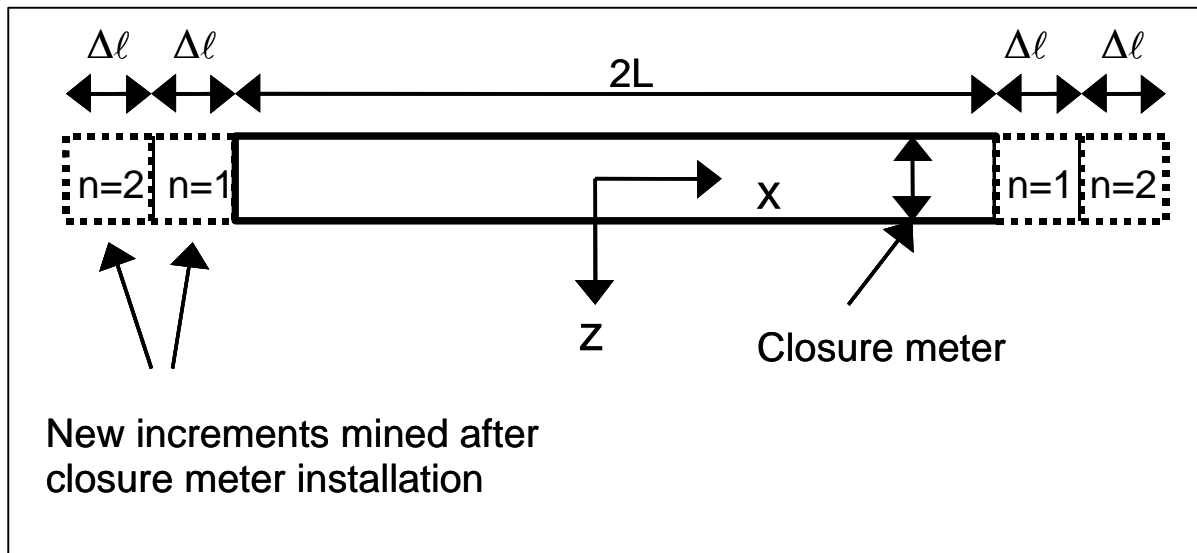


Figure 12. Incremental enlargement of a parallel sided stope panel. It is assumed that both sides of the stope are mined simultaneously (Ryder & Jager, 2002).

2.7. Aspects of closure in deep level hard rock mines,

The closure measured in the stope is a function of different factors of which some of them have been discussed in Section 2.6 above. Closure increases over time in an active mining stope even in area where mining has been stopped. This indicates that closure is not only driven by increasing mining span but there are also other factors at play. In this section the focus will be drawn to the effects of rock mass properties (intact properties and discontinuities), resultant field stress, time and the support installed in the mined area.

2.7.1. Effects of rock mass properties and stress on closure

It has been shown through many laboratory tests that different rock samples exhibit different behaviour. Most of the rock mechanics data used in mine design is derived from laboratory tests. In trying to understand rock mass deformation in underground excavations laboratory creep test has been conducted on different rock samples. Creep is defined as the continued deformation of intact rock specimen or single discontinuities due to a constant applied force over an extended period of time (Napier et.al, 1998). From creep tests conducted on quartzite and lava rocks (Drescher and Handley, 2003), there was a clear difference in deformation behaviour of the two rock samples. Figure 13 shows the creep rates of the two rock samples with quartzite having almost three times the creep rate of lava at only a third of the stress applied to the lava sample.

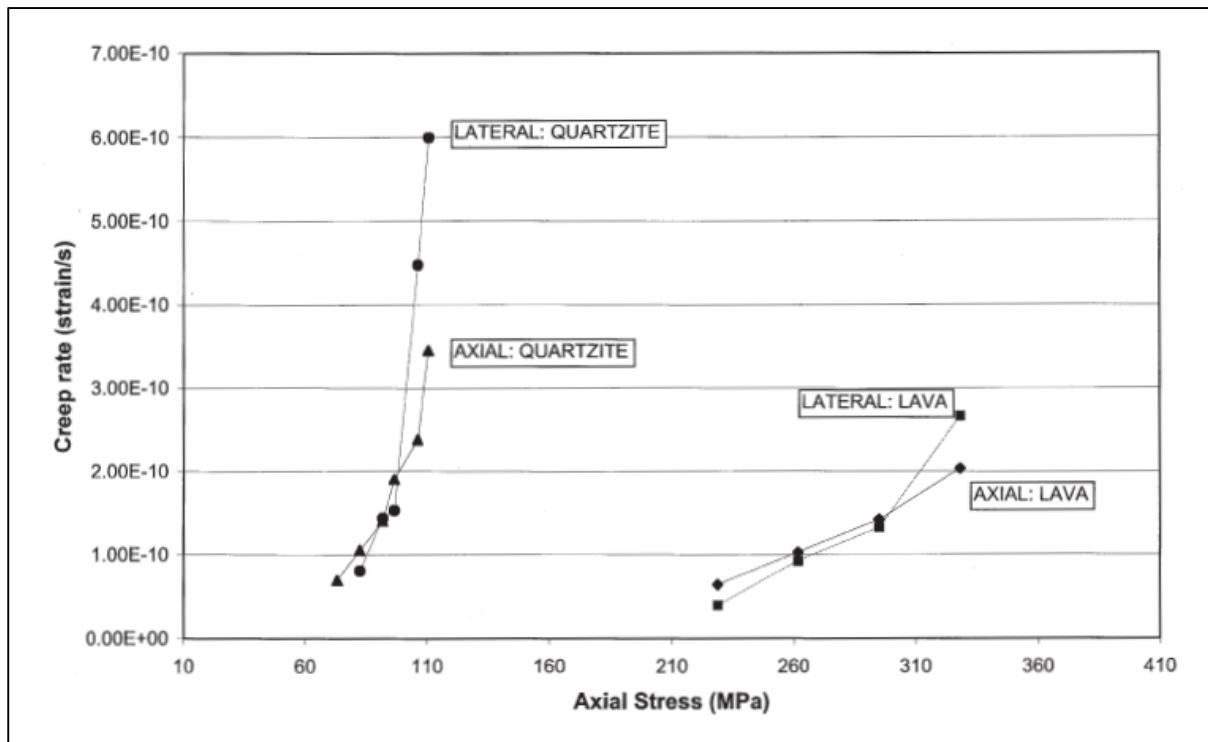


Figure 13. Creep rate versus axial stress for quartzite and lava (Drescher and Handley, 2003)

The results in Figure 13 translates into other characteristic of the two rock types such as the energy storage and release rate, plastic and elastic properties and strengths of the rock by using the stress and strain relationships. The other results of the test are shown in Table 2 which indicates that the damage sustained by quartzite is much higher than that of lava and this does

not take into account the presence of the discontinuities in the rock mass underground. Quartzite and lava have structural differences, with the quartzite being bedded and lava being massive with very little horizontal planes.

Table 2. Uniaxial compression creep test results (Drescher and Handley, 2003)

Specimen No	Creep Strength (MPa)	Nosepoint Stress (MPa)	Nosepoint as % Strength	Axial Strain at Failure $\times 10^{-6}$	Modulus Loading (GPa)	Modulus Unloading (GPa)	Damage Index
Ventersdorp Lava							
1640-23	363.7	328.2	90.3	4645	84.7	96.8	0.88
1640-53	435.4	397.4	91.3	5135	92.8	101.2	0.92
1640-55	398.7	361.9	90.8	4039	93.8	109.5	0.86
1640-63	402.2	330.3	82.1	4582	89.1	101.8	0
Elsburg Quartzite							
2056-116	117.6	91.0	77.4	3055	39.5	76.5	0.52
2056-117	114.1	91.9	80.5	3642	40.7	75.2	0.54
2056-118	112.6	91.0	80.9	4142	39.7	73.9	0.54
2056-121	135.2	105.9	78.3	3267	51.0	79.7	0.64

According to Drescher and Handley (2003) the damage index suggests that the fracture formation will extend deeper in the quartzite as compared to the lava when subjected to the same stress levels. This would mean the plastic zone in the quartzite will be much larger than that of lava. The plastic zone is where the ground has been fractured and the stress levels have also been significantly reduced. The reduced stress levels and fractured ground result in the formation of dead weight and generation on tensile fracture in the hanging wall as well as separation on bedding planes (Figure 14).

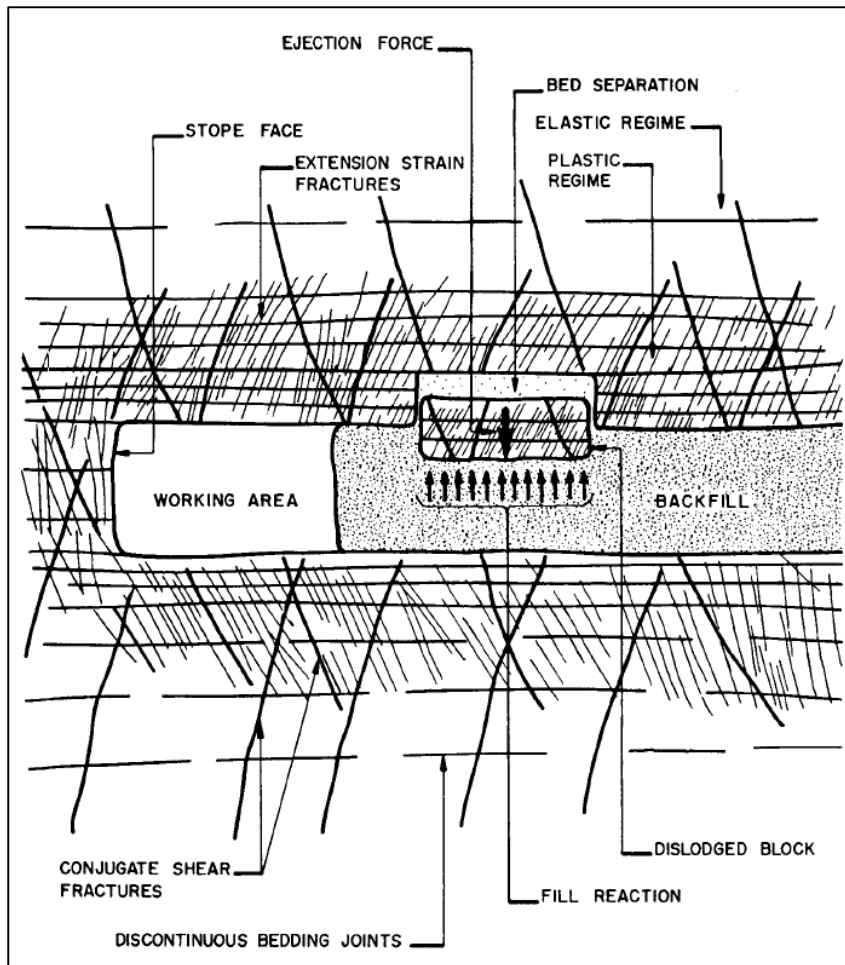


Figure 14. Fracturing in bedded rock mass around a tabular stope with backfill (Kirsten and Stacey, 1988).

Figure 11 and Figure 14 show the elastic and plastic zones around the stope. In the elastic zone the rock mass is still competent and with little fracturing. The deformation taking place in this area is of elastic nature and has small influence on the closure observed in the stope. In their work on the behaviour of the fracture zone in a deep gold mine, Napier et.al (1998) noted that the time dependent deformations are confined to the fracture zone surrounding the excavation. With the rock fracturing around the excavation, the stress is transferred to the solid rock which then also fails and the progression of failure stops when a state of equilibrium is reached, Napier et.al (1998). Following this discussion it is evident that the strength of the rock mass and the stress level determine the extent of the plastic zone which is one of the main drivers of closure. Importantly, the strength of the rock mass is determined by the intact rock properties as well as discontinuities in the rock mass.

2.7.2. Effects of time on closure

The contribution of time to closure could be both sudden (as soon after the creation of void due to blasting) or over a time period (creep behaviour). Therefore, the immediate effect could be regarded as a direct influence and the effects over prolonged time periods as indirect influence. It must be noted that the main contributor to the sudden closure is blasting and the time assists in the quantification of closure in rate terms. Time becomes useful in distinguishing the different types of closure. If mining stops the rock mass will reach a state of equilibrium with no further “sudden” elastic closure taking place, however time will still continue and creep closure will start taking effect. By representing closure as a function of time, different closure rates can be identified then be linked to either mining rate or other factors such as rock mass fracturing or seismic events.

Figure 15 illustrates different closure stages following a blast. The instantaneous closure is the sharp increase in closure during blasting followed by a reduced closure rate phase referred to as primary closure (Malan, 2003). Following the primary closure phase there is a steady state closure until the next blast and the cycle is repeated after every blast. The rate of closure is high for a short time period immediately after the blast. The closure rate decreases to a steady state for as long as normal mining activities (cleaning, making safe, supporting, marking drilling etc.) take place in the absence of any seismic events (Malan et.al, 2007).

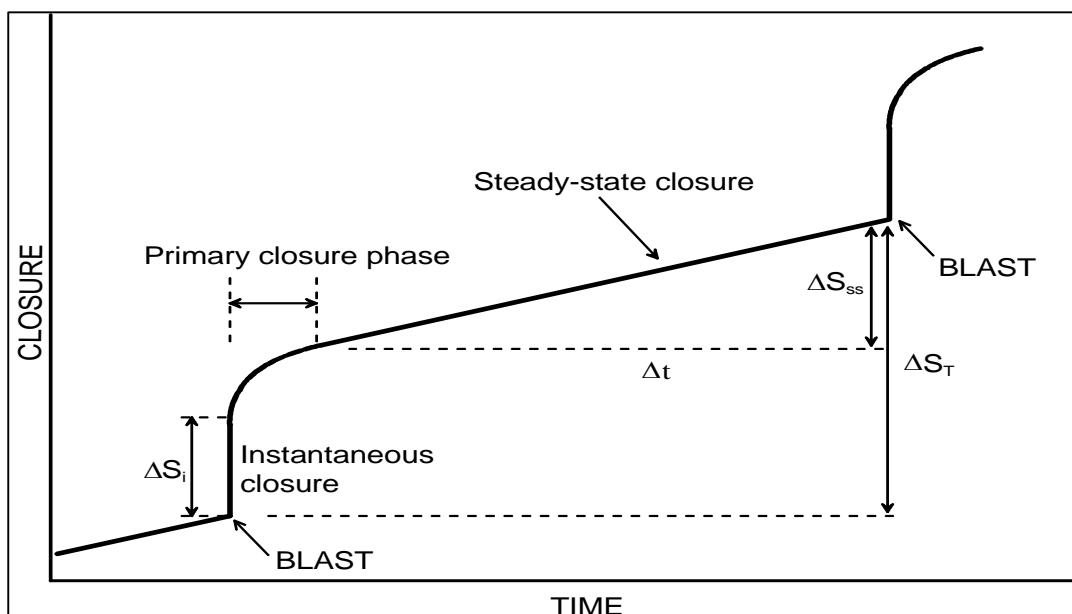


Figure 15. Typical continuous stope closure after blasting and the definition of closure terms (Malan, 2003).

2.7.3. Effects of support on closure

Backfill can significantly reduce the rate or amount of closure occurring in the stope. The forces generated by the converging hangingwall and footwall are of high magnitudes and small-scale local support units cannot withstand such high level forces. Backfill, on the other hand, can tolerate high magnitude forces to limit closure. There are different types of backfill with different properties (Ryder & Jager, 2002). One of the most important characteristics is the ability to generate high loads early before high deformation takes place. This depends on the type of backfill used.

Backfill starts to generate high loads at around 20% strain (Figure 16). The backfill can reach peak strength in excess of 180MPa which are higher than some of the stress levels encountered underground (Ryder & Jager, 2002). At these high stresses the backfill can minimise closure. Figure 14 indicates the effect of backfill in reducing and limiting closure in the stope. Mponeng uses Classified Cycloned Tailings (CCT) Backfill which can reduce closure by up to 40% of the original stoping width (Figure 16) when a good quality backfill is used. The backfill can further maintain the ERR at 40MJ/m with 80% backfill placement in the stope (Ryder & Jager, 2002).

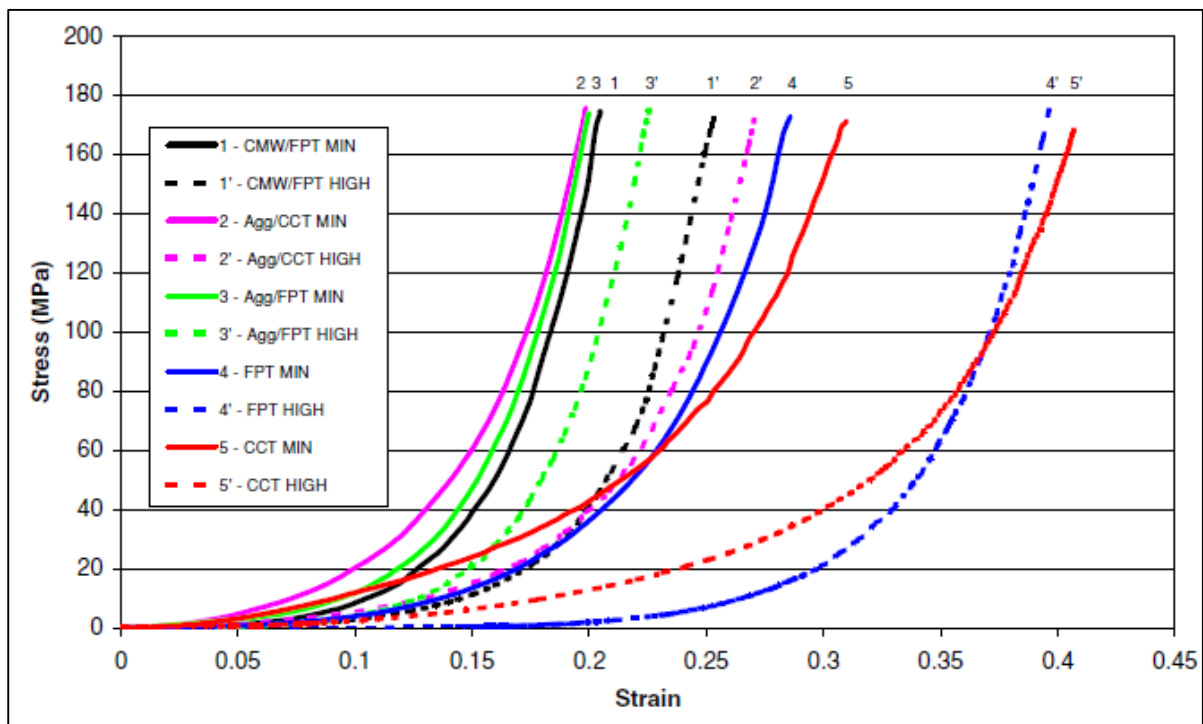


Figure 16. Stress – strain graphs of different backfill tests at different porosities (Ryder and Jager, 2002).

2.8. Correlation of seismic Potency and elastic closure

(McGarr, 1976) Suggested that the seismicity that results from ground deformation can be associated with the change in volume. In the case of mining the change in volume refers to the removal of rock through mining activities. In his (McGarr, 1976) model the seismicity is related to the volume change, ΔV , by the following relationship termed the theoretical total seismic moment:

$$\sum M_{TOT} = K\mu|\Delta V| \quad (5)$$

Where: M_{TOT} is the sum of the seismic moments of the events population, μ is the modulus of rigidity, and K is a factor close to one.

This relationship is based on the conditions that the change in volume is accommodated only by seismic failure.

This is the same relationship used to define seismic potency (P) which was used by (Scheepers et.al, 2012) to correlate seismic hazard to stope convergence. McGarr and Wiebols (1977) demonstrated that volume change due to seismic failure, ΔV_c , correlated to the mined rock volume and that the ratio $\Delta V_c / \Delta V_m$ is approximately 1 in the absence of stability pillars, where ΔV_m is the change in the mined rock volume.

It is important to note that McGarr and Wiebols (1977) highlighted that there is uncertainty in the estimations of ΔV_c as the $\sum M_{TOT}$, depends heavily on the seismic moments of the amount of large events in a particular area at a given time. In their (McGarr and Wiebols, 1977) data set it was shown that one event with local magnitude (M_L) between 2.0 – 2.25 had twice the seismic moment of ten events with M_L between 1.0 – 1.25. This simply means that the more the number of large events recorded for an area the larger the ΔV_c will be, this is regardless of the rockmass properties, mining rates, mining spans and support systems used.

The back analysis conducted by (Scheepers et.al, 2012) clearly indicates that the volumetric closure from seismic failure relies heavily on the larger event occurring in an area. The areas analysed in their study are shown in Figure 17, with focus drawn to the 120 level raise line. It can be noticed that 120-44 raise has the smallest mined area compared to the 48 and 49 raise lines. However, Figure 1 shows that the 44 raise line has the highest rate of seismic potency

per area mined compared to the 48 and 49 raise line. Of note is that the large events started occurring earlier (from 20 000m²) and more frequent in the 44 line compared to the 48 and 49.

From the discussion on elastic convergence in section 2.6 it was shown that the closure determined from elastic theory solutions depends on the properties of the intact rock and the mined span. With this in mind the closure at 120-44 should be the same to that of 48 and 49 raise lines when the same area has been mined as illustrated in Figure 3. The vertical closure that would be determined from Figure 1 for 120-44 at 22 500m² will be higher than that of 120-49 at 37 500m². This is a clear contradiction to the theoretical elastic closure solutions which are the basis for elastic numerical modelling codes. The back analysis conducted by (Scheepers et.al, 2012) shows a good correlation within the first 10 000m². This is when the mined span in the raise line is 40m according to Mponeng's mining layout.

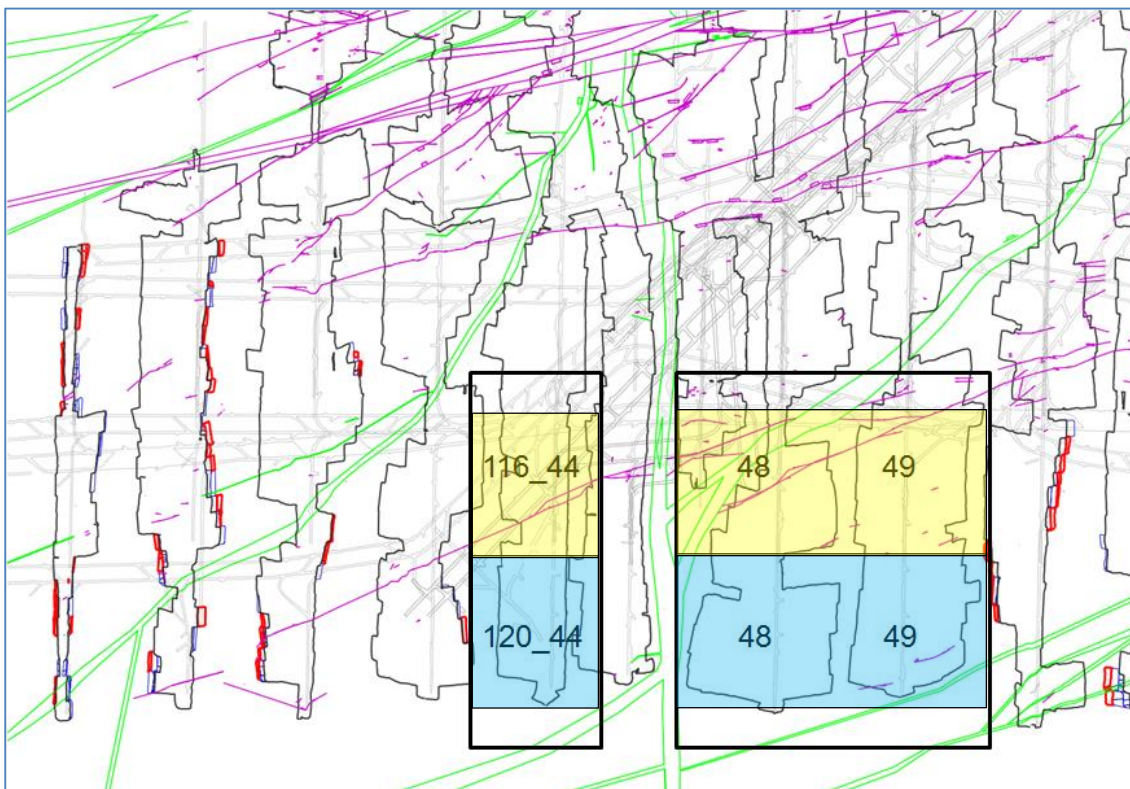


Figure 17. Detailed view of the raise lines used in the back analysis (Scheepers et.al, 2012).

2.9. Closure monitoring and measurements

Closure is one of the commonly measured and monitored behaviour of the rock mass in underground hard rock mines. This is due to the fact that closure is a simple parameter to understand and measure and also one of the major factors to understand the hangingwall behaviour. Closure is measured by simply measuring the displacement between the two opposite excavation faces (hangingwall and footwall). The methods and instruments to measure closure have over the years been simplified and depends on the user's needs. The needs include the accuracy, the durability, technology and the ease of use (Ryder & Jager, 2002).

Currently, the commonly used instruments are either mechanical or electronic and it is highly recommended that the instruments should be able to take continuous readings, i.e. all changes and the information can be plotted on a histogram. One of the closure measuring methods and instruments that was developed more than three decades ago and is still in use is the four-peg closure-ride station (Figure 18). This method can measure both the closure and the ride, with the only disadvantage being the manual reading. This method was not used for this research as the aim was to determine closure that had already occurred. Closure can still be estimated empirically using the support that was installed, this is discussed in Section 2.9.1.

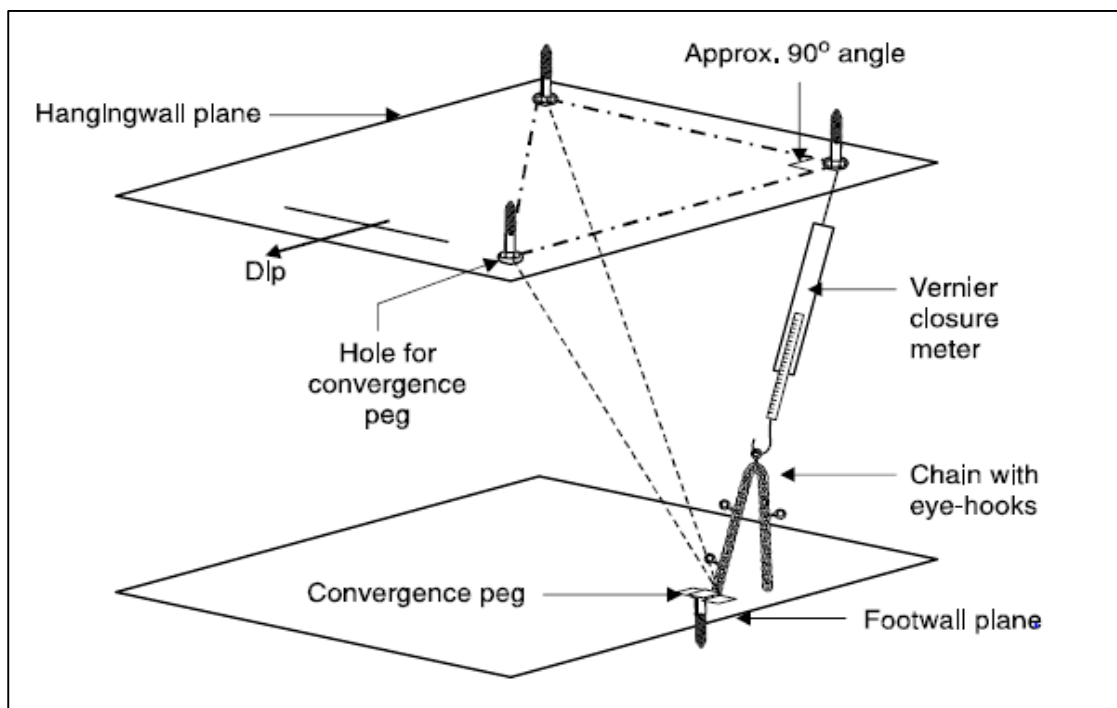


Figure 18. Schematic of the four-peg closure/ride station (Ryder and Jager, 2002).

Using the latest monitoring instruments and technology, Malan et.al, (2000) suggested a live closure monitoring system that can be implemented in a gold mine (Figure 19). This will give more understanding of the rock mass response to mining and different geotechnical districts.

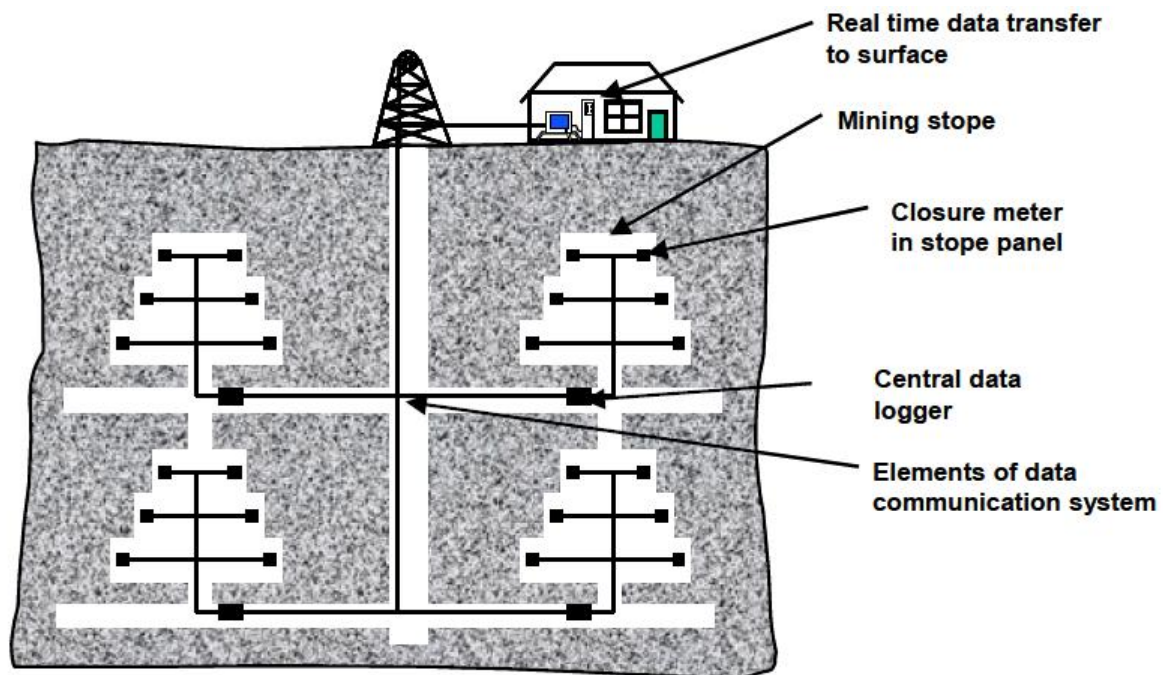


Figure 19. Idealized closure monitoring system with a closure logger in every panel (Malan, Kononov, Coetzer, Janse van Rensburg, & Spottiswoode, 2000).

2.9.1. Estimation of the closure using the deformation of installed support.

The estimation of stope closure by using old support units, specifically timber pack support is an empirical method used to make a quick assessment of the closure that has occurred in the mined out area. This method is not an officially recognized method for closure assessment. In his paper on monitoring closure, Malan (2003) did not make use or mention of this method. If applied with caution and the inherent variability taken into account, this method can be of great value in giving a picture of the amount of closure that has occurred.

Timber packs are built from single timber units that are cut to the same thickness and length. The units are similar to bricks and must be placed strategically to form a stable pack (Figure 20). Their uniform shape and size of the timber units allows one to estimate with a good degree of confidence the height of the original pack that was built before it deformed due to stope closure. Using the thickness of the timber units and summing the total number of timber units

used to build a pack one can estimate the original height of the pack. This is illustrated in Figure 20.

Pack closure measurements Example: (Figure 20)

A newly installed timber pack with 19 units has a total height of 1.9m which is equivalent to the stoping width. The packs are installed at a maximum distance of 2.5m from the face before blast.

- One timber unit = 0.1m
- $0.1\text{m} \times 19 \text{ units} = 1.9\text{m}$

The same pack in the back area following a specific face advance is measured to be 1.5m high and the units are still counted to be 19. This also depends on the closure rate of the area. Therefore there is a closure of 0.4m that has occurred. It is important to note that this is the closure that occurred at the pack and it is taken to be an average closure occurring within the vicinity of the pack. Therefore it is important to take measurement at predetermined distances along the gully.

There are no measuring instruments that can be installed at the face before blasting without completely damaging them. This leads to the immediate closure at the face not being accounted for and only considering closure taking place 2.5m to 5.0m from the face as the closest measurable closure. The immediate closure occurring on the face is taken to be negligible in this exercise.

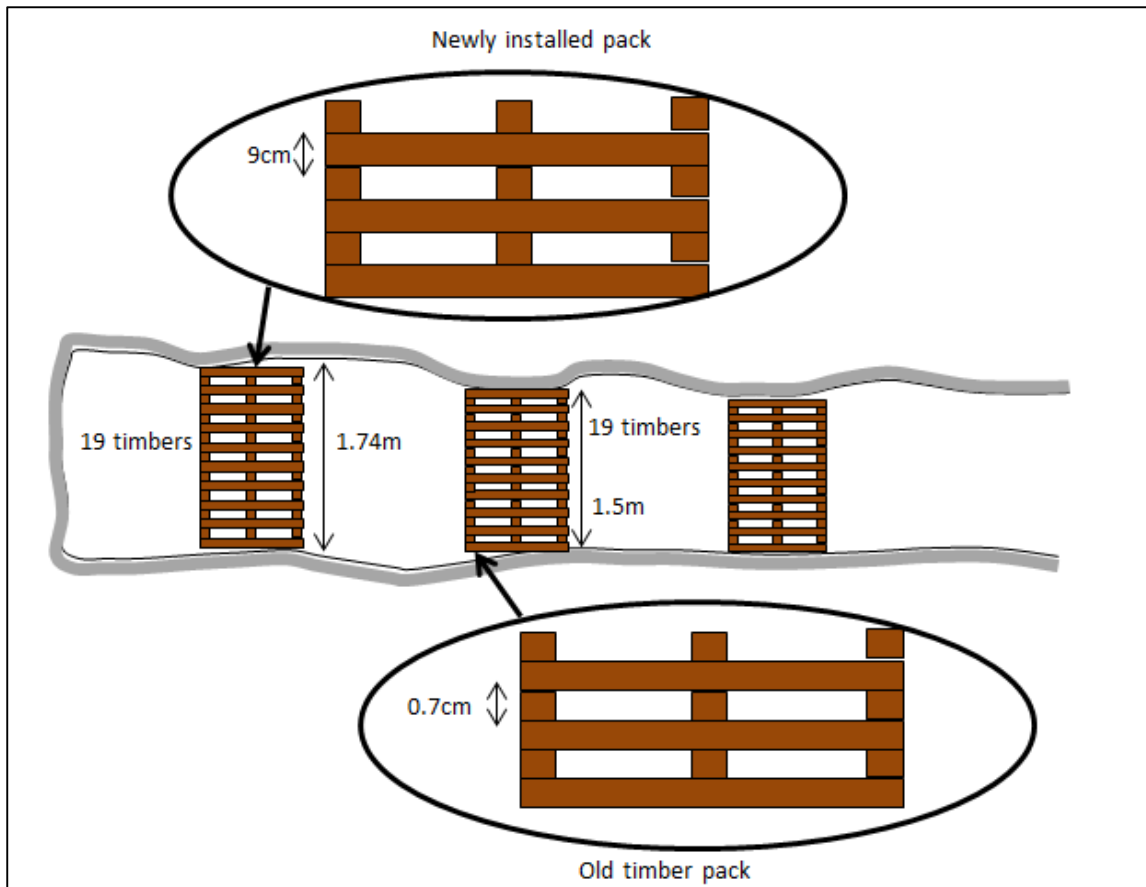


Figure 20. Timber packs deformation due to stope closure in the back area.

There are pre-stressing plates inserted in the pack which after the pack has been built the plates are inflated with water to render the pack an active support unit. The thickness of the inflated plates is negligible as when they are inflated the pack is already in contact with both the hanging wall and the footwall.

2.10. Numerical modelling as a design tool

Numerical modelling techniques have been developed and improved over the years and it has become an important tool in mine design and rock engineering fields. There are many numerical modelling software available today for different use and requirements. These software must be used with caution as they do not replace the rock engineering knowledge and engineering thinking required to make a good engineering judgement.

2.10.1. Numerical Modelling Methods

Boundary Element Method (MAP3D, 2015)

In boundary elements only the boundaries of the excavation are divided into elements. The boundary of the excavations are made up of small straight lines representing the element and the normal and shear stresses are determined for each surface. For more accurate analysis the element size must be made smaller, but the running times are still shorter when compared to finite element method.

In this project MAP 3D package which is a boundary element package is used for model building and analysis. Boundary element packages are easy and quick to use as only the excavations have to be built and not the entire rock mass.

2.11. Conclusions

It is clear that the amount of stope closure and seismic hazard has increased with the increasing depth and attempts have been made to develop mining layouts that manage and reduce rock mass deformation with the aim of managing seismicity. One of the challenges has been the measurement of seismic hazard that can be used in developing mining layouts. ERR was developed with the intention of designing less problematic mining layouts however it could not be correlated to the observed seismicity. The introduction of rock mass volume change due to seismic failure by (McGarr, 1976) aimed to correlate rock mass deformation to seismicity and this was the same principle applied by (Scheepers et.al, 2012) in correlating elastically modelled closure to volume change. Looking at the work by (Scheepers et.al, 2012) it could be shown that there is correlation only in the first 10 000m² of mining a new raise line. The relationship between elastic modelled closure and seismic volume changes becomes poor with further mining. However this is still a good indication of the anticipated seismicity. It can further be paired with an indication of the anticipated stope closure by determining the relationship of modelled closure to underground closure.

The poor correlation is mainly due to the fact that the rock mass in ultra-deep mines is highly fractured and does not behave elastically and factors such as rock mass properties, backfill and mining layouts have a significant role in the closure observed in a mined out area. The understanding of these factors is key when using elastic numerical modelling codes to analyse inelastic rock mass environments.

CHAPTER 3. EXPERIMENT AND DATA COLLECTION

To ensure that the data that is collected can be used to achieve the desired outcomes, it was important to select suitable experiment sites and relevant closure monitoring/measuring methods. Experiment sites were selected through the mine ensuring a good spread through the rock mass. Importantly, the selected raise lines had to have maturing mining spans with extensive closure already taken place. Since the raise lines had to be matured, continuous closure monitoring could be conducted in one of the raise lines to determine closure rates and possible maximum closure. Closure magnitudes could also be obtained using an empirical method. Old timber packs that had already been installed in the gullies were used to estimate the amount of deformation that had occurred, this was discussed in detail in section 2.9.1. MAP3D was used to conduct elastic numerical modelling and Salamon (1968) convergence equation was used to calculate the elastic convergence in the stope.

3.1. Continuous closure monitoring instruments

There are different instruments available to be used for this exercise however the most commonly used instrument is the closure logger from Groundworks called the Rockwatch. The Rockwatch continuously records changes in stope width and then stores the information which can later be downloaded using a device called the grabber. Figure 21 shows the complete Rockwatch kit used in monitoring closure. It includes the Rockwatch logger, Rockwatch grabber and the computer for closure analysis. (Groundwork, 2013)

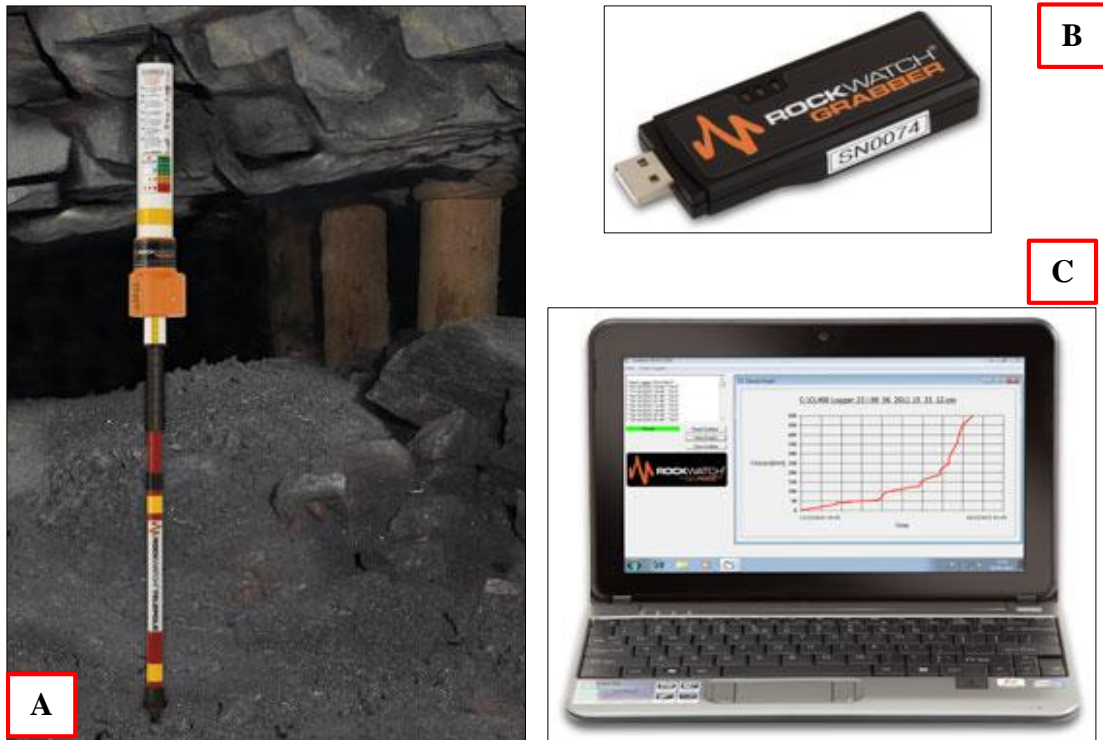


Figure 21. Rockwatch Logger and accessories used in monitoring closure, (Groundwork, 2013). (A) Rockwatch logger, (B) Grabber and (C) PC with Rockwatch software.

3.2. Experiment site selection

Four sites were selected (Figure 22) for the research. The intentions of the selected four sites were to cover different depths on the mine and also take into account the different types of rock mass conditions (Table 3). There is one site (A) on the upper east side of the mine, two sites (B, C) located at the centre of the mine towards the lower section and the last site (D) is located to the lower west side of the mine (Figure 22).

The selection of these sites ensures that the sites are placed in the two distinct footwalls found at Mponeng, the Krugersdorp quartzite and the Booyesen shale. Referring back to Malan, (2003) in section 2.6 closure at a point can be determined using elastic properties. The elastic properties of quartzite and shale are different and this is expected to be the case in the numerical model and the underground measurements. The depth below surface of the four sites ranges between 2747m to 3282m. The increase in stress due to depth should also play a role on closure.

Table 3. Experiment sites and their different environment.

	Raise	Span (m)	Back length (m)	Average Stope Width (cm)	Footwall type	Depth (Below Surface) (m)
A	104-65	210	370	127	Shale	2747
B	113-52	175	283	126	Quartzite	3073
C	116-52	180	240	130	Quartzite	3226
D	120-36	127	267	157	Quartzite	3283

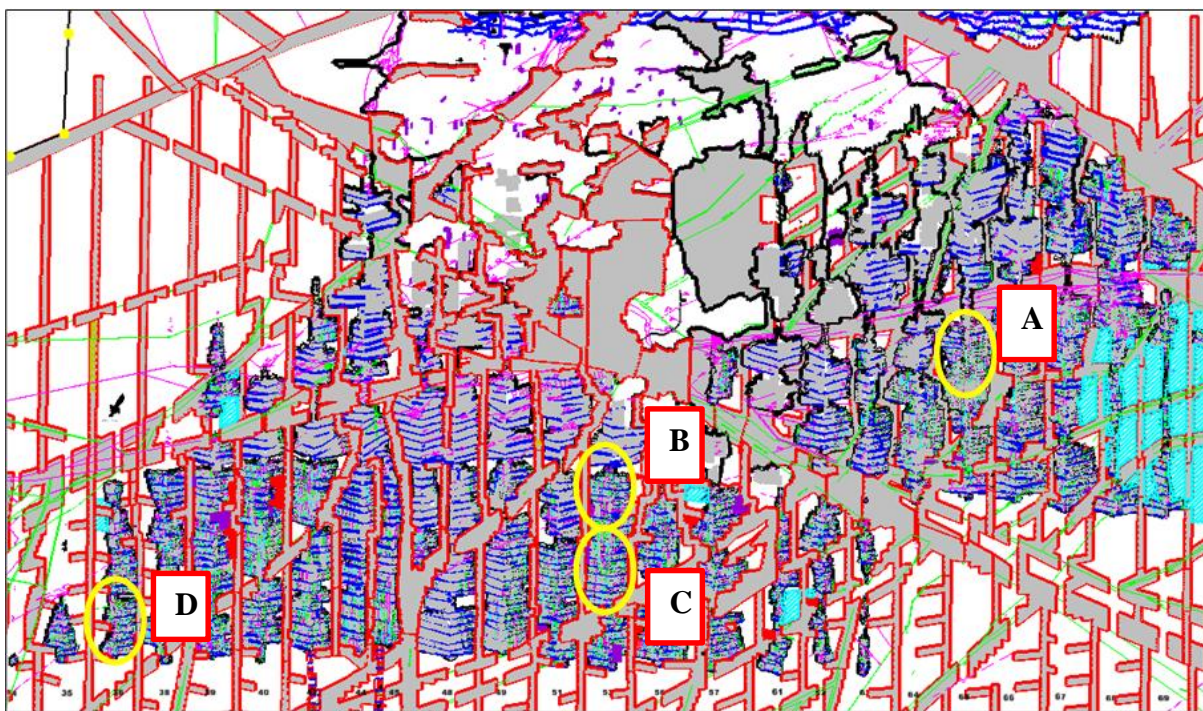


Figure 22. Plan view of Mponeng mine indicating experiment sites: A) 104-65 Raise. B) 113-52 Raise. C) 116-52 Raise. D) 120-36 Raise.

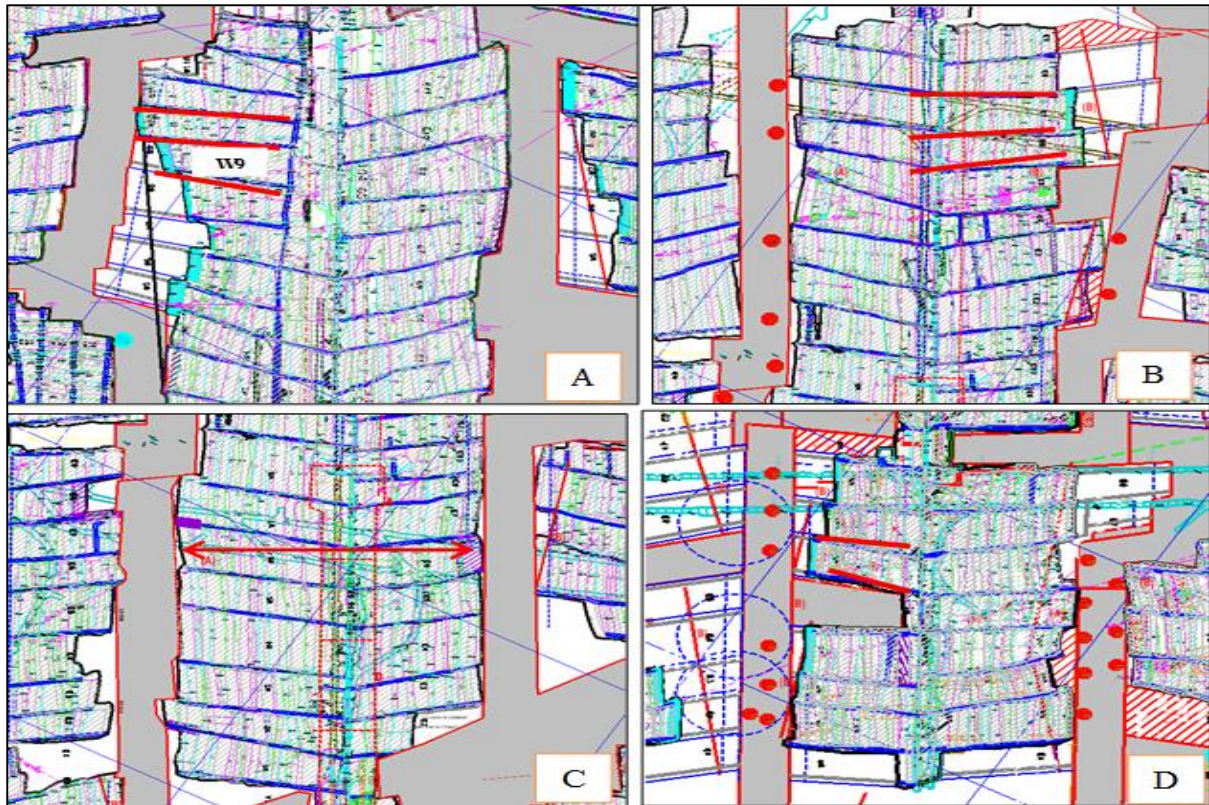


Figure 23. Plan view of 104-65 (A), 113-52 Raise (B), 116-52 Raise (C) and 120-36 Raise (D) with the gullies to be measured.

The 104-65 experiment site (Figure 23A) was being mined on the western side with the eastern side complete at the time of the project. The span was 180m in the lagging panel and 220m at the mined out panels. This is the same site also used for continuous closure monitoring instrumentations.

The 113-52 experiment site (Figure 23B) is in the final stages of mining on the eastern side of the raise line with the western side completed. The span is also at 180m with about 20m left to the final pillar position.

The 116-52- site (Figure 23C) has been completely mined out on both sites with only vamping operations taking place.

The 120-36 site (Figure 23D) had just started mining to the west when the measurements were taken with a total span of 130m.

3.3. Continuous closure monitoring at 104-65 Raise line (Site A) using closure loggers

The closure monitoring program was conducted in W9 panel which is located at the top of the 104-65 raise line. The project started on 12 November 2013 with only two closure loggers fitted in both the top and the bottom gullies of the W9. **Error! Reference source not found.** hows the position of the first two loggers, logger 671 and logger 260. The two loggers were installed 20m from the dip gully with logger 671 being 20m from the W10 face and logger 260 being 10m from the W9 face. The third logger was installed two weeks later in the W9 top gully 34m from the dip gully. Figure 25 indicated logger 260 next to an elongate that has failed due to closure,

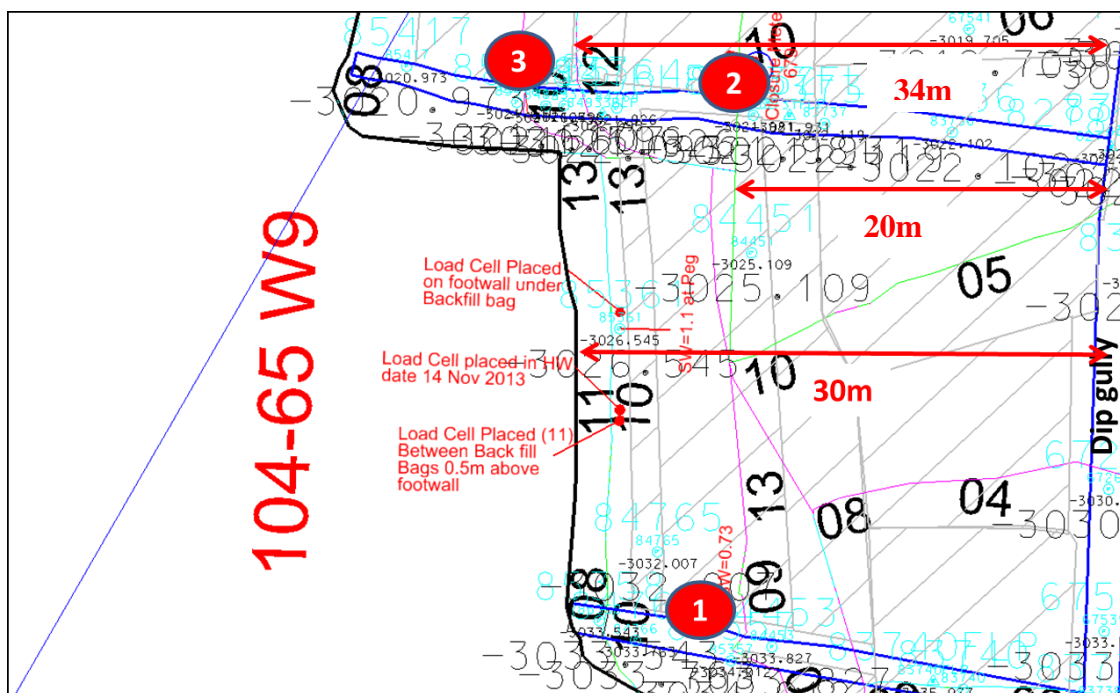


Figure 24. Position of the closure loggers in the 104-65 W9 panel. (1) Logger 260, (2) Logger 671, (3) Logger 877.



Figure 25. Logger 260 installed on the North shoulder of the W9 cleaning gully

Looking at the graphs in Figure 26 which are split into two different operation times, it can be seen that closer towards and during the Christmas break the closure rate is significantly reduced. This indicates the correlation between closure and face advance as mining activity continues. Table 4 is also split into two zones, one being within 20m from the face and the other being more than 20m from the face. Table 4 shows that the average closure rate for the two loggers during normal operations within 20m distance from the face is 2.67mm/day as compared to 0.53mm/day when mining is not taking place. The logger installed more than 20m from the face has an average closure rate of 1.21mm/day during normal operation and reduced to 0.59mm/day when there is no mining taking place.

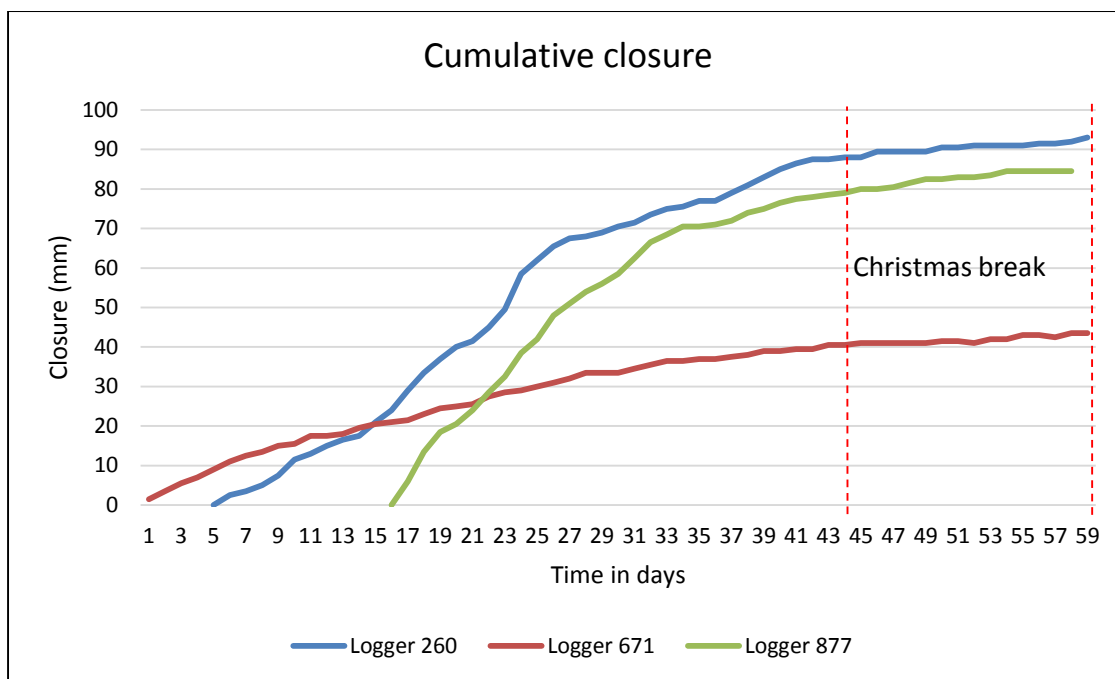


Figure 26. Closure readings from three closure loggers installed at 104-65 raise between 12 November 2012 to 08 January 2013.

The average closure per face advance is calculated to be 8.77mm/m within 20m from the face. This does not agree with the observations made earlier by (Jager and Ryder, 1999) that the closure rate in deep mines is estimated at 30-60 (mm/m). One of the factors that can result in such a significant discrepancy is the influence of backfill. This calculated closure rate can be used to estimate the expected closure at a point as the face advances.

Table 4. Closure monitoring result from 104-65 raise line.

Logger	Distance from the face (m)	Displacement (mm)	Days	Face advance (m)	Closure Rate (mm/day)	Closure Rate (mm/m)	Operation period
Closure measurements more than 20m from the face							
671	20	35	29	9.00	1.21	3.89	Normal
		10	17	0.00	0.59		Over festive break
Closure measurements within 20m from the face							
260	10	82	35	9.00	2.34	9.11	Normal
		10	17	0.00	0.59		Over festive break
877	6	76	25	9.00	3.04	8.44	Normal
		6	13	0.00	0.46		Over festive break
Ave closure rate during normal operations					2.67	8.77	
Ave closure rate over the Christmas break					0.53		

3.4. Underground stope closure measurements using timber pack support.

The measurements from the timber packs are taken to estimate the original stoping width and the closure that has occurred at that point where the pack is installed.

3.4.1. 104-65 Raise Line Underground Measurements

The 104-65 raise line is the only raise line from the four assessed raises with a shale rock mass in the footwall. A total of ten points were measured in the 104-65 raise line as indicated by the red blocks in Figure 27. The measurements are summarized in Table 5.

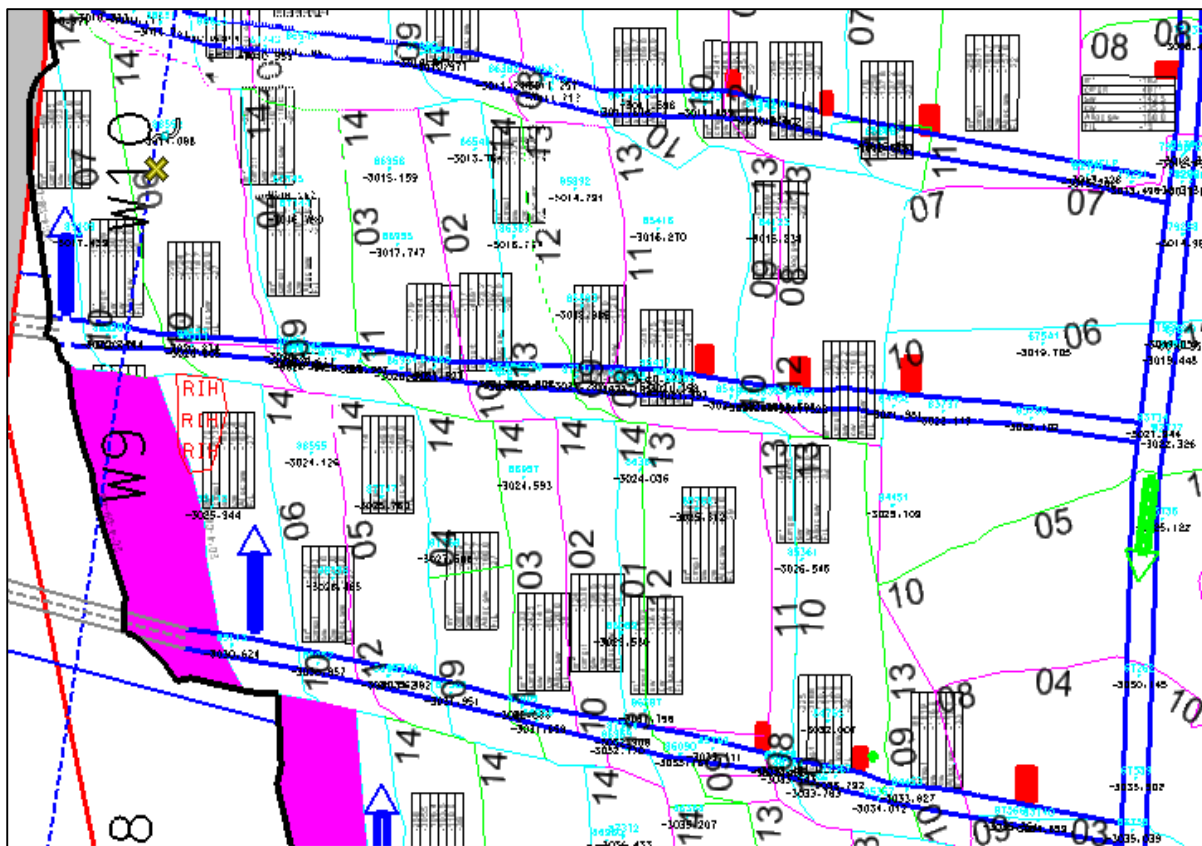


Figure 27. 104-65 experiment site and MRM mapping results in the W10 panel.

Table 5. 104-65 stope closure measurement results.

104-65 Raise	Points of measurements	Distance from centre (Half span 105m)	No of Units	Height of original pack (cm)	Measure SW (cm)	Total closure using packs
W11	1	16	12	120	60	60
	2	34	11	110	86	24
	3	40	11	110	85	25
	4	47.3	12	120	88	32
W10	1	37	9	90	65.9	24.1
	2	46	8	80	50	30
	3	53.7	10	100	82.6	17.4
W9	1	35	11	110	57	53
	2	47	10	100	50	50
	3	54.5	10	100	60	40

Looking at Figure 28 to Figure 30 the deformation in 104-65 raise line is evident. The gully shoulders are no longer accessible in certain area with highly deformed timber packs and buckled support units. Most of the movement can be observed in the footwall with some of the elongates punching into the footwall and this can be attributed to the softer nature of the shale rock mass found in the footwall.



Figure 28. Closure observed on timber pack in the 104-65 W9 cleaning gully.



Figure 29. Closure observed on timber pack and elongates in the W11 cleaning gully.



Figure 30. Closed gully shoulders and highly deformed timber packs in the W10 gully.

3.4.2. 113-52 Raise underground measurements

A total of ten points were measured in the 113-52 raise line as indicated by the red blocks in Figure 31. The measurements from 113-52 raise are summarised in Table 5.

High magnitudes of deformation could be observed in the 113-52 raise especially towards the raise with measurements up to 0.2m in the area where full cut ledging was conducted at 2.4m. The photos in Figure 32 to Figure 34 indicated closure in the respective gullies where measurements were taken. The E8 panel has seemed to have less deformation compared to both E7 and E6 panel which had similar deformation with stoping widths up 0.2m.

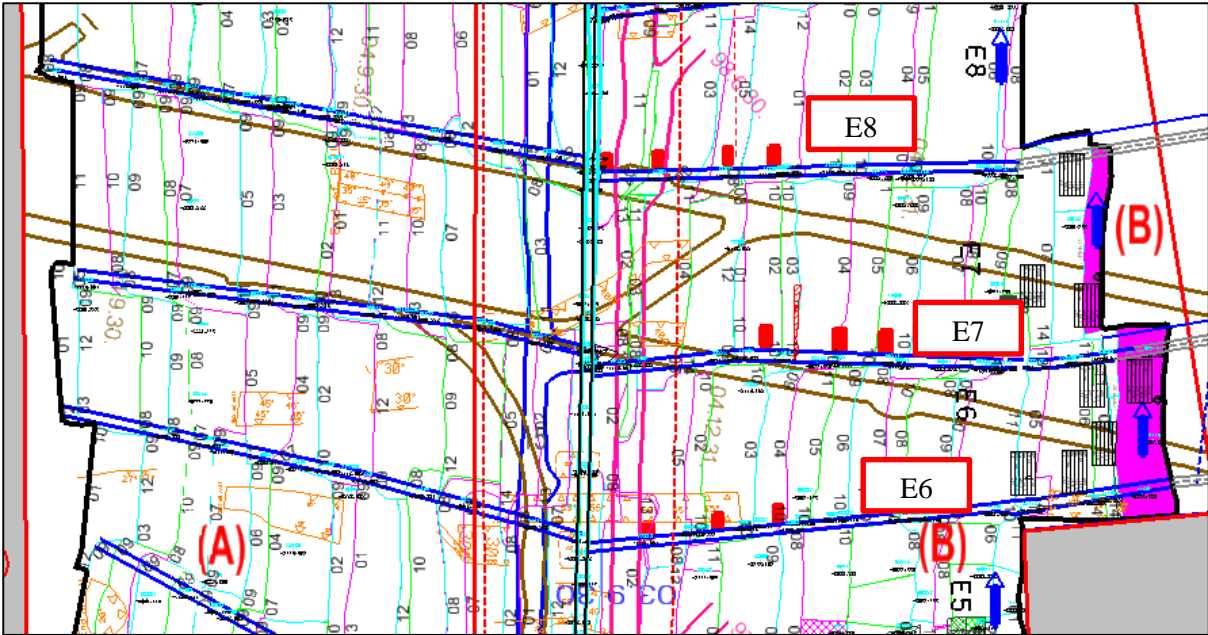


Figure 31. 113-52 experiment site.

Table 6. 113-52 slope closure measurement results.

113-52 Raise	Points of measurements	Distance from centre (Half span 87.5m)	No of Units	Height of original pack (cm)	Measured SW (cm)	Total closure using packs (cm)
E8	1	12.00	10	100.00	57	43
	2	19.30	10	100.00	69	31
	3	29.40	11	110.00	75.3	34.7
	4	36.00	14	140.00	91	49
E7	1	35.00	14	140.00	87.7	52.3
	2	44.10	11	110.00	54	56
	3	49.70	9	90.00	50	40
E6	1	20.00	11	110.00	20	90
	2	31.35	10	100.00	40	60
	3	40.55	11	110.00	59.4	50.6



Figure 32. Photos of the E8 gully cleaning gully showing deformed support



Figure 33. View into E7 stope from the E7 cleaning gully and view of the E7 gully.

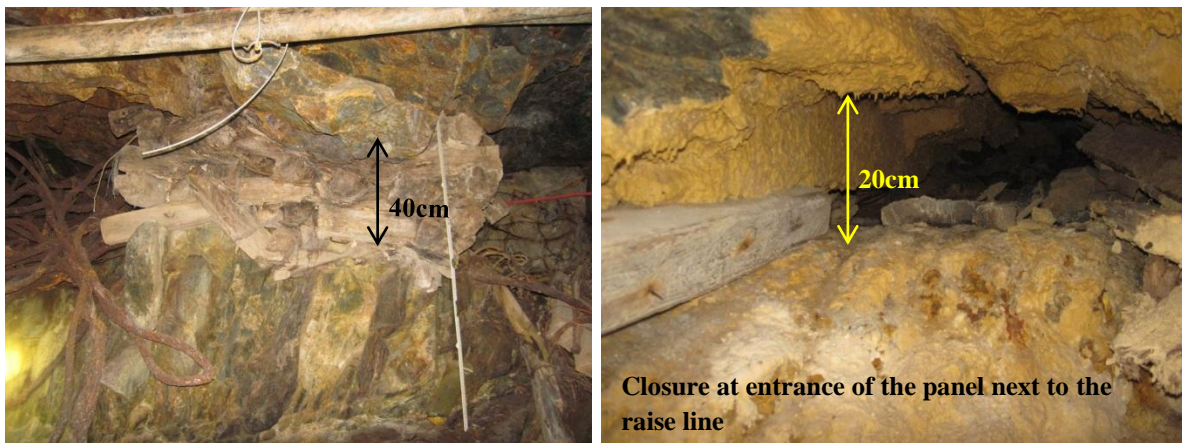


Figure 34. Highly deformed timber pack in the E6 gully and almost complete closure into the E6 stope.

3.4.3. 116-52 Raise Underground measurements

A total of ten points were measured in the 116-52 raise line as indicated by the red blocks in Figure 35. The measurements from 116-52 raise are in Table 7. No photos were taken during the underground visit to 116-52. The W6 panel stopping width was estimated to be higher than that of E4 panel however the deformation was observed to be similar.

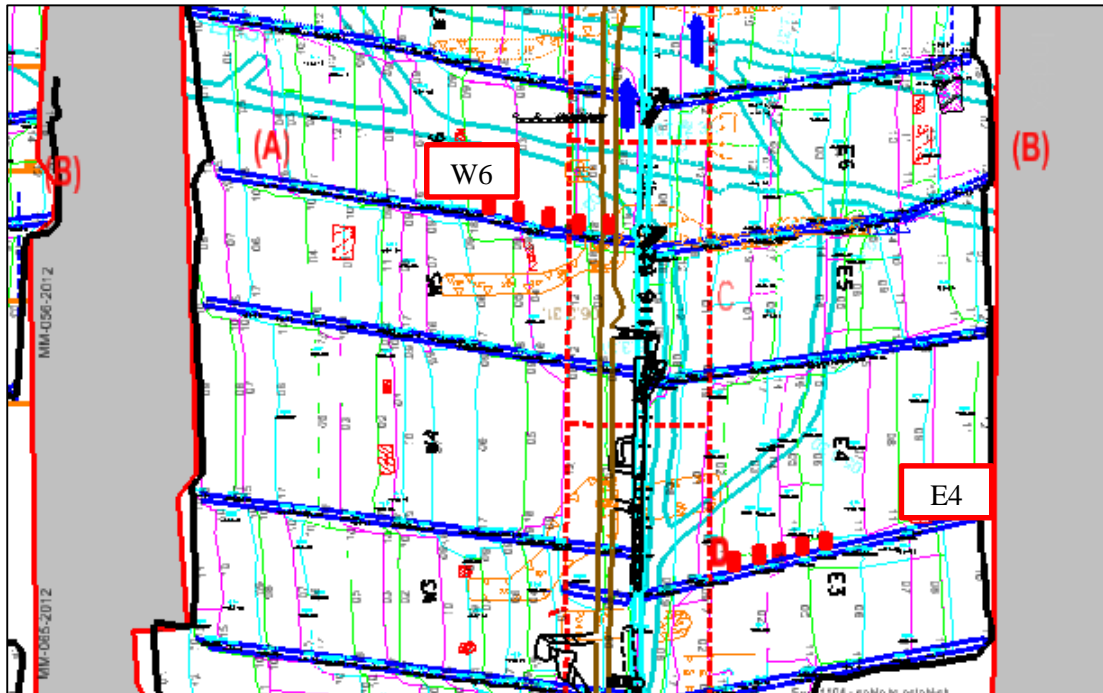


Figure 35. 116-52 experiment site indicating the points where measurements were taken.

Table 7. 116-52 stope closure measurement results.

116-52 Raise (Span 179m)	Points of measurements	Distance from centre (Half span 90m)	No of Units	Height of original pack (cm)	Measured SW (cm)	Total closure using packs (cm)
W6	1	0	13	130	80	50
	2	5.5	16	160	90	70
	3	21	17	170	80	90
	4	27.5	16	160	110	50
	5	35	17	170	100	70
						0
E4	1	29	11	110	70	40
	2	31.6	12	120	80	40
	3	34.6	15	150	70	80
	4	39	14	140	100	40
	5	44.5	12	120	90	30

3.4.4. 120-36 Raise underground measurements

A total of six points were measured in the 116-52 raise line as indicated by the red blocks in Figure 36. The measurements from 115-52 raise are summarised in.



Figure 36. 120-36 experiment site indicating the points where measurements were taken

Table 8. 120-36 stope closure measurement results.

120-36 Raise	Points of measurements	Distance from centre (Half span 63.5m)	No of Units	Height of original pack (cm)	Measured SW (cm)	Total closure using packs (cm)
W6	1	31.00	14	140.00	84.4	55.6
	2	36.40	14	140.00	114	26
	3	39.00	14	140.00	88	52
W7	1	38.00	15	150.00	120	30
	2	42.60	9	90.00	76.5	13.5
	3	45.00	13	130.00	120	10



Figure 37. Minimal deformation observed on the packs in the W6 cleaning gully.



Figure 38. Little signs of deformation on the timber packs in the W7 cleaning gully.

The western side of the 36 raise is only 40m from the centre gully hence the deformation observed on the support units was very minimal compared to the other three raise lines. Looking at the packs in Figure 37 and Figure 38 it can be noticed that the packs are still in good conditions compared to those in 113-52.

3.5. Model building to simulate closure (Using MAP3D)

Map3D is based on an Indirect Boundary Element Method. Many of the limitations of the boundary element method such as multi-step mining sequences and multiple material zones with different material properties and stress states have been overcome in Map3D. Map3D is a full three-dimensional stress analysis program designed for the stability analysis of underground (mining, tunnels, and caverns) and surface excavations (open pits, quarries, slopes) (Stacey, 2012).

Capabilities

Map3D Fault-Slip is an elastic rock mass and full plastic fault-slip stress analysis modelling programme. The stress analysis utilizes the BEM (boundary element method) and has many features: (MAP3D, 2015)

- the ability to analyse very large problem sizes (one million degrees of freedom)
- multiple elastic zones with different moduli (stiff dykes or soft ore)
- zones with different pre-mining stress states
- tabular mining with yielding pillars
- multiple mining steps are required to consider effects such as backfill placement or crack propagation

Limitations

Unlike a program such as Phase 2 which can accommodate more than one host rock in the same model, Map 3D can only have one host rock as the elements are built into the host rock. This limitation requires that the same model be run for each host rock mass properties to get different effects caused by stress on the rock mass. In this investigation two models with different rock mass properties had to be run to simulate deformation of the two different rock masses found in the footwall.

Element size

The element size is important as the resolution of the results depends on the element size used. The smaller the element size the more accurate the results will be. This is because the results are extrapolated in short distances between elements and over a large number of elements hence reducing the error margin. Larger element size results in much fewer elements in the model and much larger areas to be extrapolated between. This results in less accurate results. Figure 39 shows the closure analysed using element size of 20m and these results show there is closure up to 10cm on the stope face while the model (Figure 40) with element size of 10m shows the closure on the face is around 3cm. This shows the influence of the element size on the model results.

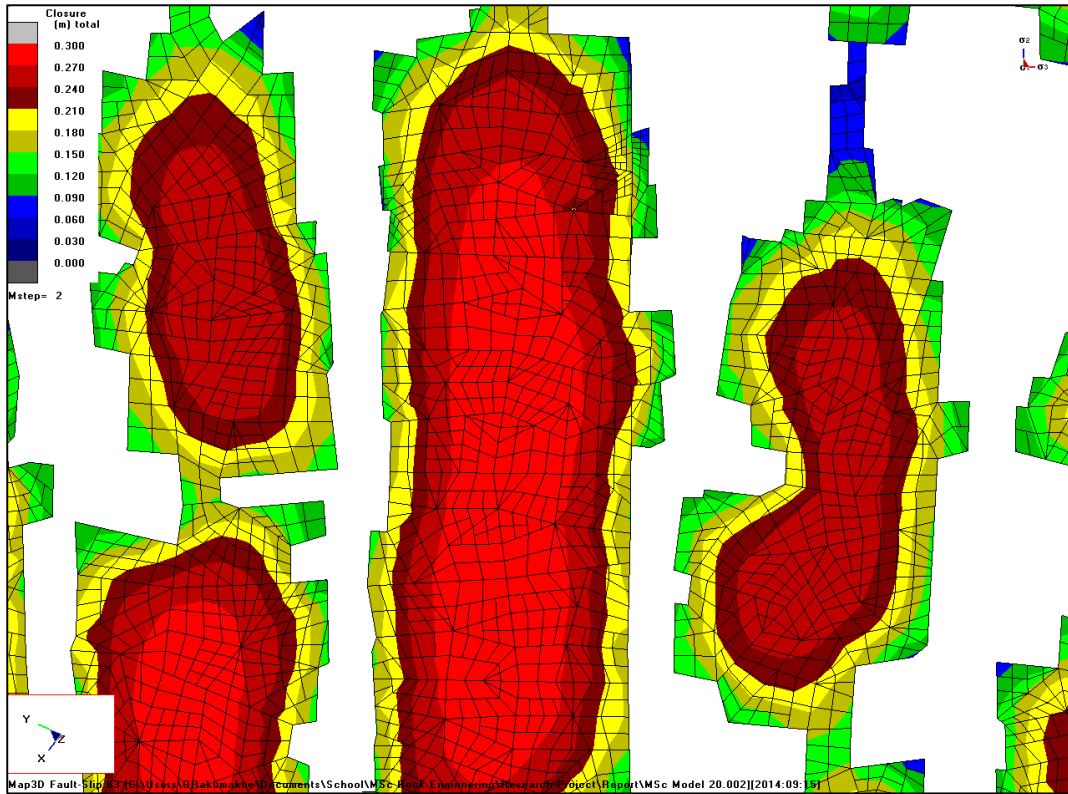


Figure 39. Closure in the stopes using element size of 20m.

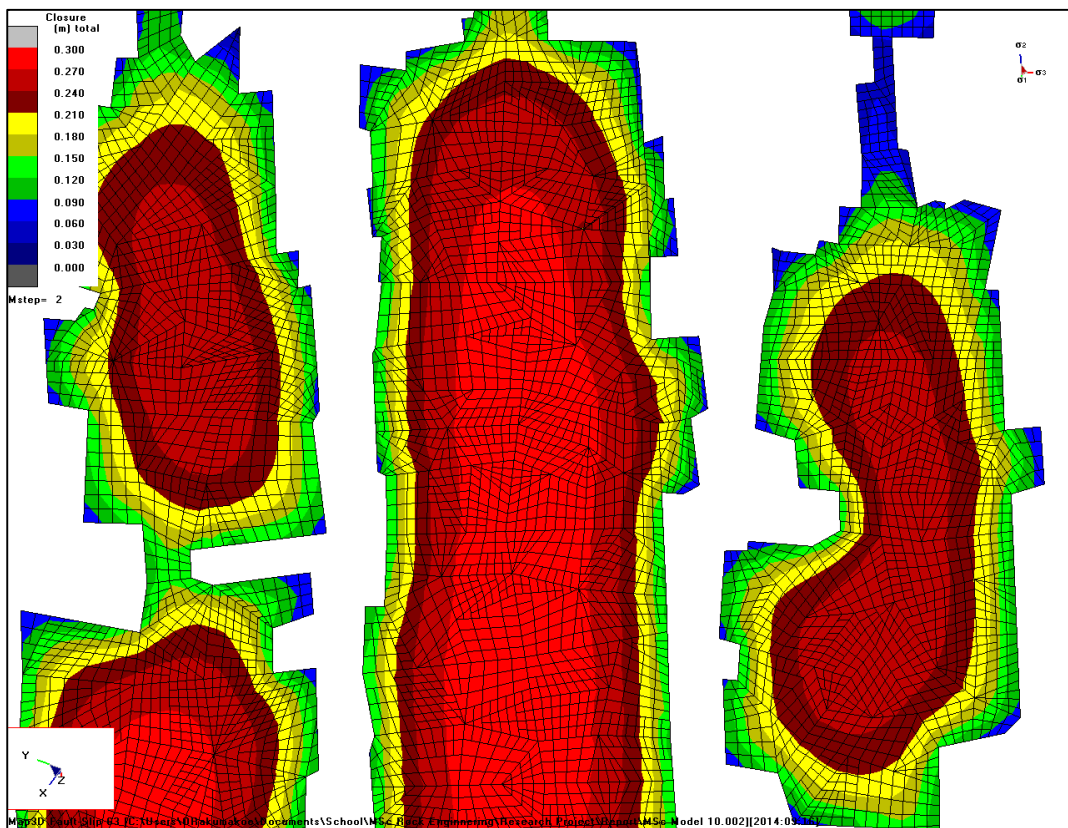


Figure 40. Closure in the stopes using element size of 10m.

There are disadvantages to finer element sizes and that is the model becomes too large due to the number of elements. This makes the model to take long time to run and at times will even require a much more powerful computer to be able to run and analyse. For this investigation the model was made finer at the areas of interest and larger at the mined out areas.

3.5.1. Experiment Model

The experimental model is set up to determine convergence in the four raise lines where underground closure measurements were conducted. The results from this model are compared to the underground closure measurements to establish the correlation between the two.

The Mponeng model is divided into two main sections which are the old long wall on the upper level which were mined without backfill and the current mining stopes which are backfilled.

The model is built in two steps:

- I. Step 1: Long walls without backfill
- II. Step 2: Current mining with backfill

The element size in this model is not fixed for step 1 and is fixed to 10m for step 2 and the raise lines for the experiment are fixed at a much finer element size of 5m. Step 1 is not fixed as it is not the area of interest and this will help reduce the model size. Two models were used to assess closure in the two different footwall rock masses found at Mponeng. Both footwalls are weaker than the Lava hanging wall hence their properties are used in the model instead of the Lava properties. The backfill properties are the same in both models.

Input parameters.

After stress measurements project was completed in late 2013 on AGA West Wits mines a stress regime was developed which is used as input into the model. The stress state is referred to at the NELSAM-CCB2013 (Figure 41) (Ogasawara et.al, 2014). The elastic properties in Figure 41 are those of the Quartzite footwall and Figure 42 indicates the elastic properties of the Shale footwall (104-65) and the backfill.

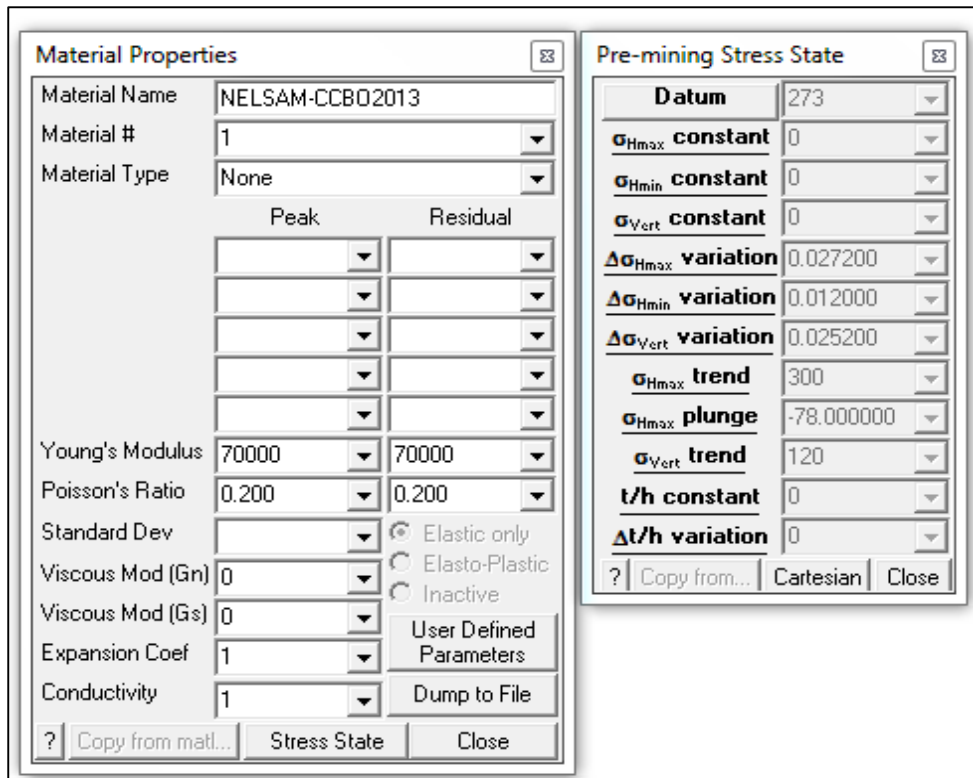


Figure 41. Stress state used in the model and the elastic rock properties for quartzite rock.

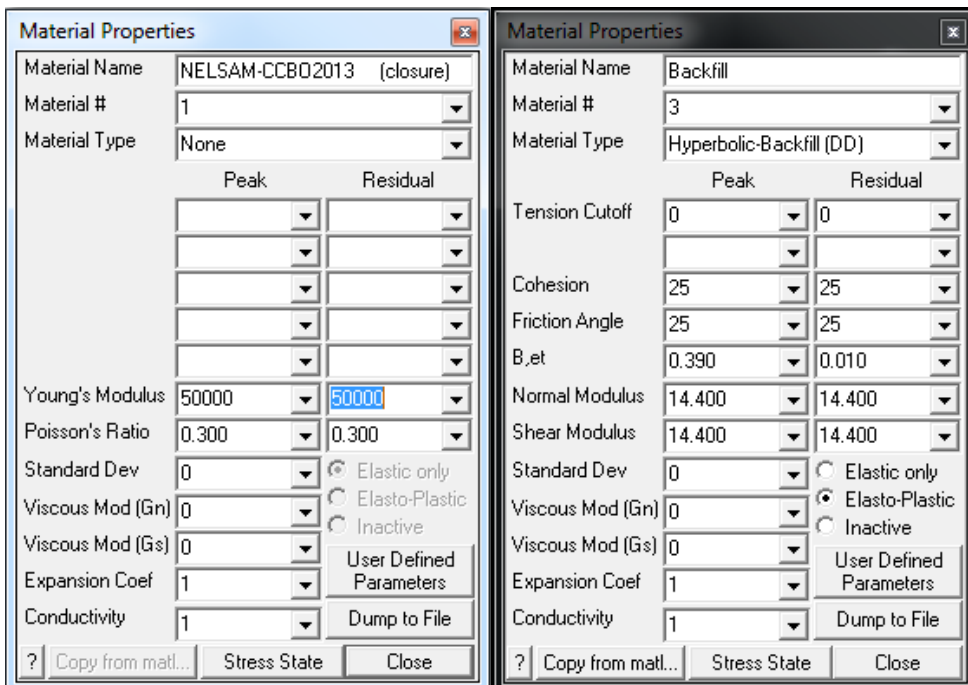


Figure 42. The elastic rock properties for shale and the material properties of the backfill material.

3.5.2. Modelled closure results per raise line assessed.

The following figures and tables indicate the modelled closure results in each specific raise line. The closure readings were taken at the same points as those used in Section 3.4. The points are counted starting from the raise towards the face with point 1 being the closest to the raise.

120-36 Raise modelled closure

Figure 43 shows the modelled closure results at 120-36 raise and in Table 9 is the modelled closure at each point of interest as indicated in Figure 43.

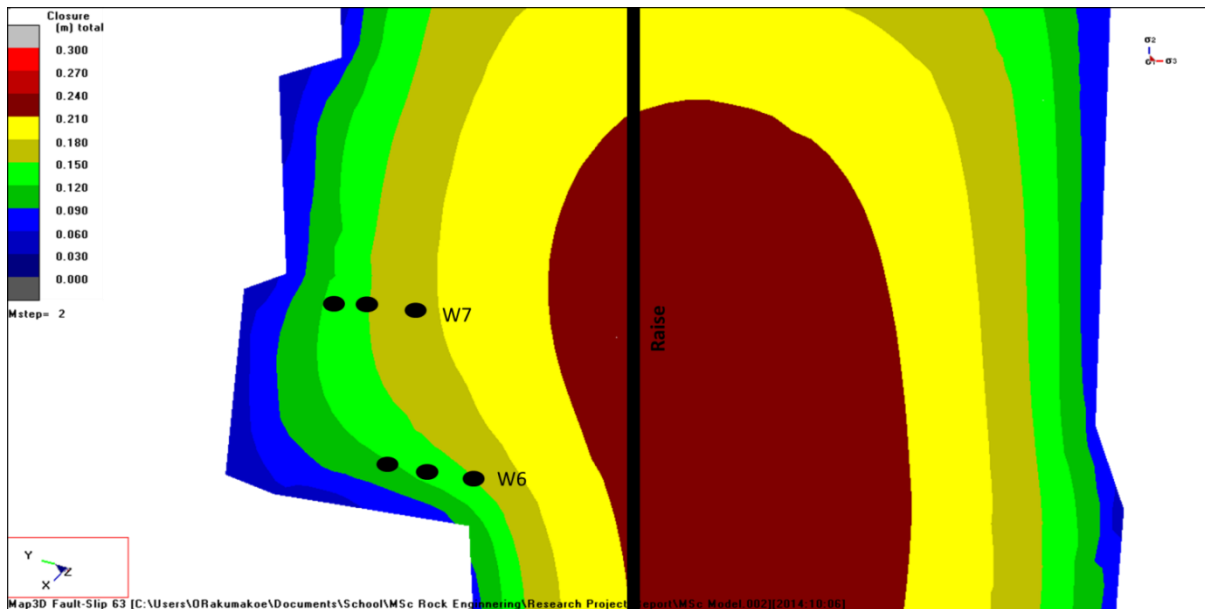


Figure 43. Points where modelled closure was measured similar to underground in 120-36 raise line.

Table 9. Modelled results of 120-36 raise at indicated points in Figure 43

120-36	Points	Distance from Centre (Half span 63.5m)	Modelled Closure (cm)
W6	1	31	16
	2	36	14
	3	39	13
W7	1	38	17
	2	43	16
	3	45	13

116-52 Raise modelled closure

Figure 44 shows the modelled closure results at 116-52 raise and in Table 10 is the modelled closure at each point of interest as indicated in Figure 44.

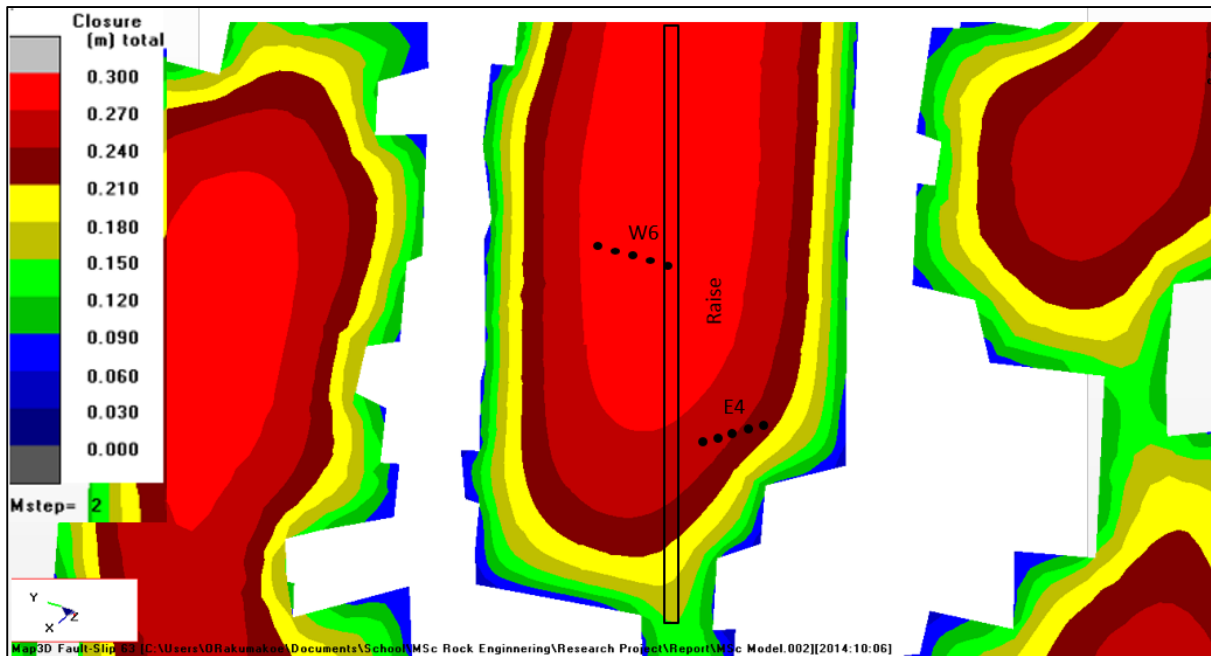


Figure 44. Modelled closure with points where measurement were taken in 116-52 raise line.

Table 10. Modelled closure results for 116-52 raise

116-52	Points	Distance from Centre (Half span 90m)	Modelled Closure (cm)
W6	1	0	29
	2	6	29
	3	21	29
	4	28	29
	5	35	28
E4	1	29	26
	2	32	25
	3	35	25
	4	39	24
	5	45	23

113-52 Raise modelled closure

Figure 45 shows the modelled closure results at 113-52 raise and in Table 11 is the modelled closure at each point of interest as indicated in Figure 45.

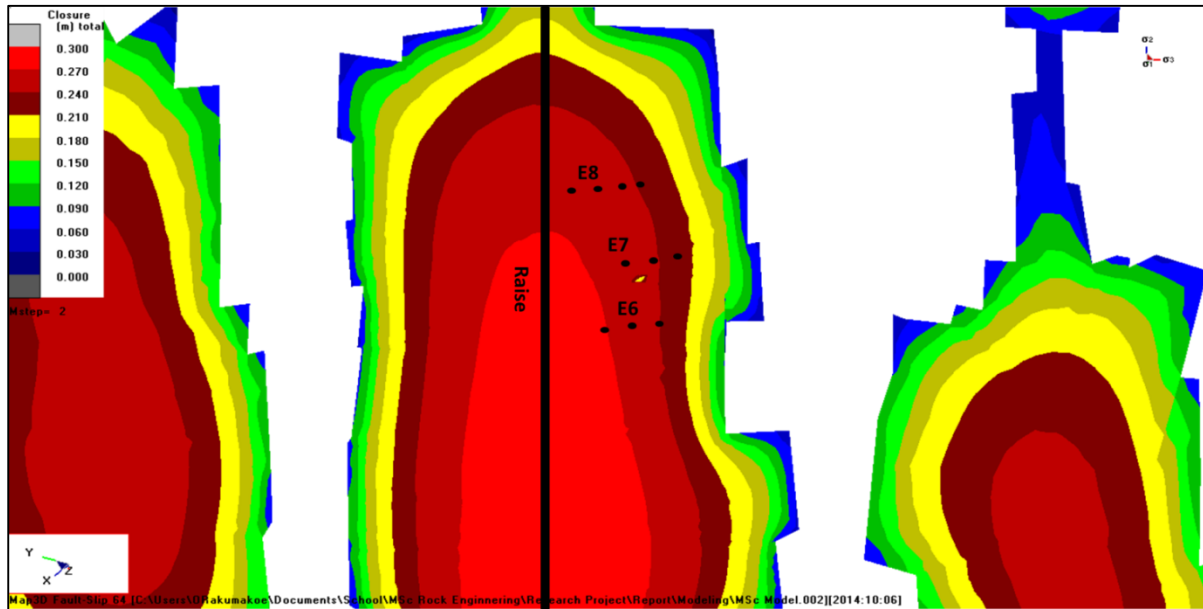


Figure 45. Modelled closure with points where measurements were taken in the 113-52 raise line.

Table 11. Modelled results for 113-52 raise at indicated points in Figure 45

113-52	Points	Distance from Centre (Half span 87.5m)	Modelled Closure (cm)
E8	1	12	26
	2	19	26
	3	29	25
	4	36	24
E7	1	35	26
	2	44	25
	3	50	23
E6	1	20	28
	2	31	27
	3	41	26

104-65 Raise modelled closure

Figure 46 shows the modelled closure results at 104-65 raise and in Table 12 is the modelled closure at each point of interest as indicated in Figure 46.

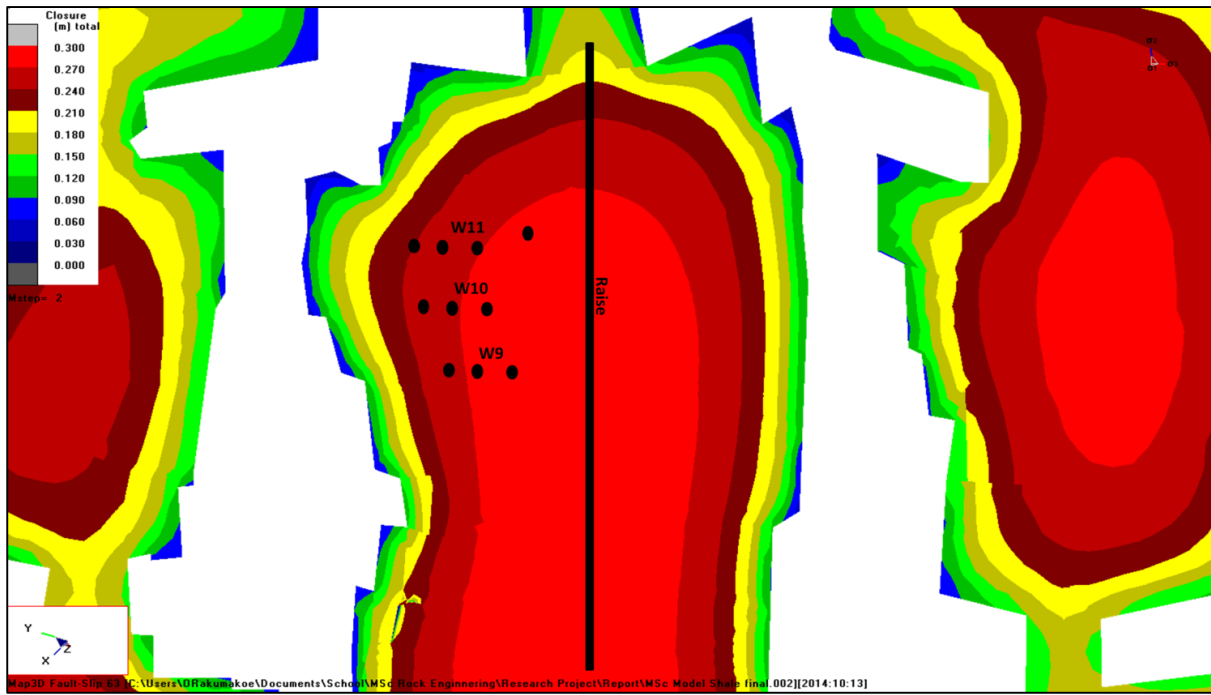


Figure 46. Modelled closure 104-65 raise line with poits where measurements were taken.

Table 12. Modelled closure results of 104-65 raise at indicated points in Figure 46.

104-65	Points	Distance from Centre (Half span 105m)	Modelled Closure (cm)
W11	1	16	28
	2	34	27
	3	40	26
	4	47	25
W10	1	37	28
	2	46	27
	3	54	26
W9	1	35	28
	2	47	27
	3	55	27

3.6. Analytical calculation of closure

The concept of analytical calculations of convergence (closure) was discussed in Section 2.6 earlier. The concept was used to calculate the expected convergence at the same points where the underground measurements were taken. Equation 3 was used to do calculation in excel program where Δl was taken to be 1, as the aim is to determine closure at maximum span and not at different mining spans. The specific parameters used in the calculations are shown in Table 13.

Table 13. Mechanical properties of the quartzite and shale rock used in the calculations.

Parameter	Quartzite	Shale	Units
Density	2700	2700	kg/m ³
Gravity	9.81	9.81	m/s ²
Young Modulus E	70	50	GPa
Poisson Ratio ν	0.2	0.3	

Using equation 3 and the parameters in the table, the expected closure at the measurement points per raise line are given in Table 14. The shale parameters were used for the 104-65 raise and other three raise lines are in the quartzite footwall.

Table 14. Calculated convergence at each experiment point per raise line.

116-52	Points	Distance from Centre (Half span 90m)	Calculated maximum convergence (cm)
W6	1	0	34
	2	6	34
	3	21	33
	4	28	32
	5	35	31
E4	1	29	32
	2	32	32
	3	35	31
	4	39	30
	5	45	29

104-65	Points	Distance from Centre (Half span 105m)	Calculated maximum convergence (cm)
W11	1	16	46
	2	34	44
	3	40	43
	4	47	42
W10	1	37	44
	2	46	42
	3	54	40
W9	1	35	44
	2	47	42
	3	55	40
113-52	113-52 Raise	Distance from Centre (Half span 87.5m)	Calculated maximum convergence (cm)
E8	1	12	31
	2	19	31
	3	29	30
	4	36	29
E7	1	35	29
	2	44	27
	3	50	26
E6	1	20	31
	2	31	29
	3	41	28
120-36	120-36 Raise	Distance from Centre (Half span 63.5m)	Calculated maximum convergence (cm)
W6	1	31	21
	2	36	20
	3	39	20
W7	1	38	20
	2	43	18
	3	45	18

CHAPTER 4. DATA ANALYSIS

In an attempt to estimate the closure underground the first step was to try and estimate the original stoping width at the time of mining. Only once the original stoping width is known then the estimated closure can be determined using the current stoping width measured. The timber pack assessment method was used to estimate the original stoping width.

4.1. Underground measured closure

To determine the estimated closure that has taken place in each assessed area the current stoping width measured is subtracted from the original stoping width determined in previous section 3.4 and listed in Table 5, 6 7 and 8. The following graphs (Figure 47, 49, 51 and 53) indicate the estimated closure plotted against modelled and analytically calculated closure.

These four graphs are split into gullies measured in each raise line. The measurements start from the half span of the raise line indicated with (S) up to the last measured point in the gully indicated with (E).

4.1.1. 116-52 Raise closure analysis

The graph (Figure 47) of the two gullies indicated similar closure pattern in the 116-52 raise line. The estimated closure in the gullies does not indicate a gradual decrease from the centre of the raise towards the solid face as it is indicated by the modelled closure and calculated convergence lines. The calculated convergence and modelled closure indicated a good correlation with the two lines parallel to each other in both gullies with an average difference of 4cm in W6 and 6cm in the E6.



Figure 47. Closures determined at each point in 116-52 raise.

The W6 gully has more closure than the E4 gully with an average closure of 66cm in the W6 compared to 46cm in the E4 gully while the modelled closure indicates 28cm and 24cm of closure respectively. The maximum estimated closure recorded in the W6 and E4 gullies are 90cm and 80cm respectively. The difference in closure measured in the two gullies can be mainly attributed to the mining sequence and the position of the gullies in relation to abutments (Figure 48). The modelled closure indicates the highest closure to be at W6 which is in agreement with underground measurements.

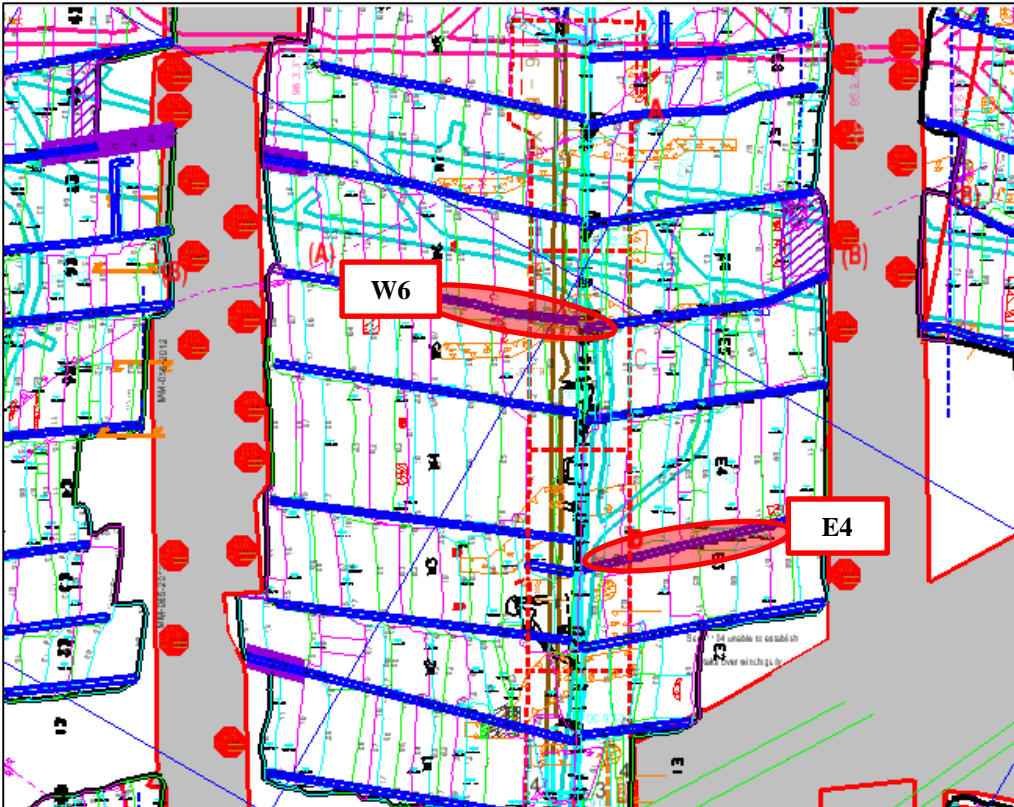


Figure 48. 116-52 raise layout indicating the position of the W6 and E4 gullies, with the E4 gully closer to the abutment.

4.1.2. 104-65 Raise closure analysis

The actual closure in the three gullies has a similar trend (Figure 49) with a uniform closure through the panel. The first point in the W11 gully was measured at the centre of the span hence indicating the highest closure and the closure is relatively constant for the rest of the three points averaging at 35cm. The W10 has similar measurement to W11. The W9 has higher closure at average of 49cm and this can be attributed to the fact that the measurements were taken closer to the centre of the raise (Figure 50). Again the actual closure does not indicate the expected decrease in closure towards the face.



Figure 49. Closures determined at each point in 104-65 raise.

The calculated convergence and modelled closure indicated a similar trend in all the gullies with a gradual decrease in closure towards the face. Although the trend is the same, the calculated convergence is much higher than the modelled closure for the shale footwall with an average difference of 15cm. The modelled closure averages indicated the highest closure to be at W9 and this corresponds with the closure estimates.

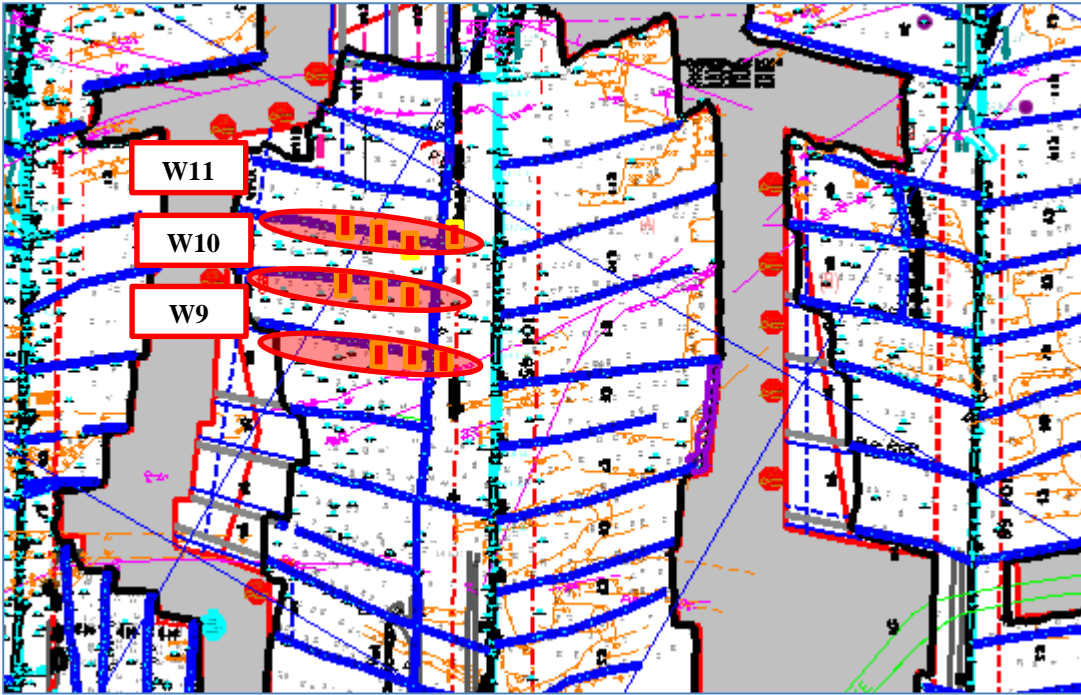


Figure 50. Layout of the 104-65 raise indicating the measured points in the W11, W10 and W9 gullies relative to the centre.

4.1.3. 113-52 Raise closure analysis

Similar to the two raise lines discussed above, the 113-52 estimated closure does not follow that of numerical modelling (Figure 51). The E8 gully shows a steady decrease in closure towards the face but there are areas where the closure increases. The E7 shows an increase in closure towards the face with high closure in the gully up to 56cm. Similarly high closure was observed in the E6 gully at the raise position with up to 90cm.

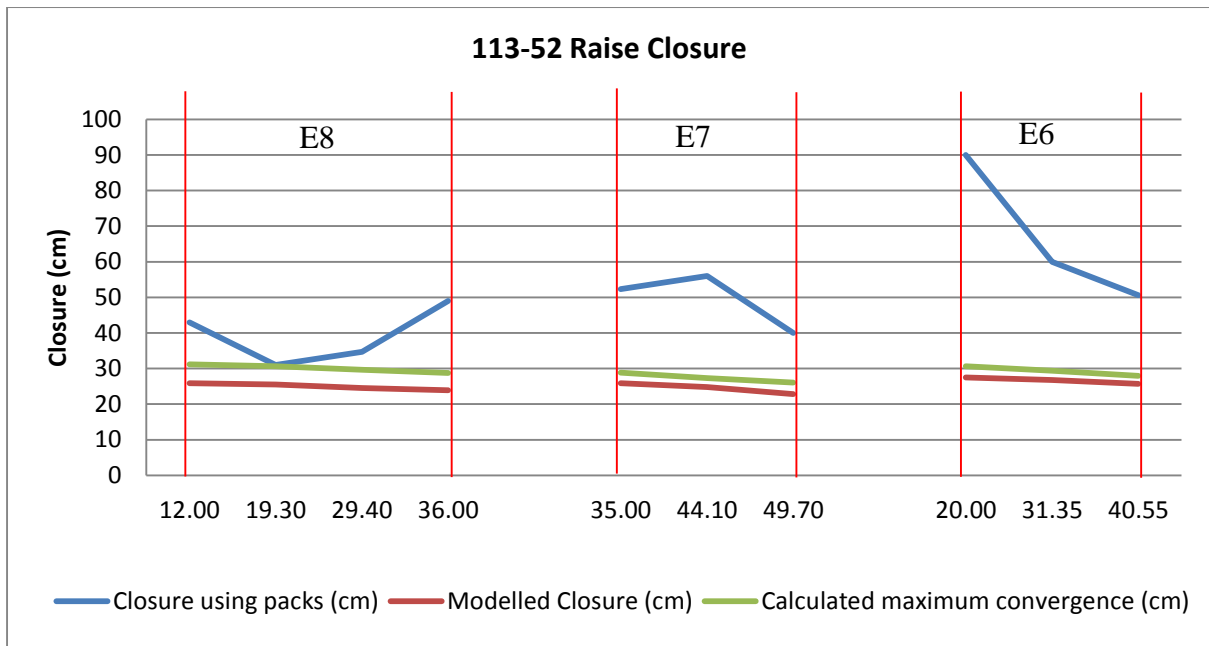


Figure 51. Closures determined at each point in 113-52 raise.

The difference between the modelled closure and estimated closure is significant in the 113-52 raise with an average of 25cm. The modelled closure indicated that the highest closure occurred in the E6 gully which was also found from the underground measurements. There is also a good correlation between the modelled closure and the calculated convergence. Comparing the modelled closure and estimated measurement in the E6, it confirms the observations in the preceding two raise lines that the layout has an influence on closure (Figure 52).

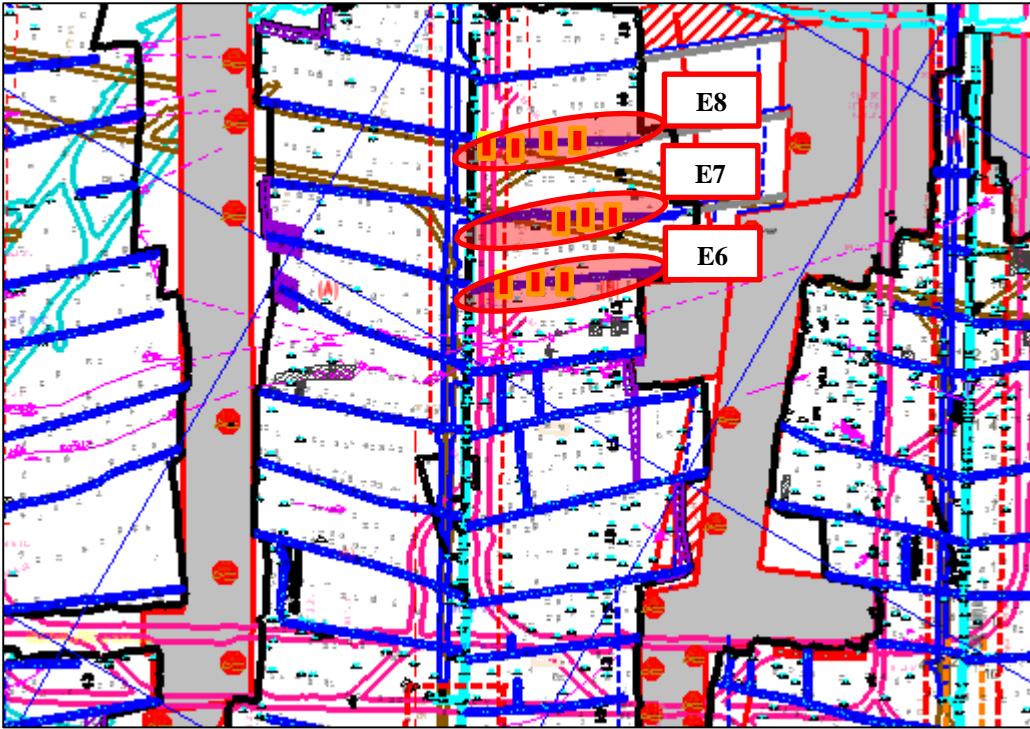


Figure 52. Layout of the 113-52 raise indicating the measured points in the E8, E7 and E6 gullies relative to the centre.

4.1.4. 120-62 Raise closure analysis

The 120-36 raise had the shortest span of the four assessed raise lines and also had strike pillars within the raise. The W6 cleaning gully is the closest to the strike pillar but had the highest closure compared to W7 with averages of 44cm and 17cm respectively. It would be expected that W6 being close to the abutment would have less closure (Figure 54). However the fact that the W6 panel is leading and is the furthest from the raise line could have contributed to the higher closure. It must also be noticed that the measurements of W6 were taken closer to the raise compared to those in W7 which were taken closer to the face. The modelled closure indicates that the highest closure is in the W7.

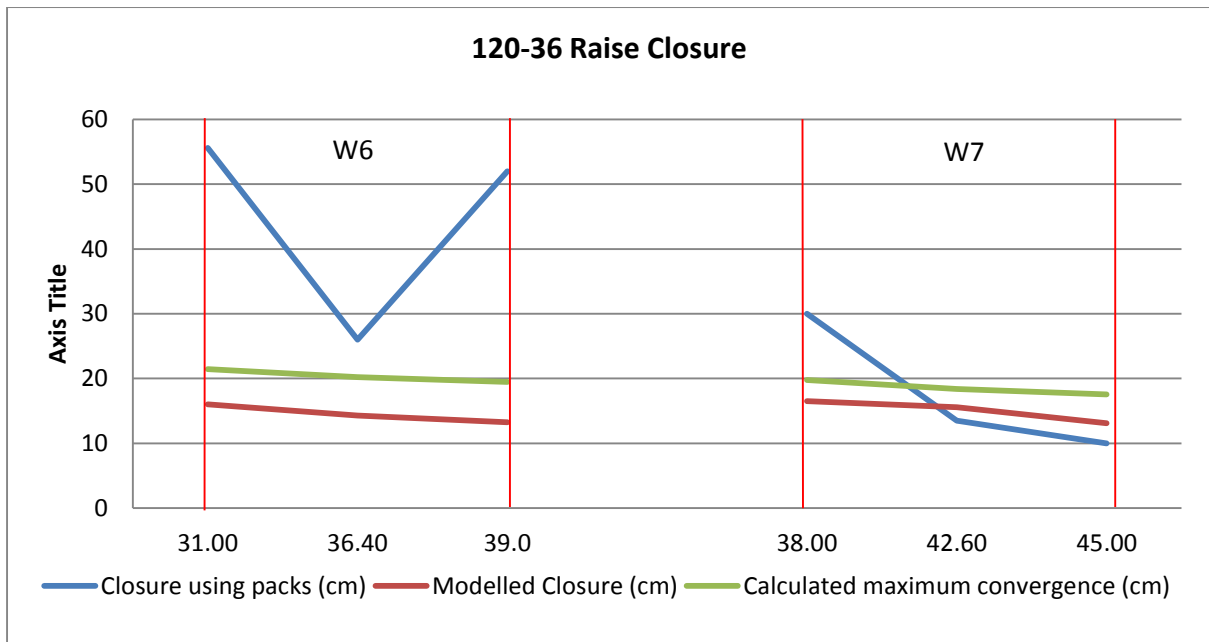


Figure 53. Closures determined at each point in 120-36 raise.

The measured closure in the W7 follows similar trend to the modelled and calculated closures and decreases towards the face. The modelled closure is almost constant in both W7 and W6. The difference between modelled closure and measured closure is much higher in the W6 at 30cm compared to the 3cm at W7 (Figure 53). The W7 approximates the assumption in the analytical solution better than W6 and this is due to the fact that the analytical solution considers infinite length in the 3rd dimension and W6 has however a pillar located nearby.

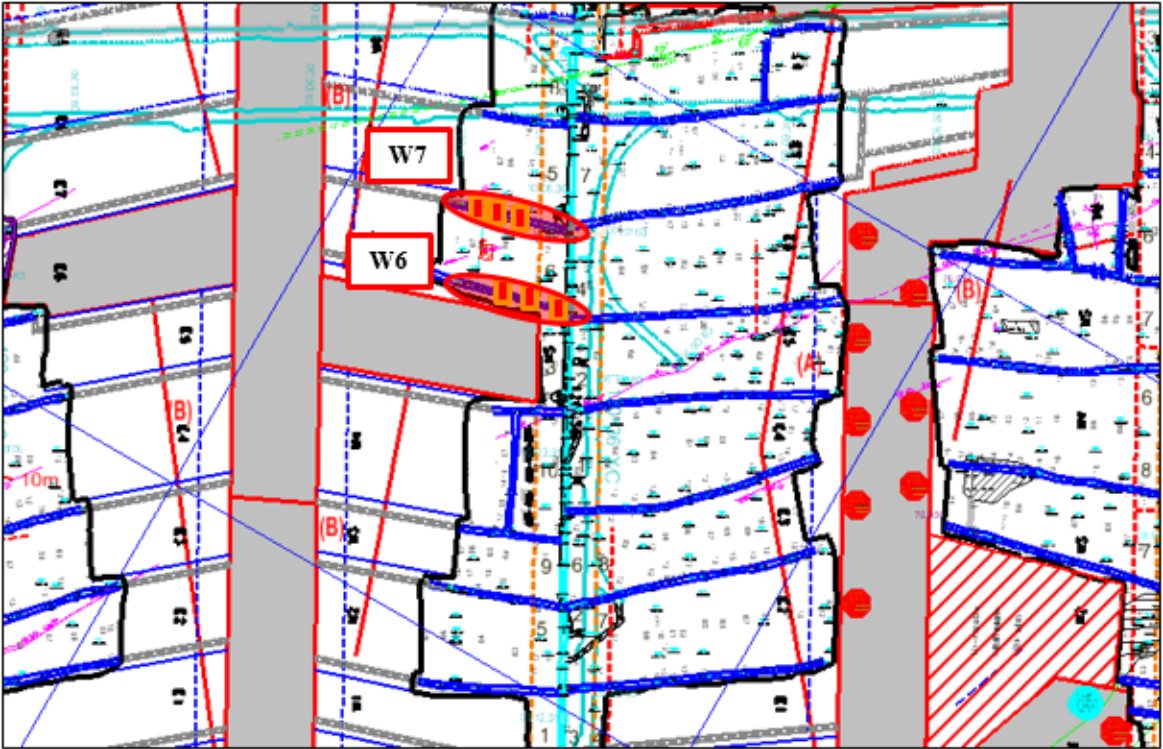


Figure 54. Layout of the 120-36 raise indicating the measured points in the W6 and W7 gullies relative to the centre.

4.2. Correlation between modelled closure and estimated closure

Due to the difference in the layouts and rock mass properties the closure in the assessed raise lines will be different as it has been shown in section 4.1. For better comparison between the modelled closure and the estimated closure the difference will be represented as a percentage. This will accommodate the different stoping widths in each raise line and the influence of layout.

The % difference between modelled closure and actual closure can be determined as follows:

$$\frac{\text{Estimated closure} - \text{Modelled closure}}{\text{Estimated closure}} \times 100\% = \text{Difference \%} \quad (4)$$

In section 4.1, in each raise line analysed it was found that the estimated closure is much higher than the modelled closure. Figure 55 indicates the distribution of the difference between the modelled closure and estimated closure. The difference is spread though the spectrum from -8.2cm up to 62.cm with the mean of 20cm and a standard deviation of 17.8cm. The 20cm difference represent 44.7% of the estimated closure resulting in the modelled closure representing 55.3% of the estimated closure. All the three raise lines with quartzite footwall have an average closure of 48.2cm with a percentage difference 51.6%. The 104-65 (shale footwall) has an average percentage difference of 25% which is 8.8cm. The lesser difference in the shale footwall is mainly due to the adjustment made to the elastic properties in the model. The lower Young's modulus results in increased deformation in the model.

If 44.7% is taken as a fair representation of the difference between the modelled closure and estimated closure it would mean that the modelled closure only represents the 55.3% of the estimated closure occurring underground with an average of 45cm.

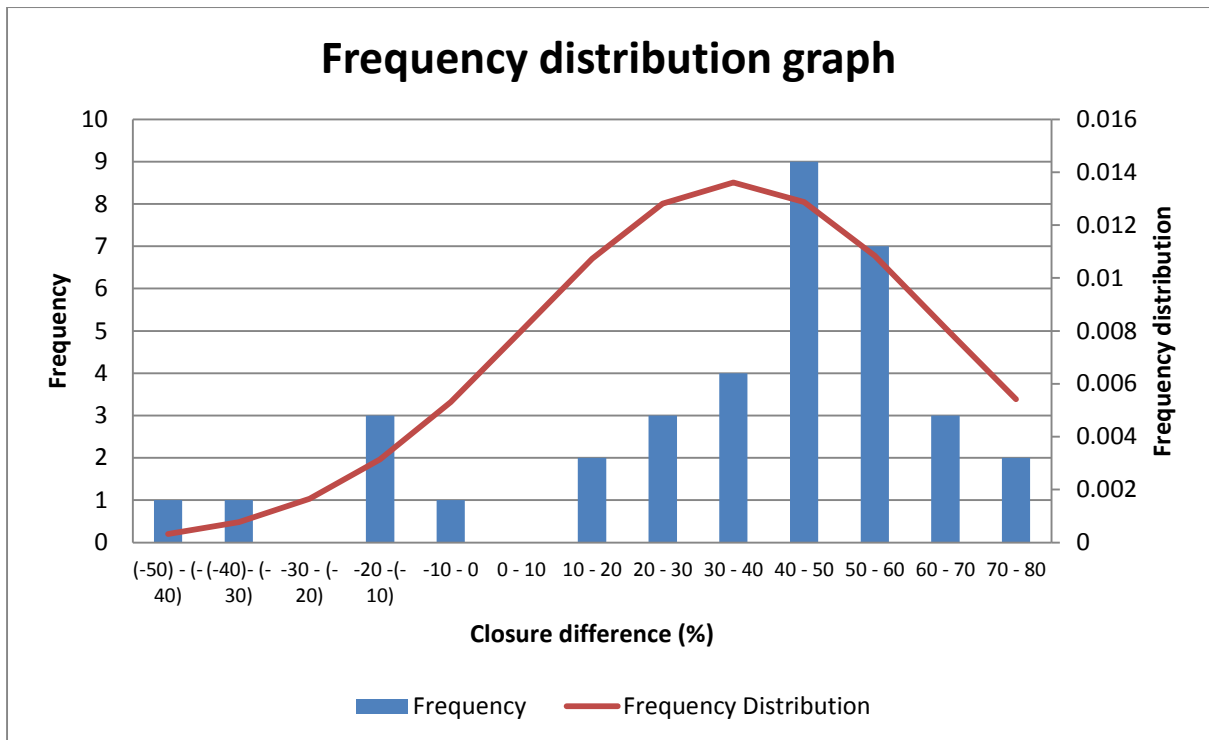


Figure 55. Frequency distribution graph of the difference between modelled closure and estimated closure.

4.3. Conclusions

From all the assessed raise lines, there is a good correlation between the calculated convergence and the modelled closure. This is simply due to the fact that the modelling program uses similar principles as the (Salamon, 1968) convergence equation. In all raise lines there is a similar trend in that the highest closure occurs towards the centre of the mining span. This trend is noticed in both the estimated closure and the two convergences based on elastic assumptions. However there is still a large difference in the total closure estimated compared to the modelled closure. The difference averages at 44.7% with the elastic modelled closure being the lesser of the two.

CHAPTER 5. DISCUSSION OF RESULTS

The analysis in chapter 4 revealed possible correlation in the trends of estimated closure and the modelled closure and yet showed major differences in the magnitudes between the two. This chapter looks at the factors that could have contributed to the observed trends and differences between the estimated closure and the modelled closure. Factors such as rock mass properties, mining layout and sequencing are discussed.

5.1. Elastic modelled closure vs estimated closure

The results in section 4 indicated that the estimated closure is much higher than what the elastic model indicates. It has been determined that the modelled closure is at least 55.3% of the estimated closure. Of interest from the closure graphs in chapter 4 is that the estimated closure underground has a similar trend to the modelled closure in that, the closure nearer to the centre of the span is higher than the closure nearer to the face. From all the ten assessed gullies only measurements from one gully did not indicate this trend. An elastic model takes into account the elastic rock behaviour and the geometry of the stope when assessing closure, particularly the span of the mined out area.

The numerical model does not take into account the deformation that has already occurred and will analyse every step as a new step. This result in the modelled closure being symmetric about the centre of the raise. Figure 56 and Figure 57 illustrates symmetric modelled closure on both sides of a raise line even though the two sides were mined at different times.

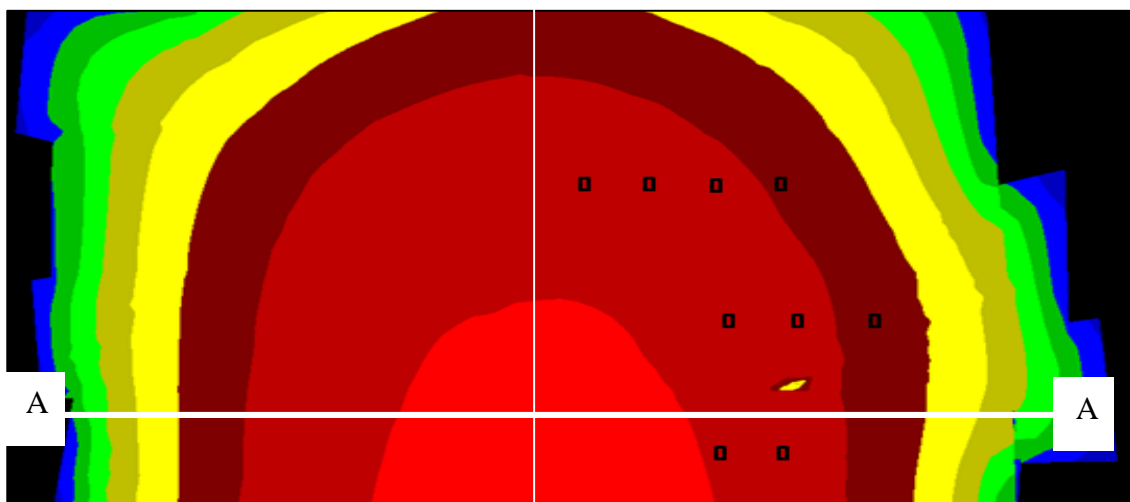


Figure 56. Modelled closure at the same points in 113-52 raise line as closure estimations .

The observed closure is not only influenced by rock properties and geometry of the excavation. Factors such as time, sequence of mining and discontinuities would have a large influence on the displacements occurring in the mined-out areas. The influences of these factors are discussed in detail in following Sections 5.2 and 5.3.

Figure 58 shows discontinuities and fracturing around a tabular deep stope. The presence of bedding planes, joints and the formation of mining induced fractures contribute to the amount of closure taking place and causing the difference between elastic modelled closure and estimated underground closure.

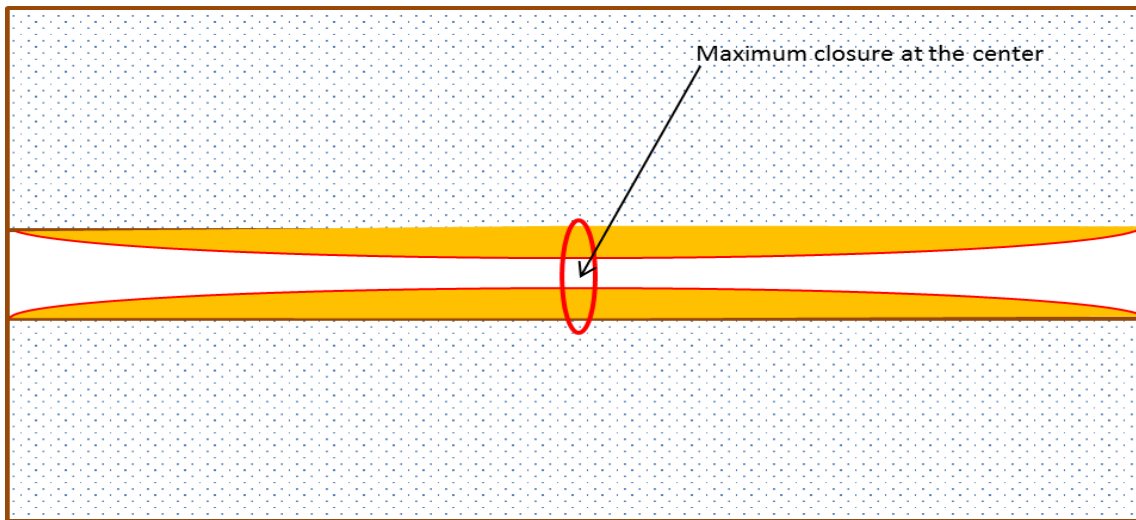


Figure 57. Cross section A-A of an elastic closure model.

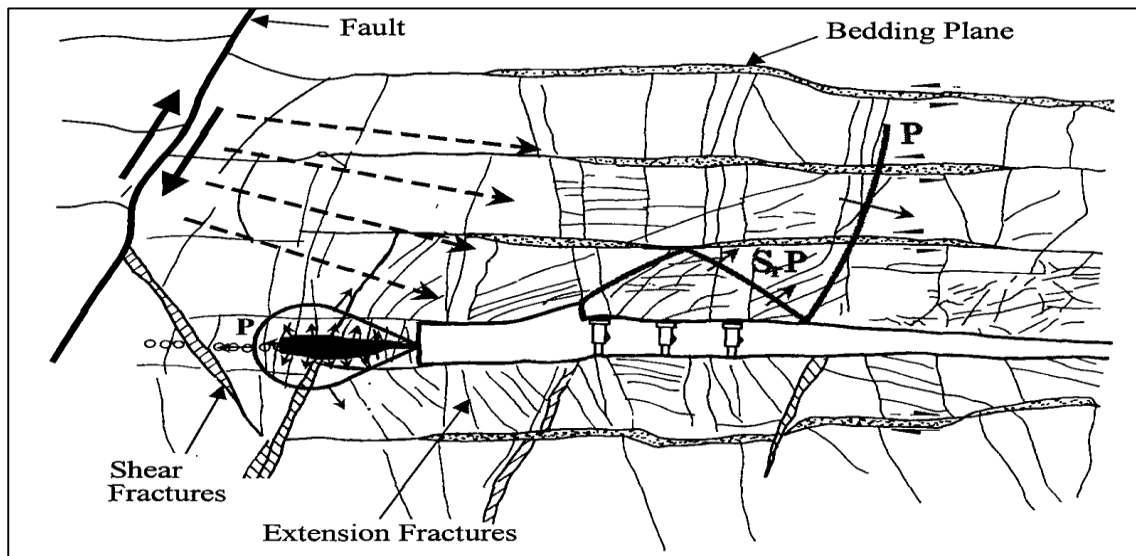


Figure 58. Typical fracturing and discontinuities formed around a tabular stope in deep mines (Napier et.al, 1998).

5.2. Correlation between estimated closure and modelled closure

The typical sequence in a sequential grid mining is to mine 10m on either side of the raise to secure the raise line, this is referred to as ledging process which results in a total span of 20m. This is followed by the second step of mining which is to mine one side up to the pillar position resulting in a total span of 100m. Then the final step is to mine the opposite side resulting in a total span of 180m (Figure 59). Assuming that Step 1 and Step 2 are considered as one mining step due to the small span during ledging and only step three is seen as a separate step then the closure in the raise can be calculated in two steps. Step three is mined more than a year later since the start of ledging. This is where the sequence of mining comes into effect regarding the extent of closure occurring.

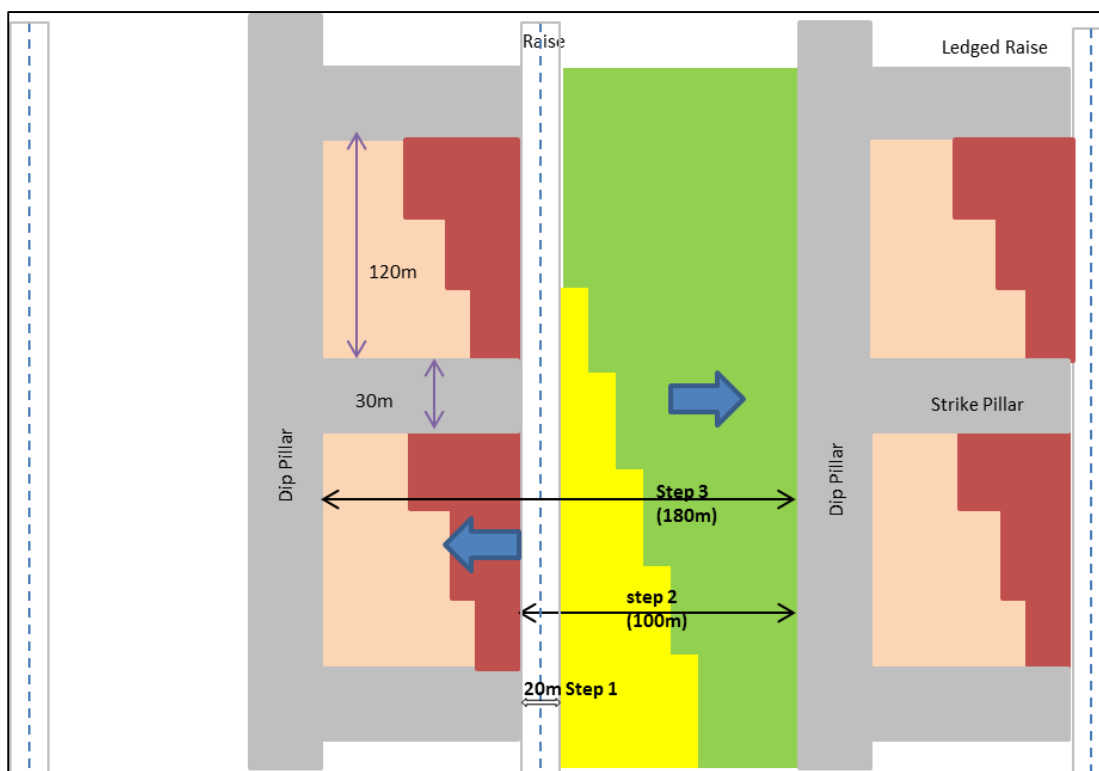


Figure 59. Mining sequence in a sequential grid raise line.

In section 3.3 the closure rates were determined from 104-65 raise line as 8.77mm/m and 2.2mm/day within 20m from the advancing face. It must be noted that the 8.77mm/m did not take into account the mining cycle which would have indicated how often the face advanced. The closure rates reduced significantly when measured at a distance more than 20m from the face, with rates as low as 3.89mm/m or 1.21mm/day. These rates are meant to enable a good estimation of the expected closure with a raise with the same rock mass properties. A simple example is used to illustrate how these rates can be used. If the closure rates per face advance

are determined for the different zones relative to the face. Then the daily closure rate is determined for when there is no mining. The sum of closure in a raise line can be determined using these three rates. The 104-65 Raise is used as an example to illustrate how this can be achieved.

Example to determine closure from closure rates (104-65 Raise with a total span of 210m and average stoping width of 1.3m)

The closure is determined from closure rates with only two mining steps required. To take into account the effects of time, the closure is determined for three different rates, the primary closure (within 20m from the advancing face), secondary closure rates (>20m from the advancing phase) and the steady state closure (measured only on the side of the raise that mined first when mining stops and changes to the opposite side) which takes place without any mining activities.

The following *assumptions* are applied in the example:

- The closure rate is constant at 8.77mm/m and 3.89mm/m within 20m from the face and after 20m from the face respectively (Table 4).
- The closure rate when there is no mining remains constant at 0.59mm/day (Table 4).
- Advancing face has no influence on the closure occurring more 90m from the face.

- Ledging and step 1 (East) span = 110m.
 - Closure = deformation with 20m + (Mined span - 20m) x deformation after 20m
 - Closure = (20m x 8.77mm/m) + ((110m - 20m) x 3.89mm/m) = 525mm

- Step 2 (West) span = 100m.
 - Closure = deformation with 20m + (Mined span - 20m) x deformation after 20m
 - Closure = (20m x 8.77mm/m) + ((100m - 20m) x 3.89mm/m) = 486mm

- Standing time on the East after completing step 1 and 2 = 5 years (1825 day). This delay was caused by difficulties in starting up the Western side following a standing period of 3 years while mining the Eastern side. Standing time on the West is neglected as the mining continued and the span increased.

- Steady state closure on the east = $1825 \times 0.59\text{mm/day} = 1076\text{mm}$

To be able to determine the influence of the time on the advancing face, first one has to determine the distance from the face where closure is no longer influenced by the immediate face advance. The 486mm closure calculated on the West side is 27% more than the estimated closure in the 104-65 raise. The estimated average closure from packs on 104-65 raise was 350mm. There is a good correlation between closure rates and estimated closure, considering the closure loggers are installed at least 10m from the face.

Unfortunately the east side of 104-65 could not be accessed for measurements mainly due to safety reasons as the area has been standing for a long period. Pictures taken in 104-66 Raise line which is adjacent to 104-65 raise showed signs of high levels of closure (full compression of backfill) on the Eastern side of the raise which was mined first (Figure 60 and Figure 61). Only 116-52 raise line was measured on both sides of the raise and it showed that the side that was mined first (W6) has higher closure (Figure 47) than the E4 which was in the last step of mining.



Figure 60. Photo of the 104-66 Raise. The pack on the raise shoulders were installed with a full cut ledge at 2.4m high and currently measure only 0.5m in height.

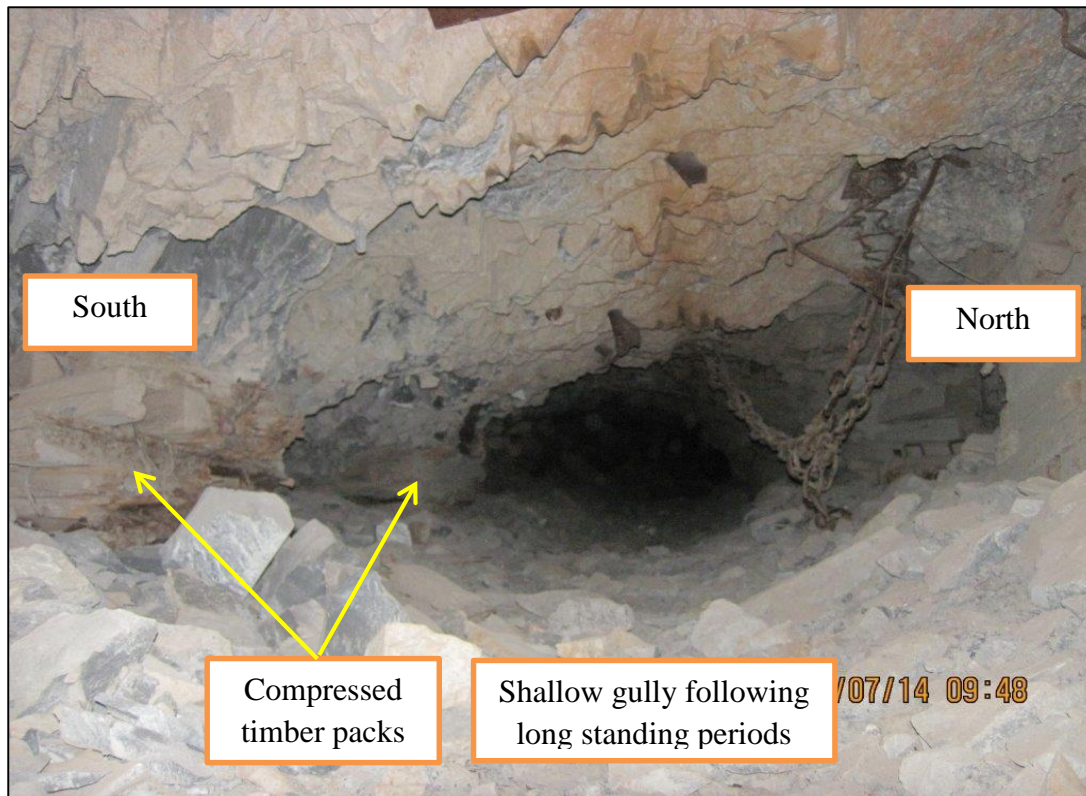


Figure 61. Closure in one of the strike gullies on the Eastern side of the 104-66 raise line.

5.3. Influence of rock mass properties on closure.

The rock mass properties are determined in a laboratory using intact rock samples. These are the parameters that are used in analytical equations to determine convergence and also used in a numerical model to analyse rock behaviour. These properties do not take into account the presence of weaknesses such as joints and bedding planes which have a large influence on the behaviour and the stability of the rock mass.

By adjusting the elastic properties for 104-65 raise line due to the shale footwall from 70GPa and 0.25 to 50GPa and 0.3 for the Young's modulus and for the Poisons ratio respectively, the calculated convergence came very close to the measured closure (Figure 49). The change in these properties did not make significant difference to the numerically modelled closure.

By adjusting the rock mass properties that are used in the model a good correlation can be drawn from the elastic model and the estimated closure. However this requires a good understanding of the estimated closure to enable calibration of the elastic model. Lower Young's modulus and Poisons ratio used in the 104-65 raise resulted in the calculated closure

being closer to the observed closure. This is an indication that the same principle can be applied for modelled closure.

5.4. Conclusions

The understanding of the factors, such as the rock mass properties, mining layouts and the sequence of mining, that have influence on the rock mass deformation is critical when using elastic numerical modelling programs. The elastic model is over simplified and does not take the factors discussed above into account, leading to inaccuracies in the rock mass behaviour underground. Adjustment made to the Young's modulus and Poisons ratio improves the correlation between the observed closure and the modelled closure. However adjusting these elastic properties of the rock mass in the model does not address the challenge of mining sequence.

CHAPTER 6. SUMMARY AND CONCLUSIONS

The objective of this research was to compare the elastic modelled closure to the estimated closure observed underground. Following the detailed literature review and analysis of the results obtained from closure comparisons, satisfactory conclusions can be made on the set objective of the research project. To understand the logic used to arrive at the conclusions, first a summary of the process followed is discussed, then conclusions are discussed.

6.1. Summary

The following sequence was followed in the research.

- i. Collect and analyse closure monitoring data from continuous closure loggers.

The data in 104-65 raise line was analysed to determine the two closure rates, closure per metre face advance and closure per day which were 8.77mm/m and 2.67mm/day respectively (Section 3.3).

- ii. Evaluate underground closure measurements using installed support.

Measurements were taken from strike and centre gullies in four different raise lines to estimate the original stoping width at some timber pack positions (Section 3.4).

- iii. Estimate closure using the stoping width at the time of pack installation and currently measured underground stoping width.

The measured stoping widths from underground assessment were subtracted from the original stoping width to estimate closure.

- iv. Build and analyse MAP3D elastic closure.

An elastic model was built using MAP3D to determine closure in each raise line. Two different models were built to accommodate the shale and quartzite footwall on the east and the west of the mine. The closure was determined for each point similar to those taken from underground.

- v. Correlate estimated closure in iii) to elastic modelled closure in iv).

In section 4.2 all the estimates of the underground closure and modelled closure were compared for each point. It was found that the underground closure estimates are higher than the modelled closure. The modelled elastic closure (average 27cm) was only 55.3% of the underground

closure due to the inability of the elastic model to incorporate inelastic and creep related closure.

vi. Correlated closure rate from closure loggers to actual closure and modelled closure.

Finally the closure rates were correlated to the estimated closure and the modelled closure and it was seen that the closure rates (8.77mm/m with 20m from the face, 1.29mm/day more than 20m from the face and a 0.59mm/day creep) will result in closure in the similar range of the estimated underground closure (average 45cm). It was also shown that over long periods there will be complete closure in the back area. The modelled closure did not result in the total closure predicted by the closure rates.

6.2. Conclusions

Scheepers et.al, (2012) attempted to correlate numerically modelled elastic closure with closure estimated from seismic events with the aim of using elastically modelled closure as a design parameter and as an indicator of expected seismic response. Earlier in section 2.8 it was shown that the correlation was observed in the first 10 000m² of a new raise. The correlation of estimated underground closure and elastically modelled closure also indicated that rock mass deformation is not linear and there are other factors that contribute to the actual closure besides rock mass properties.

According to elastic theory closure should increase with the increasing span and seismic potency should follow similar trend according to (Scheepers et.al, 2012). Elastic model is used to determine closure due to mined area purely from elastic point of view. The modelled closure is correlated to seismic potency based on the assumption that the deformation due to seismic damage manifests similar to the deformation as a result of increased mined area. However the research conducted in this report indicated that the correlation between estimated closure and modelled closure is poor, with modelled closure only representing half the observed closure. With reference to Figure 1, it was also shown in section 2.8 that high seismic activity can be experienced in an area with a small span and relatively small closure due to the stress state in the area. In this case closure would not indicate a high seismic potency. One question that requires answer from this research is the extent of influence the closure has on seismicity,

Closure is one of the observable and measurable behaviour of the rock mass in a tabular stope and monitoring conducted on closure has indicated that large seismic events are accompanied by significant stope closure (Jager & Ryder, 1999). The closure magnitudes could possibly be correlated to seismic potency, as larger seismic events have larger seismic moment and potency. The correlation of normal rock mass deformation due to increasing mining span to seismic potency required further investigation.

The modelled closure can be used as a support design parameter for ultra-deep narrow reef tabular stopes, however its use requires further study to define seismic hazard. Numerical modelling allows for prediction or simulation of rock mass behaviour once mining takes place. If the numerical modelling could simulate the expected closure it would also be possible to assess the required raise and gully height relative to the expected closure.

The use of modelling programs such as MAP3D allows for quick analysis of different scenarios with ease, however caution should be exercised. MAP3D is an elastic modelling program applied in an inelastic environment such as deep narrow reef mining. Other factors, such as time dependant deformation and discontinuities in the rock, also need to be taken into account.

MAP3D cannot simulate inelastic effects however with a good understanding of the properties and behaviour of the rock mass being modelled the elastic properties can be adjusted to yield similar behaviour to that of the actual rock mass. An extensive rock mass monitoring program must be in place to obtain information such as jointing, fracture formation and different types of closure or deformation to achieve a good understanding of the rock mass behaviour. With this understanding in mind one can calibrate the model until it reflects the actual rock mass behaviour.

Gurtunca & Adams (1991) showed that the correlation of observed underground closure with numerical modelling can be obtained if the deformation due to the fractured zone is represented by reducing the Young's modulus of the rock mass by 40% to 50%. In this report, it was also shown that a comparison between modelled elastic closure and estimated underground closure can be made by taking underground measurements and matching them to the modelled elastic closure at the same points where closure is assessed. This enables calibrating the modelled elastic closure results to be close to the actual closure.

The following calibration exercise was conducted between the elastic model and the underground closure estimations. The same numerical model was run with different input parameters and different settings. Table 15 indicates the input parameters used in each run relative to the original model used. The results of the models were analysed for 116-52 and 113-52 raise lines and shown in Figure 62 and Figure 63 respectively.

Table 15. Input parameters used in the calibration exercise.

	Young's modulus (GPa)	Poisson's ratio	Stoping width (m)
Original model	70	0.2	1
Run 1	35	0.2	1
Run 2	35	0.1	1
Run 3	70	0.2	1.4
Run 4	35	0.2	1.4
Run 5	35	0.1	1.4

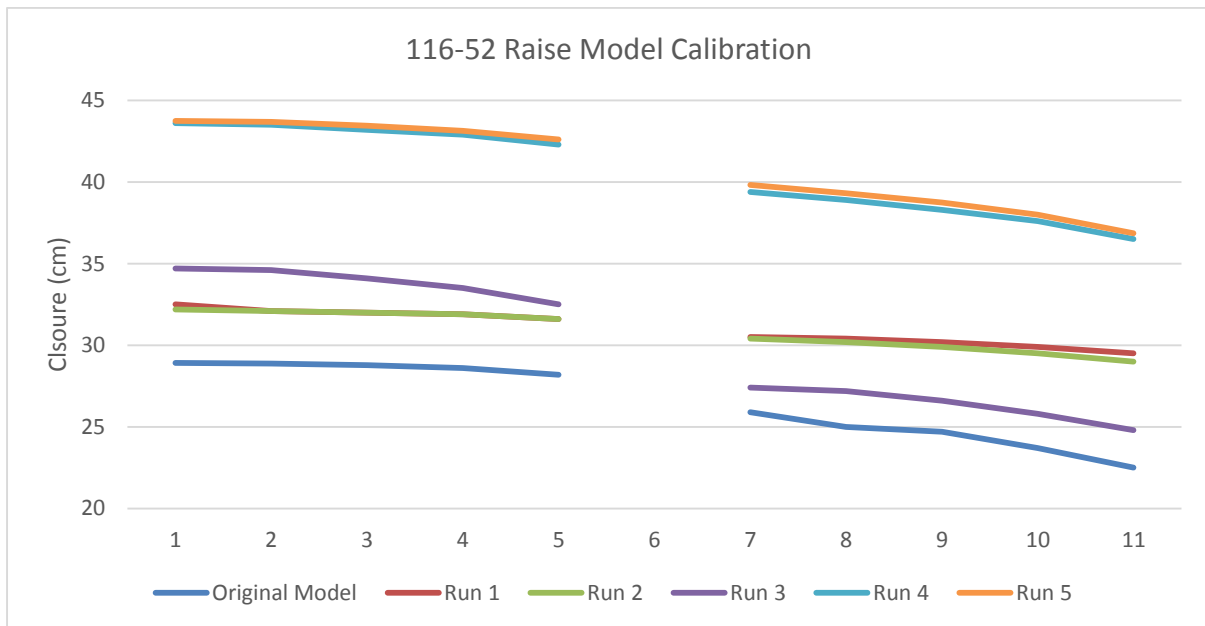


Figure 62. Calibration results for 116-52 raise line.

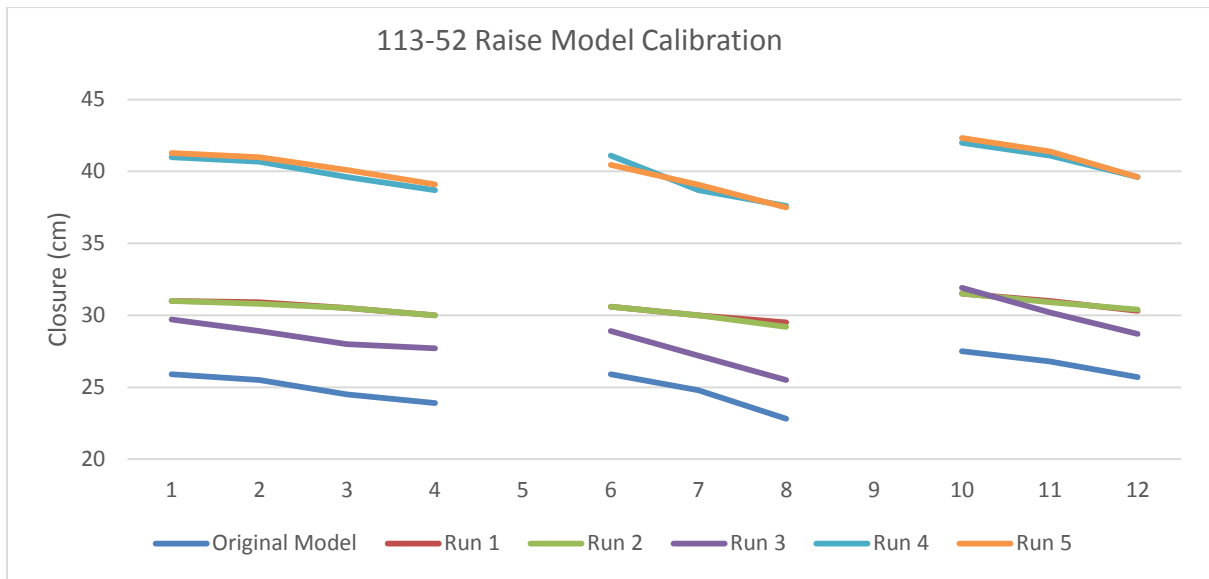


Figure 63. Calibration results for 113-52 raise line.

Reducing the Young's modulus by 50% increases the modelled closure by 5cm, however there is minimal change to the modelled closure when the Poisson's ratio is adjusted. By adjusting the stoping with from 1m to 1.4m (average stoping width) and further reducing the Young's modulus by 50%, the modelled closure increases to an average of 40cm compared to an average of 45cm for estimated closure. The correlation between the estimated closure and the modelled closure becomes improved.

CHAPTER 7. RECOMMENDATIONS FOR FUTURE WORK

To allow for the application of modelled elastic closure as a design parameter for ultra-deep narrow reef stopes more work need to be done to develop the relationship between the estimated closure and the modelled elastic closure. Below is the work that needs to be done to develop this relationship:

i. Investigate the use of inelastic modelling in narrow reef stope

Inelastic modelling programs such as FLAC and UDEC take into account factors such as mining sequences and discontinuities and can simulate inelastic closure. Having inelastic affects would result in a better estimation of closure. It must also be kept in mind that any model can only give output based on the input data. Therefore it is still of utmost importance to understand the mechanical properties of the rock mass.

ii. Gather data regarding closure rates and types of closure

Even if one does an inelastic modelling exercise, without the actual rock mass behaviour to refer to, the result can still be misleading and one would not know if the results represent the expected rock mass behaviour. Therefore it is highly recommended that different geotechnical districts be monitored to gather the closure rates.

iii. Understand the influence of discontinuities on closure.

Weakness in the rock mass can lead to large block formation and failure in the back area which can result in back breaks. Falls of ground could be associated with shear fractures in the stope and the interaction of these shear fractures with bedding can result in increased closure in the de-stressed mined out areas. Therefore it is recommended to conduct geotechnical mapping of joints, factures and bedding planes to gain a better understanding of their influence on closure.

iv. Define suitable mechanical properties of the rock mass to be used in numerical modelling.

Tools such as Rock Mass Rating (RMR) allow for assessment of quality of rock masses. The perception is that the RMR is not suitable for ultra-deep mining environment. However if used with caution and consideration RMR can give a good indication of what the suitable input parameters could be in the models.

CHAPTER 8. References

- AngloGold Ashanti. (2013). *Anglogold Ashanti South Africa*. Retrieved June 26, 2013, from <http://www.aga-reports.com/12/ir/operating-reviews/south-africa>
- Applegate, J. D. (2001). *Rock Mechanics Aspects of Sequential Grid Mining*. Johannesburg: Project Report submitted to the University of the Witwatersrand in partial fulfilment of the Degree of Master of Science in Engineering.
- Budavari, S. (1983). *Rock Mechanics in Mining Practices. SAIMM Monograph Series 5*.
- Cook, N. G., Hoek, E., Pretorius, J. P., Ortlepp, W. D., & Salamon, M. D. (1966). Rock Mechanics applied to the study of rockbursts. *J.S.Afr.Inst. Min.Meta*, 66, 435-714.
- Drescher, K., & Handley, M. F. (2003). Aspects of time-dependent deformation in hard rock at great depth. *The Journal of The South African Institute of Mining and Metallurgy*, 103(5), 325 - 335.
- Durrheim, R. J. (2010). Mitigating the risk of rockbursts in the deep hard rock mines of South Africa: 100 years of research. In *Extracting the Science: a century of mining research*, ISBN 978-0-87335-322-9, 156-171.
- Durrheim, R. J., Spottiswoode, S. M., Roberts, M., & van Z. Brink, A. (2005). Comparative seismology of the Witwatersrand Basin and Bushveld Complex and emerging technologies to manage the risk of rockbursting. *The South African Institute of Mining and Metallurgy*, 105(6), 401 -409.
- Groundwork. (2013). *Groundwork, Products*. Retrieved 2013, from Groundwork: <http://www.groundwork.co.za/products.html#rw>
- Gurtunca, R. G., & Adams, D. J. (1991). Determination of the in situ modulus of rock mass by the use of backfill measurements. *J. S. Afr. Inst. Min. Metall*, 91(3), 81-88.
- Handley, M. F., De Lange, J. A., Essrich, F., & Banning, J. A. (2000). A review of the sequential grid mining method employed at Elandsrand Gold Mine. *The Journal of The South African Institute of Mining and Metallurgy*, 100(3), 157-168.
- Jager, A. J., & Ryder, J. A. (1999). A Hand Book on Rock Engineering Practice for Tabular Hard Rock Mines. In J. J. A., & A. R. J, *A Hand Book on Rock Engineering Practice for Tabular Hard Rock Mines* (p. 46). Johannesburg: SIMRAC.
- Jooste, Y. (2013). *Modified Sequential Grid Layout to Increase Production Rates in Deep Level Hard Rock Mines*. Pretoria: University of Pretoria.
- Kirsten, H. A., & Stacey, T. R. (1988). Hangingwall behaviour in tabular stopes subjected to seismic events. *Journal of The South African Institute of Mining and Metallurgy*, 88(5), 163 -171.
- Lachenicht, R. (2001). *Relationship between ERR, system stiffness parameters and seismic energy release for different geotechnical areas*. Johannesburg: SIMRAC.
- Mahne, W. L. (2004). Pre – Conditioning: A tool to combat Face Bursts at Mponeng. Johannesburg: The Miner's Guide through the Earth's Crust, South African National Institute of Rock Engineering.

- Malan, D. F. (2003). *Guidelines for Measuring and Analysing Continuous Stope Closure behaviour in Deep Tabular Excavations*. Johannesburg: SIMRAC.
- Malan, D. F., Kononov, V. A., Coetzer, S. J., Janse van Rensburg, A. L., & Spottiswoode, B. S. (2000). *The feasibility of a mine-wide continuous closure monitoring system for gold mines*. Johannesburg: Safety in Mines Research Advisory Committee.
- Malan, D. F., Napier, J. A., & Janse van Rensburg. (2007). Stope deformation measurements as a diagnostic measure of rock behaviour: a decade of research. *The Journal of The Southern African Institute of Mining and Metallurgy*, 107(11), 743-765.
- MAP3D. (2015). *Map3D Fault Slip*. Retrieved 2015, from http://www.map3d.com/fault_slip.php: <http://www.map3d.com/index.php>
- McGarr, A. (1976). Seismic moments and volume changes. *Journal of Geophysical Research*, 81(Solid Earth and Planets), 1487 - 1494.
- McGarr, A., & Wiebols, G. A. (1977). Influence of Mine Geometry and Closure Volume on Seismicity in Deep-Level Mines. *Int. J. Rock Mech, Min, Sci, & Geomech*, 14, 139-145.
- Mendecky et.al. (2010). Routine Micro-Seismic Monitoring in Mines. *Australian Earthquake Engineering Society*. Perth, Western Australia.
- Milev, A. M., & Spottiswoode, S. M. (1997). Intergrated seismicity around deep level stope in South Africa. *Int. J. Rock Mech and Min Sci.*, 34(3-4).
- Murphy, S. K. (2012). Linear elastic numerical modelling for failure prediction-an assesment. *The Southern African Institute of Mining and Metallurgy*, 112(8), 736-748.
- Napier et.al. (1998, December). Deep gold mine fracture zone behaviour. *Safety in mines research advisory committee*.
- Napier et.al. (1998). *Deep gold mine fracture zone behaviour*. Johannesburg: SIMRAC.
- Ogasawara et.al. (2014). In situ stress measurements in earthquake prone areas in South African gold mines. *South African Rock Engineering Symposium*. Johanesburg: SAIMM.
- Riemer, K. L., & Durrheim, R. J. (2012). Mining seismicity in the Witwatersrand Basin: monitoring, mechanisms and mitigation strategies in perspective. *Journal of Rock Mechanics and Geotechnical Engineering*, 4(3), 228 - 249.
- Russo-Bello, F., & Murphy, S. K. (2000). Longwalling at great depth in a geologically disturbed environment—the way forward. *The South African Institute of Mining and Metallurgy*, 100(2), 91-100.
- Ryder, J. A., & Jager, A. J. (2002). *Rock Mechanics for Tabular Hard Rock Mines*. Johannesburg: SIMRAC.
- Salamon, M. D. (1968). Two-dimentional treatment of problems arising from mining tabular deposits in isotropic ground. *International Journal of Rock Mechanics*, 5(2), 159-185.
- Scheepers et.al. (2012). The Study of Seismic Response To Production for A Grid Mining Layout. *Southern Hemisphere International Rock Mechanics Sysposium SHIRMS*.

Spottiswoode et.al. (2000). *The Relationship between ERR and seismic energy release for different geotechnical areas*. A. Johannesburg: SIMRAC.

Stacey, T. R. (2012). Map 3D (Numerical Model course notes). *Numerical Modelling Techniques in Rock Engineering*. Johannesburg: Wits University.